An Out-bred Animal Model of Cottontail Rabbit Papillomavirus Latent Infection

Dissertation

der Mathematisch-Naturwissenschaftlichen Fakultät

der Eberhard Karls Universität Tübingen

zur Erlangung des Grades eines

Doktors der Naturwissenschaften

(Dr. rer. nat.)

vorgelegt von

Jin Xi

aus Sichuan, China P.R.

Tübingen

2017

Gedruckt mit Genehmigung der Mathematisch-Naturwissenschaftlichen Fakultät der Eberhard Karls Universität Tübingen.

Tag der mündlichen Qualifikation: 26.09.2017

Dekan: Prof. Dr. Wolfgang Rosenstiel

1. Berichterstatter: Prof. Dr. Thomas Iftner
2. Berichterstatter: Prof. Dr. Friedrich Goetz

CONTENT

ABSTRACT

Cutaneous Human Papillomaviruses (cuHPVs) cause the most common HPV infections and are frequently detected and tend to persist asymptomatically in the skin of the general population. The cuHPV types are mainly represented by the beta and gamma genera, of which the beta-HPV infections has been suspected to be involved in the development of non-melanoma skin cancers (NMSC), besides well-known risk factors, such as immunosuppression and ultraviolet (UV) light radiation. The ability of cuHPVs to persist in the absence of disease, i.e latency, has long being suspected. In humans, administration of immunosuppressive drugs such as cyclosporine A (CsA) to organ transplant recipients (OTRs) and/or sun exposures are risk factors that have been proposed to activate cuHPV latent infections leading to apparent tumors.

Cutaneous infection of New Zealand White rabbits with CRPV represents an attractive animal model that enables *in vivo* investigation of cuHPV infection. In this study, we employed the CRPV/rabbit model to investigate whether latent cuHPVs infections are controlled by the immune system and/or UV radiation. We observed that a level of one viral DNA copy per 200 to 1000 cells can be detected in 88% of the latently infected skin sites more than 14 months post infection (p.i.). Viral copy numbers dramatically increased, when latent skin samples were explanted in tissue culture. Low-dose UV alone showed no significant effect on viral latency. We observed an increase in viral genome copy numbers in latently infected skin sites upon immunosuppression. Although the appearance of three papillomas on only one rabbit in latent period was likely to be activated by immunosuppression, the majority of latently infected sites showed no papilloma formation. Surprisingly, the combination of immunosuppression and UVA + UVB radiation showed no significant difference compared to immunosuppression alone.

During the course of our latency experiment, we observed a dramatic increase of pre-existing papilloma growth upon CsA-based immunosuppression. We demonstrated that the fast-growing papillomas were not associated with the levels of viral DNA copies or viral gene expressions. T-cell counts and T-cell associated cytokines were significantly decreased due to systematic immunosuppression. Interestingly, the pro-inflammatory cytokines such as IL-8 and IL-1β were significantly upregulated

specifically in the fast growing papillomas. Although, it has been shown that CsA can induce cell proliferation and tumorigenesis independent of host immune system, it has been widely used as an immunosuppressant in previous PV-related studies, and the side effect of CsA on PV-induced tumorigenesis has not been investigated. Our results here indicate that the proliferation of rabbit-derived cells was increased upon CsA treatment.

In conclusion, we have established an outbred CRPV/rabbit model for the study of latent infections with cutaneous PVs which allows investigating factors controlling the latent state.

We demonstrated that short-term immunosuppression increased latent viral genome copy numbers, but did not lead to new papilloma formation at majority of latently infected sites. Low-dose UV alone showed no significant effect on viral latency. The combination of short-term immunosuppression and UV radiation showed no significant difference compared to immunosuppression alone. However, it is still possible that the reactivation of latent viral infection may require longer-term systematic immunosuppression or multiple UV radiations.

In addition, we demonstrated that CsA-based immunosuppression facilitates pre-existing papilloma growth likely via reduction of immune surveillances, upregulation of pro-inflammatory cytokines such as IL8 and IL-1β, and maybe CsA-related tumorigenesis.

Our findings here may provide implications for the clinic treatment of CsA-based immunosuppression of OTRs associated with cuHPV infection.

ZUSAMMENFASSUNG

Infektionen mit kutanen Papillomviren (cuHPVs) sind sehr häufig in der Allgemeinbevölkerung, wo sie zumeist symptomlos in der Haut über längere Zeit persistieren und nachgewiesen werden können. Die cuHPV-Typen werden hauptsächlich durch die Beta- und Gamma-Gattungen repräsentiert, von denen, neben bekannten Risikofaktoren wie Immunsuppression und Ultraviolette (UV) Strahlung, die Beta-HPV-Infektionen vermutlich an der Entwicklung von Nicht-Melanom-Hautkrebs (NMSC) beteiligt sind. Die Fähigkeit der cuHPVs, in Abwesenheit von Läsionen zu persistieren, d.h. ein Latenzzustand, wurde in der Literatur immer wieder diskutiert. Beim Menschen wurde die Verabreichung von immunsuppressiven Medikamenten wie Cyclosporin A (CsA) bei Organtransplantationsempfängern (OTRs) sowie UV-Strahlung als Risikofaktoren vorgeschlagen, die zur Aktivierung latenter cuHPV Infektionen und somit zur Tumorbildung führen können.

Die kutane Infektion von Weißen Neuseeländer Kaninchen mit CRPV (Cottontail Rabbit Papillomavirus) ist ein ideales Tiermodell, was die *in vivo* Untersuchung der cuHPV-Infektion ermöglicht. In dieser Arbeit wurde dieses Modell eingesetzt, um zu untersuchen, ob latente cuHPVs Infektionen durch das Immunsystem und/oder UV-Strahlung reguliert werden können. Wir haben festgestellt, dass im Durchschnitt eine virale DNA-Kopie pro 200 bis 1000 Zellen in 88% der latent infizierten Hautstellen mehr als 14 Monate nach der Infektion (p.i.) nachgewiesen werden kann. Die Kopienzahlen sind dagegen drastisch erhöht, wenn latente Hautproben in Zellkultur explantiert wurden. Niedrigdosierte UV-Strahlung allein zeigte keinen signifikanten Effekt auf die Viruslatenz. Wir beobachteten eine Zunahme der Virusgenom-Kopienzahlen in latent infizierten Hautstellen bei Immunsuppression. Obwohl das Auftreten von drei Papillomen auf einem Kaninchen im latenten Zustand wahrscheinlich durch die Immunsuppression aktiviert wurde, zeigte die Mehrheit der latent infizierten Stellen und die anderen Kaninchen keine Papillomneubildung. Überraschenderweise zeigte die Kombination von Immunsuppression und UVA/UVB-Strahlung keinen signifikanten Unterschied im Vergleich zur alleinigen Immunsuppression.

Wir beobachteten außerdem eine dramatische Zunahme des bereits vorhandenen Papillom-Wachstums unter CsA-induzierter Immunsuppression. Diese sehr schnell wachsenden Papillome korrelierten allerdings nicht mit der viralen DNA-Kopienzahl oder der viralen Genexpression. Die Anzahl der T-Zellen und die Expression T-Zell-assoziierter Zytokine waren aufgrund der systemischen Immunsuppression signifikant verringert. Interessanterweise waren die proinflammatorischen Zytokine wie IL-8 und IL-1β in den schnell wachsenden Papillomen signifikant hochreguliert. Obwohl bekannt ist, dass CsA die Zellproliferation und die Tumorentstehung unabhängig vom Wirtsimmunsystem induzieren kann, wurde es in früheren PV Studien weithin als Immunsuppressivum verwendet und die Nebenwirkungen von CsA auf die PV-induzierte Tumorentstehung wurden nicht untersucht. Unsere Ergebnisse zeigen, dass die Proliferation von Kaninchenzellen durch CsA-Behandlung erhöht wurde.

Zusammenfassend haben wir das Outbred-CRPV/Kaninchen-Modell für die Untersuchung von latenten Infektionen mit kutanen PVs etabliert. Dies ermöglicht es, Faktoren zu kontrollieren, die den latenten Zustand regulieren könnten. Wir haben gezeigt, dass die kurzfristige Immunsuppression die latenten Virusgenom-Kopienzahlen erhöhte, aber nicht zu einer Papillomneubildung bei der Mehrheit der latent infizierten Stellen führte. Niedrigdosierte UV-Strahlung allein zeigte keinen signifikanten Effekt auf die Viruslatenz. Die Kombination von kurzfristiger Immunsuppression und UV-Strahlung zeigte keinen signifikanten Unterschied im Vergleich zur Immunsuppression allein. Es ist jedoch möglich, dass die Reaktivierung der latenten Virusinfektion eine längerfristige systemische Immunsuppression oder mehrere UV-Expositionen erfordert. Darüber hinaus haben wir gezeigt, dass die CsA-basierte Immunsuppression das bereits vorhandene Papillomwachstum durch die Reduktion der Immunüberwachung, der Hochregulierung von entzündungshemmenden Zytokinen wie IL8 und IL-1β, sowie die CsA-induzierte Tumorgenese fördert.

Unsere Ergebnisse liefern neue Einblicke in die klinische Behandlung von OTRs, die eine CsA-basierte Immunsuppression erhalten und mit einer cuHPV-Infektion assoziiert sind.

ABBREVIATIONS

ACK	Ammonium-Chloride-Potassium
ATF3	Activating transcription factor 3
AVS	Asian Virus Stock
Bak	Bcl-2 homologous antagonist/killer
BCC	Basal cell carcinoma
Bp	Base pair
BPE	Bovine pituitary extract
BPV	Bovine papillomavirus
CCL	Chemokine (C-C motif) Ligand
CD3+	Cluster of differentiation 3
CD4+	Cluster of differentiation 4
CD5	Cluster of differentiation 4
CD8+	Cluster of differentiation 8
Cdk	Cyclin-dependent kinase
CNI	Calcineurin Inhibitor
CPD	Cyclobutane Pyrimidine Dimer
CpG	5'-C-phosphate-G-3'
CRPV	Cottontail rabbit papillomavirus
CsA	Cyclosporine A
Cu-HPV	cutaneous HPV
ddH_2O	Double distilled water
DAPI	4',6-diamidino-2-phenylindole
Dex	Dexamethasone
DNA	Deoxyribonucleic acid
dsDNA	Double-stranded DNA
E.coli	*Escherichia Coli*
EBV	Epstein-Barr virus
EGFR	Epidermal growth factor receptor
ESC	Epidermal stem cells
EV	*Epidermodysplasia verruciformis*
FACS	Flow cytometry

Fas-l	FAS-ligand
GAPDH	Glyceraldehyde 3-phosphate dehydrogenase
HF	Hair follicles
HIV	Human immunodeficiency virus
HPV	Human papillomavirus
HSPG	Heparan sulfate proteoglycans
HSV-1	Herpes simplex virus 1
IFE	Interfollicular epidermis
IFN-γ	Interferon-γ
IL	Interleukin
K14	Cytokeratin 14
K15	Cytokeratin 15
Kb	Kilobase pairs
KDa	Kilo Dalton
KSFM	Keratinocyte-SFM
LCM	Laser capture microdissection
LCR	Long control region
LE6	Long Early protein 6
Lgr-5	Leucine-rich G-protein-coupled receptor 5
MHC	Major histocompatibility complex
mL	Millilitre
mM	Millimolar
MmuPV1	*Mus Musculus* papillomavirus 1
MnPV	*Mastomys Natalensis* papillomavirus
mTOR	mammalian target of rapamycin
muHPV	Mucosotropic human PV
NFATc1	Nuclear factor of activated T cells c1
nm	Nanometres
NMSC	Non-melanoma skin cancer
nt	Nucleotide
NZW	New Zealand white
ORF	Open reading frame
ori	*Origin of replication*

OTR	Organ transplant recipient
p.i.	Post-infection
PBMC	Peripheral blood mononuclear cells
PBS	Phosphate buffered saline
PCR	Polymerase chain reaction
PE	Early promoter
Pfr-1	Perforin-1
Poly-AE	Early polyadenylation
Poly-AL	Late polyadenylation
pRb	Tumor suppressor retinoblastoma protein
PV	Papillomavirus
RCA	Rolling circle amplification
RNA	Ribonucleic acid
RNase	Ribonuclease
ROPV	Rabbit oral papillomavirus
ROS	Reactive oxygen species
rpm	Revolutions per minute
RRT	Renal transplant recipients
RT-qPCR	Rea-time quantitative PCR
SA	Splice acceptor
SD	Splice donor
SDS	Sodium dodecyl sulphate
SE6	Short Early protein 6
sec	second
sfPV1	Sylvilagus floridanus Papillomavirus 1
SG	Sebaceous gland
SGR	Specific growth rate
SRL	Sirolimus
SSC	Squamous cell carcinoma
TGF-β	Transforming growth factor β
TGN	Trans-Golgi network
TPA	12-O-Tetradecanoylphorbol-13-acetate
TLC	T lymphocytes

TNF-α	Tumor necrosis factor α
URR	Upstream regulatory region
UTR	Untranslated region
UV	Ultraviolet
V	Volume
wt	Wild type
WST-1	Water-soluble tetrazolium-1

1 INTRODUCTION

1.1 Papillomavirus (PV)

PVs comprise a diverse group of viruses that establish infections in the mucous membranes and cutaneous epithelia (1). PVs are highly host specific and have been discovered in a wide range of vertebrates such as humans, bats, birds and reptile species (2, 3). To date, more than 240 distinct PV types in 49 *genera* have been characterized at the nucleotide level (**FIG 1.1**), of these over 170 belong to Human papillomavirus (HPV) types, which are divided into five species: *Alpha*, *Beta*, *Gamma, Mu* and *Nu* (4-6). Mucosotropic human PVs (muHPVs) that belong to the *Alpha* HPV species can be further divided into high-risk types and low-risk types according to their potential of causing cancer in humans. At least 13 high-risk muHPVs types (16, 18, 31, 33, 35, 39, 45, 51, 52, 56, 58, 59 and 68) have a high risk of causing cancer in humans (7, 8). Low-risk muHPV types, such as HPV 6 and 11 can cause benign tumors (9, 10). Cutaneous HPVs (cuHPVs) represented by the species of *Beta*, *Alpha* species 4, *Gamma* species 1 to 5, *Mu* and *Nu* are commonly found in the healthy skin of the general population (10-12) and have been found to cause skin lesions such as benign skin warts, actinic keratosis (AK), keratoacanthomas, and be associated with non-melanoma skin cancer (NMSC) (13-15). The role of oncogenic muHPVs in the development of cancer is fully recognized. However, the role of cuHPVs in skin carcinogenesis has not yet been elucidated.

PVs are circular dsDNA genomes with sizes close to 8 kb and replicate within the nuclei of host cells. Viral genomes contain approximately 8 open reading frames (ORFs), which are located on one DNA strand of the viral genome (1). These ORFs encode PV early genes (E1, E2, E4, E5, E6 and E7), late genes (L1, L2), as well as a non-coding region called the upstream regulatory region (URR). Briefly, the regulatory genes E1 and E2 modulate transcription and replication of the viral genome, the three oncogenes E5, E6, and E7 modulate the transformation process of host cells, and the two structural genes L1 and L2 compose the viral capsid (16, 17). Although there are many similarities in between the PV genomes organization (5), there are differences in term of gene expression patterns. For instance, gamma

species 6 HPVs (HPV101, 103 and 108) lack an E6 gene (18, 19), and most cuHPVs do not encode E5 protein (20).

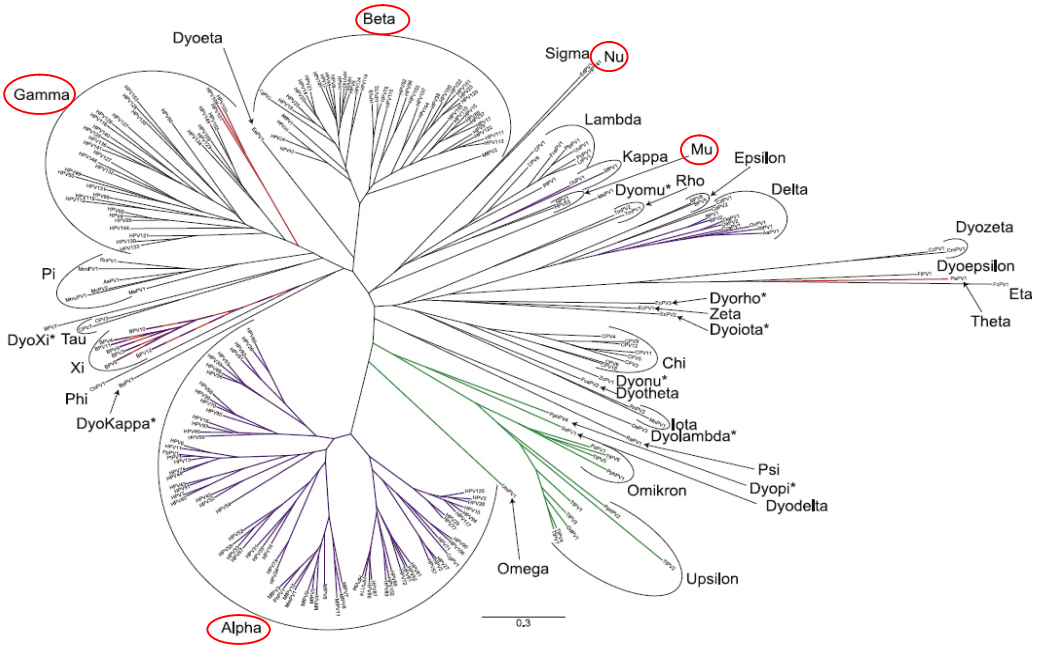

FIG 1.1 Papillomavirus phylogenetic tree. The DNA sequence coding for E1, E2, L1 and L2 for all 241 papillomaviruses were used for construction of the phylogenetic tree. (Adapted from Van Doorslaer, *et al* 2013).

PV virions are non-enveloped particles, about 55nm in diameter. Their outer shell contains 72 pentamers of the major capsid protein L1 situated at the vertices of a T = 7 dextro icosahedral lattice (21). The features of papilloma virions are conserved despite significant differences in amino acid sequences of L1 (22) (**FIG 1.2**).

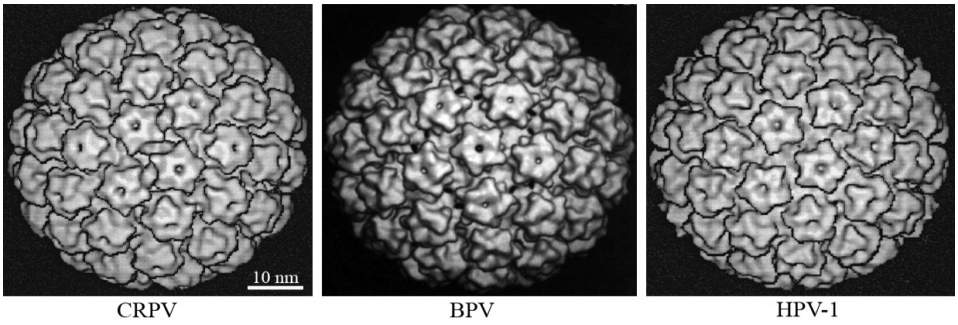

FIG 1.2 Papilloma virions. CRPV: Cottontail rabbit papillomavirus; BPV: Bos taurus papillomaviruses, also known as bovine papillomaviruses; HPV1: Human papillomavirus 1 (Adapted from Trus, *et al*. 1997 & Belnap, *et al*.1997).

1.2 The life cycle of PVs

1.2.1 Attachment, entry, uncoating and intracellular trafficking

PVs infect the undifferentiated basal cells of the stratified epithelium only when wounds or abrasions allow the virus to penetrate the physical barrier of the upper skin layers. The infectious entry of PV particles into basal cells occurs via the "micropinocytosis" pathway, which requires receptor signaling and actin cytoskeleton rearrangement (23). The viral major capsid L1 protein mediates initial binding to heparan sulfate proteoglycans (HSPG) within the basement membrane. This binding process induces exposure of the hidden amino terminal portion of the viral minor capsid L2 protein, which is facilitated by the host cell chaperone cyclophilin B (24-26). The exposed L2 is subsequently cleaved by a furin convertase. These processes result in a loss of affinity to the primary attachment receptor and a transfer to an elusive second receptor that probably resides in or is associated with the tetraspanin-enriched microdomains (26). However, the complete early process of PV remains poorly understood at the molecular level.

The infectious entry of PVs into basal cells occurs via a clathrin and caveolin independent endocytic pathway. The tetraspanin CD151 is essential for PVs endocytosis (23). Internalized PV virions initially reside in smooth endocytic vesicles. The uncoating of PV virions is triggered by acidification of the endocytic vesicles followed by cyclophilin-mediated dissociation of the majority of L1 proteins from the viral genome (27). For intracellular trafficking, the viral DNA along with L2 is retrogradely transported by the retromer complex and Rab GTPases via microtubules to the trans-Golgi network (TGN) (26).

1.2.2 Viral transcription, replication, transformation and release

The transcription of PVs is regulated by viral transcription and cellular factors, and viral promoters, cellular differential RNA splicing, transcription termination signals etc. One of the major regulators of PV's transcription is the viral early protein E2, which activates or represses transcriptional processes, depending on the binding of E2 to the context of the E2 binding sites (E2BS) in relation to the early viral promoter during viral life cycle (28). One well-known cellular interactor of E2 is the Bromodomain-containing protein 4 (Brd4) which recruits cellular transcription factors

and chromatin regulators to control transcription (29). The binding of Brd4 to E2 stabilizes E2, regulates E2-mediated transcription, as well as anchors E2 and viral genomes to the host chromosome during mitosis (28, 30). PVs initiate transcription via two major viral promoters, the early promoter (PE) and late promoter (PL). The regulation of PV's gene expression is tightly controlled by the differentiation of epithelia cells. In the early stage, transcription from viral PE generates mRNAs encoding the early genes (E1, E2, E4, E5, E6 and E7), whereas at the late stage, the terminal differentiation of the host cells downregulates the activity of PE, resulting in the activation of the viral PL to express late genes (L1 and L2) (24).

The replication of PVs' genomes is mainly controlled by the interaction of E2 with the viral helicase protein E1. E2 forms heteromers with E1 to stimulate initiation of viral replication. The binding of viral E1/E2 complex to the viral origin of replication (*ori*) within the URR recruits the cellular DNA polymerase to the episomal viral genome for the replication (31, 32). E1 unwinds viral DNA and attracts replication proteins to proceed the replication bi-directionally. Initially, the viral genome replicates at low levels in the basal cells (33). For viral episomal maintenance during persistent infection, PVs control their copy number via E2 and E8^E2 (former name E8^E2C) repressor proteins. E2 repressor proteins only retain the carboxy-terminal domain that mediates dimerization of E2 proteins and viral DNA recognition. The E8^E2 protein consists of the small E8 peptide fused to the C terminus of E2, which is an important negative regulator during viral life cycle (34).

As the infected cells differentiate towards the upper layer of the epithelium, the host cell downregulates the expression of cellular factors that are essential for viral DNA replication (28). This downregulation is counteracted by the viral oncoprotein E7, which binds to the tumor suppressor retinoblastoma protein (pRb) releasing E2F transcription factors to restore the expression of DNA replication factors in the infected cell. Another consequence of a high-level E7 is an induction of the tumor suppressor protein p53 (35), which is targeted by most of the alpha HPV E6 for proteasomal degradation. In addition, the protein E5 localizes to the membrane of the infected cell, where it binds to epidermal growth factor receptor (EGFR) and causes receptor dimerization. This results in the transmission of mitogenic signals to the nucleus, thus stimulating cell growth (36). With the help of E1 and E2, the

oncoproteins E5, E6, and E7 create a suitable environment that promotes efficient viral replication. However, it has being shown that the accumulation of E1 proteins in the cell nucleus triggers a DNA damage response and causes cell arrest in S-phase (33), whereas high levels of E2 can inhibit the early promoter and downregulate the expression of the growth-promoting oncoprotein E6 and E7, which lead to the differentiation of the infected cell in response to cellular signals (28). Induction of the late genes L1 and L2 is delayed until the host cell becomes terminally differentiated and E2 no longer represses the promoter PL, resulting in the production of progeny virions in the superficial layer of the epithelium. Finally, the viral protein E4, which has been shown to cause a collapse of the cellular intermediate filament network, might aid the release of virions (37).

In the past few decades, studies have been mainly focused on the lifecycle of muHPVs, especially the high-risk types such as HPV 16 and 18. However, cuHPVs have been less studied compared to muHPVs. Most cuHPVs express E6 and E7 gene products that are structurally similar to those of the muHPVs but their genomes do not encode E5 protein (20). The E5 protein plays a role in the productive phase of the viral lifecycle and stimulates mitogenic signals of growth factors in most muHPVs (36). However, it is yet unclear what the consequences on the lifecycle are for cuHPVs lacking E5 (38). In addition, E6 proteins of cuHPVs such as cuHPV 1 and 8 neither bind to p53 or E6 associated protein (E6-AP) (39). E7 proteins of cuHPVs such as type 5 and 8 showed lower binding affiliate to pRb compared to HPV16 E7 (40). The E6 or E7 protein of cuHPV 1 and 8 showed no true immortalizing activities in primary human keratinocytes (41), but E6 and E7 of cuHPV 38 were shown to immortalize primary human keratinocytes (42). Instead of directly binding to p53, the cuHPV 5, 8, and 38 E6 interact with the histone acetyltransferase p300 and block p53-mediated apoptosis, which suggests a role in skin carcinogenesis (43, 44). E6 protein of cuHPV 5, 8, 20, 22, 38, 76, 92, and 96 has also been shown to degrade Bak protein - a pro-apoptotic effector expressed in human epidermal keratinocytes, and protect UV-treated keratinocytes from apoptosis *in vitro* (45).

1.3 CuHPV and Non-melanoma skin cancer (NMSC)

CuHPVs induced skin warts are benign, often regress spontaneously. Skin warts differ in clinical morphology and histological appearance, which include common

warts (cuHPV 2, 4, 7 and 57), deep plantar and palmar, myrmecial warts (cuHPV 1), plane warts (cuHPV 3, 10 and 41), intermediate warts (cuHPV 26, 27, 28 and 29) and cystic or punctate, mainly plantar warts (cuHPV 60, 63 and 65) (46).

It has been implicated that some cuHPV infections are associated with the etiology of NMSC, other than the well-known factors such as cumulative sun exposure, age, gender, fair skin type, and immunosuppression (47). NMSC is more common than lung, breast, prostate, and colon cancer combined, and its rate is increasing by 4 - 8% each year (48). The most common types of NMSC are basal cell carcinoma (BCC) and squamous cell carcinoma (SCC) which account for approximately 80% and 16%of all skin cancers, respectively. SCC and BCC are both derived from the basal layer of the epidermis of the skin, but SCCs can be highly invasive and metastasize, whereas BCCs are slow growing and rarely metastasize (49).

1.3.1 *Epidermodysplasia Verruciformis* (EV)

The first evidence that cuHPV infection associated with SCC has been found in patients with the rare genetically determined condition EVs (50). EV is a heritable disease, which is characterized by an abnormal susceptibility to specific types of HPV infection, namely EV-HPV (now classified β-HPV) which include HPV types 5, 8, 9, 12, 14, 15, 17, 19-25, 36, 38 and 47 (15, 51). In early childhood, EV patients have a propensity to develop warts and characteristic macular lesions on the face, dorsa of the hands, and legs, which usually persist throughout lifetime (15, 52). In approximately 30 – 60% of the cases lesions progress to SCC at sun-exposed body sites, more than 25 – 30 years after their onset (52, 53). All EV individuals share at least 7 mutations in the EVER1 gene and 5 mutations in EVER2 gene, which are involved in ion transportation and signal transduction (54-56). A Defect of these two genes in EV patients appears to specifically enhance susceptibility to EV-HPV infections (55). However, the exact role of the EVER genes in the pathogenesis of EV-HPV infection has not been clearly elucidated (38, 55). It is also likely that immunogenic and environmental factors, particularly UV light radiation, are important for EV-HPV infections in EV individuals, due to partial defects in cell-mediated immunity, such as inhibition of natural killer cell activity and of cytotoxic T cells (57, 58).

1.3.2 Organ Transplant Recipients (OTRs)

SCC is a most common skin cancer in OTRs, occurring 60 to 250 times more frequent than in the general population (59). A diverse group of cuHPV DNAs has been frequently detected in SCC lesions raising the question of a possible role of the viruses in skin carcinogenesis (51, 60, 61). The incidence of cuHPV related warts in renal transplant recipients (RTRs) steadily increases over the years post-transplantation and these lesions are refractory to most therapeutic strategies (59, 62). RTRs have a 200 fold increased incidence of SCCs, which arise on sun-exposed areas (60). The presence of cuHPV DNA in SCCs of OTRs suggests parallels to EV patients in terms of the association between HPV infection and skin cancer. However, notable differences between these two types of patients include: In OTRs, 1) multiple cuHPV types can frequently be found in the SCCs of OTRs instead of one single predominant type. 2) the viral DNA loads in SCCs are very low, more than five log fold lower compared to the warts associated with HPV infection (61, 63). 3) no viral transcripts could be found in the SCCs (64, 65). To date, although cuHPV types can induce various skin lesions, their role in the pathogenesis of SCCs remains controversial.

1.3.3 UV radiation and cuHPV infection

Solar UV light is composed of three classes: UVA (320–400 nm), UVB (280–320 nm), and UVC (200–280 nm). It is well known that UV radiation plays a significant etiological role in NMSC development, primarily due to the DNA-damaging properties of UVB (66, 67). UVB light has long been implicated as an important risk factor for the development of cuHPV associated cutaneous carcinomas in immunosuppressed OTRs (68) and in the non-immunosuppressed general population (69), as most lesions appear in sun-exposed body sites versus sun-protected sites (13, 68). It has been shown by several studies that cuHPV E6 can increase the tolerance of cells to UVB radiation via targeting and abrogating Bak function to impair the cellular apoptosis signaling to DNA damage response (DDR) (45, 58, 70). Moreover, the ataxia-telangiectasia-mutated (ATM) and ataxia telangiectasia and Rad3-related (ATR) kinase that is involved in UV-induced DDR is also inhibited by cuHPV 5, 8 E6 (70, 71).

Beyond modulating of the cellular DDR, UVB has also been shown to play a key role in inhibiting cell-mediated immune response both in short-term and long-term (72, 73), and reducing T-cell sub-population in the skin (74). The decreased immune surveillance might therefore help to drive PV-induced disease. Recently, Uberoi, et al., have shown that UVB-induced immunosuppression increases the susceptibility of *Mus Musculus* papillomavirus 1 (MmuPV1) infection in immunocompetent mice (75).

1.3.4 Epidermal stem cells (ESC) and cuHPV infection

The epidermis forms the outer layer of the adult skin, which comprises a multi-layered epithelium, the interfollicular epidermis (IFE), hair follicles (HFs) and sebaceous glands (SGs) (76). ESCs residing in the epidermis and HFs ensure adult skin homeostasis, hair regeneration and the repair of the epidermis after injuries (77). In the viral life cycle, it is known that PVs establish infections in the basal layer of the epidermis. Considering the transit time of cells through the differentiation program of the epidermis from the basal layers to being shed, PVs must reside in cells that are retained for long periods in the epidermis. Whether PV infects and is maintained in ESCs, or confers stem cell-like properties to more differentiated cells, is currently unknown (15). Cells in the HF stem compartment were regarded as the primary target (78) and the natural reservoir of cutaneous PVs (61). The cuHPV DNA has been frequently detected in plucked eyebrow hairs, which contain cells of the HF stem cell niche, although the exact target cells of the cuHPV was not determined (79, 80). It is possible that cuHPV may increase the self-renewal capacity of ESCs, which may lead to the generation of cancer stem cells driving NMSC development. A better understanding of the effects of cuHPV on ESCs may be beneficial for disease management and treatment in the future (15).

1.4 PV latent infection

Viral latency is defined as “a reversible state in which the viral genome is present in a cell without production of infectious virus particles” (81). Although many viruses are capable of asymptomatic infections, only a few are known to undergo truly latent infection. To qualify as viral latency, infections must display persistence and reactivation. Infection by herpesvirus species such as Herpes simplex virus 1 (HSV-1; α-herpesvirus), cytomegalovirus (β-herpesvirus), Varicella virus (α-herpesvirus)

and Epstein-Barr virus (EBV; γ-herpesvirus) leads to a lifelong latent infection (82). It is believed that similar to these latent viruses, PVs can also establish latent infections (32, 83, 84).

At present, the ability of PVs to establish latent infection is still controversial (84). Although no direct evidence for a solely latent HPV infection has been found, a number of clinical observations and studies in animal models suggest that it may occur.

1.4.1 Clinical evidence for HPV latency

1.4.1.1 Immunocompromised patient

Human immunodeficiency virus (HIV) infected patients have a higher incidence of cervical HPV infection than HIV-negative patients (85). Studies have shown that women with a historic infection of high-risk HPV might be at risk of reactivation of viral infection even in the absence of sexual activity, and the risk is higher in individuals with HIV infection (86, 87). An increased reactivation of latent cervical HPV infection has been shown to be associated with a reduction in peripheral blood $CD4^+$ cell counts suggesting that a reduction in cell-mediated immunity is important in permitting persistence of such infection (87).

There is also evidence that OTRs undergoing iatrogenic immunosuppression to prevent rejection of transplanted organs are at greater risk for cuHPV infections. In general, cuHPV DNAs were detected in plucked eyebrow hairs (68, 88, 89) and on clinically normal skin (12, 90, 91), where they predominantly induce asymptomatic infections in immunocompetent individuals. However, beta-HPVs have more frequently been found predominantly with higher viral loads in immunosuppressed OTRs (68, 92, 93).

1.4.1.2 Recurrent respiratory papillomatosis (RRP)

RRP, also known as laryngeal papillomatosis, is characterized by exophytic, wart-like lesions of the upper airway that tend to recur and have the potential to spread throughout the respiratory tract (94). Lesions of this disease are caused by infection with low-risk muHPV type 6 or 11. Despite the removal of infected tissues by laser treatments, papillomas constantly and rapidly recur. It is thought that recurrent lesions are caused by reactivation of HPV infection in a latent state with subsequent

spreading of infectious virions (95). This is supported by the frequent detection of HPV type 6 or 11 DNA in biopsy samples taken from non-diseased regions of the respiratory tract of RRP patients (96, 97).

1.4.1.3 Recurrent genital papillomas

Genital warts are the most common venereal disease, which are mainly caused by infection with low-risk muHPV type 6 or 11 (98). The infection is considered to have a high rate of transmission with lesions arising within two or three months of infection that mostly spontaneously regress. Treatments of these lesions include surgery cryotherapy, anti-proliferative agents and topical immunomodulatory agents. However, recurrence rates of 25% within three months are reported and can be as high as 67% despite treatment being given (99). Recurrences of genital warts are typically seen at sites of previous infection suggesting that HPV can persist in long-lived cells at these sites in the absence of clinical signs of disease with subsequent reactivation leading to re-emergence of lesions (100).

1.4.1.4 Latent infection of the cervix

There is growing evidence from recent studies that some cervical HPV infections may be present in a latent state. Most notable is the detection of HPV DNA at low copy number in histologically normal cervical epithelial cells (101). Analysis of HPV DNA was performed on tissue sections taken from histologically normal tissue adjacent to cervical lesions. Highly sensitive laser capture micro-dissection (LCM) and real-time PCR techniques were used for analysis. It was found that the determined viral DNA copy numbers were indicative of infections of single cells or small groups of cells harboring low levels of viral DNA among hundreds of cells analyzed. It is possible a representation of latent phase (84, 102).

1.4.2 Animal models of PV latent infection

Animal PV models are essential in order to study the pathogenesis of PV infections and to develop strategies for treatment and prevention. Animal models have been used to study latent PV infection.

1.4.2.1 Latency of Rabbit oral papillomavirus (ROPV)

ROPV is a naturally occurring virus infecting mucosal tissues of domestic rabbits (103). Typically, infection of ROPV induces papillomas on the underside of the tongue, which regress spontaneously in 100% whitin to 8 weeks p.i. (104). However, the immune-mediated regression does not result in completely clearance of viral infections. Maglennon *et al*., (105) have shown that a low copy number of ROPV DNAs (1 copy/ 10,000 GAPDH) were still detectable up to 52 weeks p.i.. Using LCM they were able to determine that cells harboring persistent viral DNAs were only retained in the basal layer of epithelium. In addition, Maglennon *et al*., (106) have further demonstrated that systematic immunosuppression using cyclosporin A (CsA) and Dexamethasone (Dex) led to the elevation of viral copy numbers in a minority of the infected sites and subsequent formation of only one papilloma. They believed that activated T-cells accumulate within and beneath the lesion, which may lead to the suppression of latent viral infection, but the balance can be affected by factors such as immunosuppression and allow reactivation to occur with the possible reappearance of visible papillomas (32, 83). So far no convincing data are available on the reappearance upon immunosuppression.

1.4.2.2 Latency of Cottontail rabbit papillomavirus (CRPV)

CRPV infection of New Zealand White (NZW) rabbits is the only small animal model that enables the study of PV infection and disease, including malignant progression (107, 108). This animal model was the first proposed *in vivo* model system for latent PV infection (109, 110). It has been shown that inoculation of domestic rabbit skin with a low-titer virus leads to asymptomatic infection. CRPV DNA can be detected at the asymptomatic sites 18 weeks post-infection (109). Further irritation of these sites with a photosensitizer resulted in subsequent papilloma formation at some sites (109). Moreover, irritation of asymptomatic infected sites with UV light during the incubation period led to an increase expression of E6 and E7 gene as early as one week after irradiation and subsequently papillomas formation at 26% of all irritated sites. However, attempts to activate infections that remained latent by repeating UV irradiation at the end of the three months observation period were unsuccessful (110).

In addition, our group earlier analyzed skin tissue from CRPV infected rabbits following immune-mediated regression of papillomas (111). We found that viral DNA and mRNA encoding early viral proteins were detectable during the regression of papillomas by *in situ* hybridization, but were not detectable using these methods after full regression. However, using more sensitive PCR methods, it was possible to detect viral DNA as late as 17 months after regression. Analysis of viral DNA copy numbers showed that papillomas contained about 7.5 copies per cell whereas regressed sites contained one copy per 40 - 1000 cells (111).

1.4.2.3 Latency of Bovine papillomavirus 2 (BPV2)

BPV2 induces classical skin warts and was originally isolated from the neck and shoulder of a British cattle (112). It has been shown that the virus was also involved in bladder cancer in cattle (113). The infection of BPV2 was frequently found latent in the healthy skin and in the bladder. Campo *et al*., (113) has shown that latent BPV2 could be activated by immunosuppressive treatment -either by feeding bracken fern or by azathioprine treatment, as in the bladder and skin(114).

1.4.2.4 Latency of *Mastomys natalensis* papillomavirus (MnPV)

MnPV was first isolated from adult animals of the inbred line “GRA Giessen” of *Mastomys natalensis* that is a common rodent in South Africa (115). MnPV induces keratoacanthomas and papillomas of the animal skin, in an age-dependent manner (116). Persistent infections of MnPV lead to stomach cancer in 28 – 53% of animals older than one year (117). The inbred *Mastomys* colony (Heidelberg colony) is free from malignances, and was found to retain endogenous latent MnPVs (116). Tumors never appeared in the inbred animals under one year of age, but 80% of the animals developed tumors around 16 months of age (116). Treatment of the latently infected skin with TPA, a tumor-promoting molecule drug, dramatically increased latent viral DNA copy numbers (100 fold) and tumor formations (118).

1.4.2.5 Latency of *Mus Musculus* papillomavirus 1 (MmuPV1) model

MmuPV1, also designated ‘‘MusPV1’, was first discovered in an inbred colony of NMRI-*Foxn1*^{nu}/*Foxn1*^{nu} (nude) laboratory mice by Ingle and colleagues (119). The infected nude mice spontaneously developed papillomas at the mucocutaneous junction of the nose and mouth (119). MmuPV1 virons isolated from papillomas also

showed the ability to infect mucosal tropism such as vaginal, cervical and anal (120). Most recent studies have shown that the infection of the MmuPV1 is species-specific to mouse strains (121). The depletion of CD3+ cells permits the virus efficiently to infect non-susceptible immunocompetent mice. However, neither the depletion of CD4+ nor CD8+ cells alone increased the susceptibility of MmuPV1 infections (121). Remarkably, Wang, *et al*., (122) showed that despite no appearance of papillomas in CD4+ or CD8+ depleted mice upon MmuPV1 infection, the viral DNA can still be detected up to 5 weeks p.i.. When anti-CD3 antibody was applied to the mice, papillomas significantly appeared only in the CD4+ depleted group (14/15) within ten weeks indicating a possible reactivation of latent infection from the asymptomatic site, but not in the CD8+ depleted group (1/15).

1.5 Introduction to CRPV model system

CRPV, also known as Shope rabbit papillomavirus or *Sylvilagus floridanus* Papillomavirus 1 (SfPV1), was the first PV to be identified in wild cottontail rabbits bearing large warts around the head and neck in 1933 (123). Early investigations demonstrated that CRPV could infect laboratory rabbits of various strains, such as NZW rabbits, as well as wild snowshoe rabbits and jack rabbits (124). Since then, the CRPV NZW rabbit model has been used extensively to study virological aspects of PV infections *in vivo*, virus-induced carcinogenesis, immunological features of virus infection leading to host immune-mediated regression, interactions between papillomas and cocarcinogens and viral gene function (124-126). One unique property of the CRPV model is that infections can be initiated using purified viral DNA (127). This property allows for the functional testing of viral mutants *in vivo* (128), which is why this model was widely used to explore the interaction between host and virus; and to develop vaccines against PV infections (107, 108, 129).

1.5.1 Molecular biology of CRPV

The CRPV genome is 7868 bp in size. It has a similar genome organization, expresses in similar differentiation-specific patterns in lesions, and encodes proteins with conserved sequence and function as other PVs (130).

1.5.1.1 Viral transcriptions

Like other PVs, the CRPV genome consists of early genes and late genes (**FIG 1.3**). To better reflect the expression pattern *in vivo*, as well as the organization of the CRPV genome, the genome can be divided into early genes (E1, E2, E4, E5, E6, E7, and E10) and late genes (L1 and L2). Unlike other PVs, mapping of viral transcripts from CRPV-induced tumors strongly suggests that two different E6 transcripts, long E6 (LE6) and short E6 (SE6), are produced. LE6 initiates at the first AUG, and SE6 is translated from a separate mRNA starting at the second AUG (131).

In the early stages of the CRPV life cycle, transcription from the early promoters (PE-1, PE-2, and PE-3) generate mRNAs encoding all early genes, which are polyadenylated at the early polyadenylation signal (Poly-AE) (FIG 1.3). These polycistronic viral mRNAs are subject to alternative splicing through the differential use of various early splice donors (SD) and splice acceptor (SA) sites. As the infected epithelial cell differentiates, the late promoter (PL) is activated. Expression from the PL bypasses E6 and E7 genes and induces expression of E1, E2C, E8^E2 (former name E9^E2C) and E1^E4 mRNAs. These mRNAs are also polyadenylated at Poly-AE. The E1 and E2 proteins bind to the origin of replication (*ori*), which is located in the URR of the CRPV viral genome. Terminal differentiation of the host cell downregulates the activity of Poly-AE resulting in a read-through into the late region of the genome, encoding L1 and L2 protein, followed by polyadenylation at late Poly-A (Poly-AL) to generate L2 and L1 mRNAs (24, 132-134).

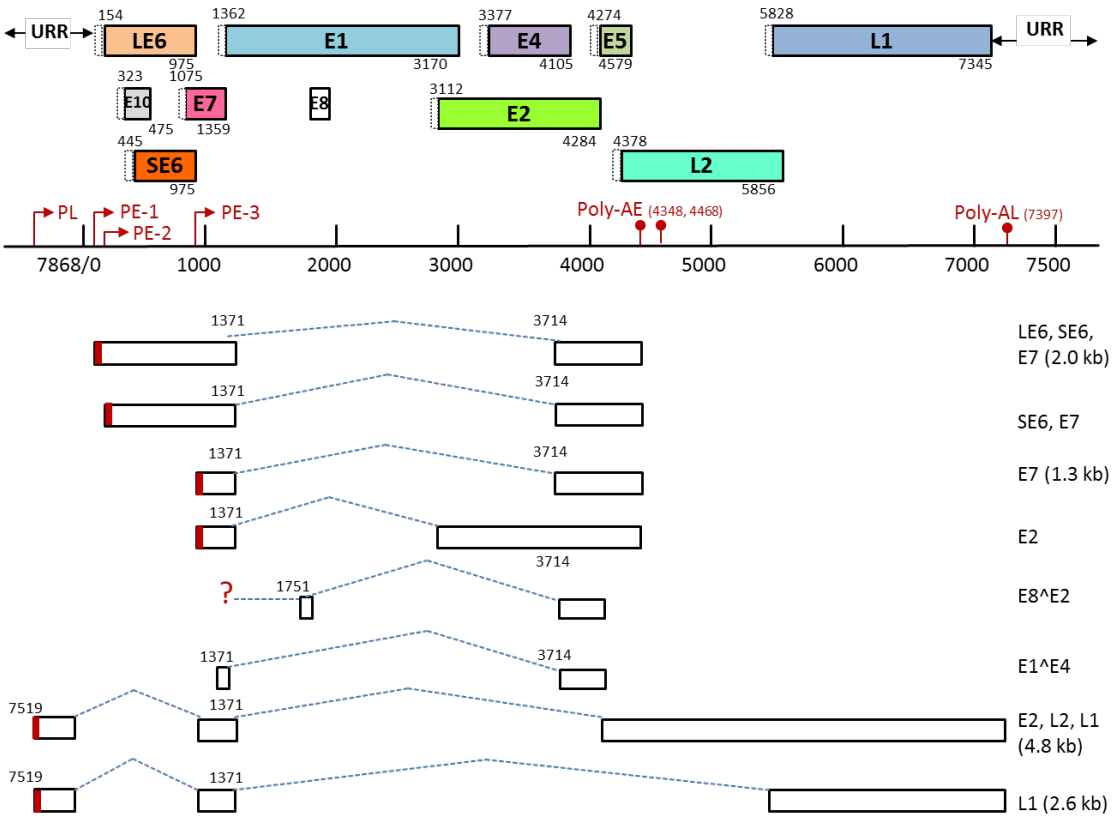

FIG 1.3 CRPV genome and representative mRNAs. A, distribution of the open reading frames on CRPV genome. B, each mRNA represents the likeliest candidate mRNA for production of the corresponding proteins. (Adapted from Wettstein, *et a*l.,1983, 1987; Nasseri, *et al*., 1984; Georges, *et al*., 1984; Danos, *et al*., 1985; Zeltner, *et al*., 1994)

1.5.1.2 Viral proteins

The CRPV genome encodes two E6 oncoproteins, LE6 and SE6 (135, 136). The LE6 protein is 39 kDa and predominantly present in the nucleus in which it appears to be associated with the nuclear matrix, with minor portions present in the cytoplasm and the membrane fraction. Unlike LE6, the 24 kDa SE6 is a soluble cytoplasmic protein phosphorylated at serine residues (135). Both E6 proteins contain Cys-X-X-Cys zinc-binding motifs and are able to block p53 mediated apoptosis via binding to p300 for cellular immortalization and tumorigenesis (43, 132).

The 14 kDa CRPV E7 oncoprotein is 56% identical to the HPV16 E7 protein and, like its human counterpart, can transform established cell lines, bind pRB, disrupt pRB-E2F complexes (41, 137-139).

The CRPV E10 gene (former name E8) encodes 51 amino acids and CRPV E5 genome encodes 101 amino acids (130). Both are able to stimulate rodent fibroblast proliferation, promote cell cycle transition, and induce anchorage-independent growth and that CRPV E10 and E5 transfected C127 cells were weak tumorigenic in nude mice (140). Other studies showed that CRPV E10 provides an essential function in papilloma formation and growth, most likely by promoting stem cell proliferation (141). However, unlike its human counterpart, the CRPV E5 located downstream from poly AE is dispensable for the viral infection in domestic rabbits (142, 143).

The 68 kDa CRPV E1 protein is an ATP-dependent DNA helicase and is essential for viral genome replication and amplification. However, there are still some controversies in regarding to whether E1 is required to maintain the viral episomal DNA in undifferentiated cells (33).

The 49 kDa CRPV E2 protein consists of an N-terminal domain and a C-terminal domain which is connected by a flexible hinge region. The C-terminal domain of E2 is responsible for the binding to the specific sequences - ACCN6GGT located within the URR of the viral genomes, whereas the N-terminal domain is involved in viral transcription activity (28). The CRPV E2 protein stimulates both viral DNA replication and transcription. The transactivation domain in the N-terminal CRPV E2 protein is essential for induction of papillomas in NZW rabbits, which functionally depends on amino acids isoleucine at position I73 (I73) and arginine at position 37 (R37) (144). In addition to CRPV E2, the fusion protein CRPV E8^E2, which is a partial C-terminal E2 protein fused to a short stretch of protein derived from the small E8 open reading frame was shown to be a repressor of viral promoters (134). CRPV E8^E2 represses the E1/E2 dependent replication of the CRPV genome origin and counteracts the transactivation effect of the full-length E2 on minimal promoters containing several E2BS. However, mutated CRPV E8^E2 within the whole virus genome showed no phenotype during tumor induction in NZW rabbit models (134).

The CRPV E4 protein is produced in the late stage of the viral life cycle. It was shown not to be required for papilloma development and extrachromosomal viral DNA status. The expression and the amplification of the E4 protein correlated with the expression of the L1 protein and were detected in the more differentiated epithelium layers (37, 145).

1.5.1.3 State of CRPV DNA

The rabbit papillomas, primary carcinomas, and metastatic carcinomas caused by CRPV in domestic rabbits contain 10 to about 100 copies of the CRPV viral genome per diploid cell equivalent of DNA. In its natural host cottontail rabbits, the viral gene copy number of papillomas is higher, ranging from 1,000 to 10,000 copies (146). The average number of viral gene copies per neoplastic cell decreases dramatically to less than 100 copies per cell as cottontail papilloma progress to carcinoma (147). In papillomas, most viral DNA is maintained as nicked or supercoiled episome DNA (147-149). The situation can be different in carcinomas. Most of the viral DNA was maintained in form of extrachromosomal multiple head-to-tail DNA, and a minority of tumors contained a fraction of integrated viral DNA (149). Thus, the transplantable VX2 and VX7 carcinomas of domestic rabbits were found to contain only integrated DNA with 10 - 40 or 100 - 400 CRPV copies per cell (150).

CRPV DNA methylation between rabbit papillomas and carcinomas is different. In cottontail rabbit papillomas, CRPV DNA was not methylated and the degree of methylation increased from domestic rabbit papillomas to carcinomas and was very high in the transplantable VX2 carcinoma (126, 151). The most methylated genes were located in the late region and E2 of the CRPV genome (126).

1.5.2 Immune response and regression

Neutralizing antibodies had been found to recognize both capsid proteins, CRPV L1 and L2 (152, 153). Antibody response to the L1 protein was detected in essentially all rabbits with papillomas 4 to 6 months after infection. An antibody response to the L2 minor protein was detected only in some rabbits. A limited immune response to the early protein E1, E2, E6, and E7 was only detected in a fraction of the animals, and no specific response was found for E4 and E5 protein (152, 154). The response to E6 and E7 peaked around 7 months and decreased thereafter. In contrast, that to E1 and E2 remained high after an initial raise. A much higher response to the E2 protein was observed in regressor rabbits (111, 154).

Spontaneous regression of PV-induced papillomas in humans and cottontail rabbits is relatively common. However, the regression of CRPV induced papillomas in domestic rabbits is rare. If it happens, most regressions occur within 30 to 60 days post infection, but some begin as late as 90 days. Once initiated, the regression

proceeds at a steady pace and is complete within 1 - 2 weeks. However, when papillomas reach a certain size, there is a much lower chance for spontaneous regressions to occur (155). It has been shown that the papilloma regression process was associated with infiltration of leucocytes (156), most notably of $CD8^+$ cells (111); and an immune response to the CRPV E2 protein (154).

During regression, expression of the early genes E6 and E7 remains at levels comparable to those in persisting papillomas. After complete regression, viral transcripts are no longer detectable, but surprisingly regression does not result in the elimination of all cells which harbor viral DNA. The viral DNA was maintained extrachromosomally in the cells after regression and persisted in on case in a latent stage for prolonged periods for 17 months (111).

In a former study, Hu *et al* (157) have shown that administration of the immunosuppression drug CsA could prevent the regression of cutaneous papillomas induced by CRPV. They also demonstrated the ability of CsA to cause a reduction in CD4+ and CD8+ stained peripheral blood leukocytes.

1.6 Study objectives

In summary, cuHPV infections are highly prevalent and tend to persist in the skin of the general population (11, 90, 91, 158). The presence of beta-HPV infections has been suspected to be involved in the development of NMSC, besides well-known risk factors, such as immunosuppression and UV radiation (38, 63, 93, 159). The ability of PVs to persist in their host in the absence of causing overt disease, i.e latency, has long been suspected (83). Several lines of clinical evidence support the hypothesis that PVs can establish latent infections such as HIV individuals with high rate of multiple infections to specific types of HPVs; and OTRs with a high prevalence of cuHPV associated infections especially in sun-exposed body sites. In addition, drug-induced immunosuppression and UV light radiation have been implicated as contributing factors for the reactivation of latent PVs infections. In animal model systems, systematic immunosuppression has been shown to play a role in PVs latent infection caused by ROPV, BPV2 or MmuPV1 (106, 122). UV radiation may also contribute to PVs latent infection as shown in the CRPV animal model (109, 110). Cutaneous infection of NZW rabbits with CRPV represents a tractable animal model

that enables *in vivo* investigation of cuHPV infection. The objective of this study was to employ the CRPV/rabbit model to investigate whether the latent cuHPVs infection is controlled by the immune system and/or UV-mediated radiation.

2 MATERIALS AND METHODS

2.1 Materials

2.1.1 Animals and viral DNA

Animals: Three weeks old out-bred female New Zealand White (NZW) rabbits were purchased from Charles River, Kisslegg, Germany.

Viral DNA: The recombinant CRPV genome pLAII-CRPV was used in this project. The 7.8 kb CRPV genome has been inserted into the SalI site of pLAII vector resulting 11.3 kb pLAII-CRPV. This construct has been shown to induce papillomas on NZW rabbits (107, 160).

2.1.2 Equipment

Application	Name	Supplier	Location
Real-time PCR	LightCycler® 480 system	Roche Applied Science	Penzberg, Germany
Gene-Gun	Helios Gene Gun	BIO-RAD	Munich, Germany
	Tubing Prep Station		
	Tubing Cutter		
	Tefzel® tube		
Sonification	SONOPLUS	Bandelin electronic	Berlin, Germany
	Sonifier® S-250A	Branson	Dietzenbach, Germany
PCR-Machine	PTC-0200 DNA Engine Cycler	BIO-RAD	Munich, Germany
Electrophoresis chamber	Mini-Sub Cell GT	BIO-RAD	Munich, Germany
	Wide Mini-Sub GT		
Power Supply	PowerPac 200	BIO-RAD	Munich, Germany
Camera system	Gel Doc 2000	BIO-RAD	Munich, Germany
Incubator	CO_2 Incubator US AutoFlow (Nuaire)	NuAire, Inc	MN, USA
	Kelvitron T (Heraeus)	Thermo Fisher Scientific	MA, USA

	CO_2 Incubator C200	Labotect	Goettingen, Germany
Microscope	Axiovert 200 Inverted Microscopes	Carl Zeiss	Goettingen, Germany
	Leica DMIRB	Leica	Bensheim, Germany
Centrifuges	Centrifuge 5810R / 5804R	Eppendorf	Hamburg, Germany
	Centrifuge 5417R / 5417C		
	Thermomixer 5436		
Shaker	Certomat® IS	B. Braun Biotech	Goettingen, Germany
Vortexer	REAXtop	Heidolph Instruments	Schwabach Germany
	MR3001K		
Spectro-photometer	BioPhotometer	Eppendorf	Hamburg, Germany
	NanoDrop -1000 Spectrophotometer	Thermo Fisher Scientific	MA, USA
Tissue homogenization	T 18 digital ULTRA-TURRAX®	IKA	Leiden, Netherlands
UVB lamp	Vilber Lourmat lamps	VILBER LOURMAT	Eberhardzell, Germany
UVA lamp	Vilber Lourmat lamps		
UVX radiometer	Ultra-Violet Products, LLC	Ultra-Violet Products Ltd	CA, USA
ELISA reader	Cytation 3 Imaging Reader	BioTek® Instruments	VT, USA
Flow Cytometry	FACSCalibur	Becton Dickinson	Heidelberg, Germany

2.1.3 Accessories

Disposable culture dishes were purchased from Eppendorf, Falcon, Greiner and Nunc.

Accessories	Name	# Catalog	Supplier	Location
Real-time PCR plate	LightCycler® 480 Multiwell Plate 96, white	04729692001	Roche	Penzberg, Germany
	LightCycler® 480 sealing foil	04729757001		
Gold particle	Biolistic 1.0 µm Gold Microcarriers	1652263	RIO-RAD	Munich, Germany
Sandpaper	P030 180	8633000	Wolfcraft	

Sterile filter	0.22 µm	Pro04064	Millipore	Billerica, UK
	0.45 µm	Pro04065		
Cell Counter	Countess	C10227	Invitrogen	CA, USA

2.1.4 Chemicals

Chemicals were purchased from the following companies: BioRad, Biozym, Calbiochem, Fluka, Merck, Peqlab, Perkin-Elmer, Roche, Roth, and Sigma.

2.1.5 Medical drugs

Drug	Trade name	Supplier	Class of drug	Species, dose, and route
Ketamine	KETAMIN10% 100 mg/mL	Bela-Pharm, Vechta, Germany	Dissociative anesthetic	Rabbit: 10 – 25 mg/kg, s/c or im
Sedative	Sedator® 1 mg/mL	Eurovet Animal Health B.V. Bladel, Netherlands	Sedatives hypnotics	Rabbit: 0.05 – 0.1 mg/kg, s/c or im
Dexamethasone	Dexadreson® sodium, 2 mg/mL	Intervet Millsboro Germany	Steroid medication	Rabbit: 0.15 – 0.25 mg/kg, s/c
Cyclosporine A	Sandimmun® 50 mg/mL	Novartis Pharma Basel, Switzerland	Immunosuppressant medication	Rabbit: 7.5 – 15 mg/kg, s/c

Note: s/c, subcutaneous; im: intramuscular

2.1.6 Commercial kits

Application	Kit	# Catalog	Supplier	Location
Plasmid purification	EndoFree Plasmid Maxi Kit	12362	Qiagen	Hilden, Germany
	Plasmid Mini Kit	27106		
DNA extraction	QIAamp DNA Mini Kit	51306		
Gel Extraction Kit	QIAquick Gel Extraction Kit	28706		
RNA extraction	RNeasy Mini Kit	74106		
cDNA Synthesis	QuantiTect Reverse Transcription Kit	205313		
Gene cloning	Rapid DNA Ligation Kit	K1422	Thermo Fisher Scientific	MA, USA
	CloneJET PCR Cloning Kit	K123		
Real-time PCR	LightCycler® 480 SYBR Green I Master Mix	04887352001	Roche	Penzberg, Germany
	PrimeTime® Gene Expression Master Mix	1055772	Integrated DNA Technologies	Leuven, Belgium

Normal PCR	*GoTaq*® Green Master Mix	9PIM712	Promega	WI, USA
Transfection	FuGENE HD Transfection Reagent	E2311	Roche	Penzberg, Germany
Rolling circle amplification	Illustra empliPhi100 Amplification Kit	25640010	GE Healthcare	Milan, Italy
DNA methylation	EZ DNA Methylation™ Kit	D5001	Zymo Research	Freiburg, Germany
Cell proliferation	Cell Proliferation Reagent WST-1	11644807001	Roche	Penzberg, Germany

2.1.7 Enzymes

Application	Kit	# Catalog	Supplier	Location
Polymerases	Pyrobest™ DNA- polymerase	TBR005A	Takara Bio Inc.	Shiga, Japan
Restriction enzymes	SmaI	R0141S	New England Biolabs,	MA, USA
	DpnI	R0176S		
	PspGI	R0611S		

2.1.8 Antibodies

Primary antibodies

Antibody	Clone	Species	Dilution	Conjugation	#Catalog	Supplier /location
T-lymphocytes	KEN-5	Mouse	1:20	FITC	MCA800F	AbD Serotec /Puchheim, Germany
Rabbit CD4	KEN-4	Mouse	1:20	FITC	MCA799F	
Rabbit CD8	C7	Mouse	1:20	FITC	MCA1576F	
IgG1	N/A	Mouse	1:20	FITC	MCA928F	
IgG2a	N/A	Mouse	1:20	FITC	MCA929F	
Cytokeratin 15	LHK15	Mouse	1:50	No	sc-47697	Santa Cruz Biotechnology, Inc. /CA, USA

Note: N/A, not available.

Secondary antibodies

Antibody	Species	Conjugation	Dilution	#Catalog	Supplier /location
Anit-Mouse (green)	Goat anti-Mouse,	IRDye® 800. Odyssey Infrared Imaging	1:15000	925-32210	LI-COR® /NE, USA

2.1.9 Oligonucleotides

Name	Primer/ probe	Sequences (5′ - 3′)	Position	Target size	References
CRPV E6	Forward	CATGCGTTGTACAGTTTGCG	444-463	149 bp	Designed in this study
	Reverse	TCACCTTGGTCTGACAGTTTG	573-593		
	TaqMan probe	AAGAACTGCAATGACCCCTCCACT	548-571		
GAPDH	Forward	GGATTTGGCCGCATTGG	N/A	N/A	Maglennon, et al. (105)
	Reverse	CAACATCCACTTTGCCAGAGTTAA			
	TaqMan probe	CGCCTGGTCACCAGGGCTGC			
CRPV E1^E4	Forward	GTGCCCGGAGTGTTGTAA	1338-1355	71 bp	Culp, et al. (161)
	Reverse	GGTGTCTTCAGGGGCACT	3733-3750		
	TaqMan probe	TGAAAATGGCTGAAGCTCCCC	1357-1370 ^ 3713-3719		
CRPV E1 full length	Forward	ATGGCTGAAGGTACAGACCCT	1362-1382	1809 bp	Designed in this study
	Reverse	TCATAGAGACTGAGAAGTTCC	3150-3170		
CRPV E2 full length	Forward	ATGGAGGCTCTCAGCCAGCGCTTA	3112-3135	1173 bp	Designed in this study
	Reverse	CTAAAGCCCATAAAAATTCC	4265-4284		
CRPV SE6/LE6	Forward	CTGCAGAGACTGCACTGTATTG	3330-251	137 bp	Designed in this study
	Reverse	CTTCCGCAAACTGTACAACG	448-467		
GAPDH RNA	Forward	GGGTGGTGGACCTCATGGT	N/A	58 bp	Seol, et al. (162)
	Reverse	CGGTGGTTTGAGGGCTCTTA			
Bisulfite Methprimer 1	Forward	TTAAAGTGGTTTGTAAAGAATTGGTATAAAAAG	N/A	306 bp	Designed in this study
	Inner reverse	CTACCTACRATCAAACTCAATACCAACC			
	Outer reverse	CAACCATCATTAAATCAAAATACATAACACC		576 bp	
Bisulfite Methprimer 2	Forward	GTATTYGGTGGTATGTGATGATATATTATATAG	N/A	397 bp	Designed in this study

		TAAG			
	Inner reverse	AAGYGTTTTTATTAATTTTGGGGTATTTTTAAG			
	Outer reverse	ATCTCAAATACACAATACCAACAACC		513 bp	
Bisulfite Methprimer 3	Forward	GATATYGGTTGTTGGTATTGTATATTTGAG	N/A	254 bp	Designed in this study
	Inner reverse	ACCCCRTACATTTAAACAATTATTTTTCTAC			
	Outer reverse	CCCCAAATCACCTTAATCTAACAATTTACAAAAACTAC		562 bp	
IFN-γ	Forward	TTCTTCAGCCTCACTCTCTCC	N/A	224 bp	Godornes, et al. (163)
	Reverse	TGTTGTCACTCTCCTCTTTCC			
TNF-α	Forward	GTCTTCCTCTCTCACGCACC	N/A	335 bp	
	Reverse	TGGGCTAGAGGCTTGTCACT			
IL-10	Forward	GAGAACCACAGTCCAGCCAT	N/A	179 bp	
	Reverse	CATGGCTTTGTAGACGCCTT			
Fas-ligand	Forward	ACACCTATGGAATTGCCCTGG	N/A	312 bp	Dewals, et al.(164)
	Reverse	TGACCAGTGATATCTCAGAGAC			
Perforin-1	Forward	CAGTACAGCTTCAACACGGAC	N/A	176 bp	
	Reverse	ATGAAGTGGGTGCCATAGTTG			
IL-6	Forward	CTACCGCTTTCCCCACTTCAG	Exon 2 from ,5; NCBI ID: NM_001082064	135 bp	Schnupf, et al. (165)
	Reverse	TCCTCAGCTCCTTGATGGTCTC			
IL-8	Forward	CCACACCTTTCCATCCCAAAT	Exon 2 and 3 from 4; NCBI ID: NM_001082293	122 bp	
	Reverse	CTTCTGCACCCACTTTTCCTTG			
IL-17A	Forward	CCAGCAAGAGATCCTGGTCCTA	Exon 3 from 3; NCBI ID: XM_002714498	112 bp	
	Reverse	ATGGATGATGGGGGTTACACAG			
IL-1β	Forward	TTGAAGAAGAACCCGT	Exon 3/4 and 4	128 bp	

		CCTCTG	from		
	Reverse	CTCATACGTGCCAGAC AACACC	,6; NCBI ID: NM_001082201		
TGF-β	Forward	CAGTGGAAAGACCCCA CATCTC	Exon 6 and 7 from ,8; NCBI ID: NM_001082660	140 bp	
	Reverse	GACGCAGGCAGCAATT ATCC			
CCL-4	Forward	GAGACCACCAGCCTCT GCTC	Exon 2 and 3 from 3; NCBI ID: NM_001082196	123 bp	
	Reverse	TCAGTTCAGTTCCAAGT CATCCAC			

Note: N/A, not available.

2.1.10 Bacterial strains

E. coli DH5α (Catalog #9057, Takara Bio Inc. Shiga, Japan): An endonuclease and recombinase-deficient *Escherichia coli* strain were used for DNA amplification.

SCS110 Competent Cells (Catalog #200247, Stratagene, CA, USA): SCS110 is derived from the JM110 strain, which is ideal for preparing plasmid-free of Dam or Dcm methylation.

2.1.11 Eukaryotic cell lines

AVS cell line: A cell line derived from CRPV particles transformed New Zealand White rabbit keratinocytes. The cell line was designated AVS (Asian Virus Stock).

Vx2 cell line (Catalog #90030912, supplied by European Collection of Authenticated Cell Cultures): Derived from a rabbit Oryctolagus cuniculus tumor of unspecified tissue origin, which was caused by a CRPV infection. The CRPV DNA was found in head-to-tail tandem integrated repeats within the host cell genome (150).

2.1.12 Cell culture Medium

Keratinocyte-SFM (KSFM): Catalog #10744-019, Gibco-BRL, Thermo Fisher Scientific, MA, USA.

Epidermal Growth Factor (EGF) and Bovine Pituitary Extract (BPE): Catalog #37000-015, Thermo Fisher Scientific, MA, USA.

2.1.13 Reagents and solution buffers

10× PBS: 137 mM NaCl, 2.7 mM KCl, 10 mM Na_2HPO_4, 2 mM KH_2PO_4, pH 7.4 .

1× PBS-T: 1× PBS + 0.1% Tween-20.

10× TBS: 50 mM Tris, 150 mM NaCl, pH 7.6.

1× TBS-T: 1× TBS + 0.1% Tween-20.

FACS buffer: 1× PBS with 2% fetal calf serum (FCS).

Ammonium-Chloride-Potassium (ACK) buffer: NH_4Cl (ammonium chloride) 8.02 g; $NaHCO_3$ (sodium bicarbonate) 0.84 g; EDTA (disodium) 0.37 g; adjust to 100 mL with Millipore water, stored at 4°C for six months.

LB-medium (Luria-Bertani-medium): 25 g LB Broth Base (GibcoBRL) were solved in 1 L H_2O.

LB-Agar: 15 g/L select agar (GibcoBRL) in LB medium.

SOC-Medium: 2% (*w/v*) Bactotrypton, 0.5% (*w/v*) Bacto yeast Extract, 10 mM NaCl, 2.5 mM KCl, 10 mM $MgCl_2$, 10 mM $MgSO_4$, 20 mM Glucose.

2.1.14 Software

GraphPad Prism 5 (La Jolla, CA, USA); Vector NIT® software (Thermo Fisher Scientific, MA, USA); Edit seq (DNASTAR. Inc. WI USA); Gen5™ software (BioTek® Instruments, Inc, VT, USA); ZEN 2 software (Carl Zeiss Microscopy GmbH, Göttingen, Germany); CellQuest Pro software (Becton Dickinson, Heidelberg, Germany).

2.2 Methods

2.2.1 Molecular biology methods

2.2.1.1 General cloning

The restriction enzyme digestion was typically performed in a volume of 20 µL containing up to 1 µg DNA fragments with 1 µL of each unit of enzyme. Reactions were incubated at appropriate temperature overnight followed by 15 min at 65°C to inactivate the enzyme activity. The ligation of DNA fragments was performed using the Rapid DNA Ligation Kit according to the manufacturer's instructions. The ligation mixture was then used directly for bacteria transformation.

2.2.1.2 Transformation and propagation

E. coli DH5α competent cells were used for the propagation of plasmids. 100 µL competent bacteria were thawed on ice, mixed with 15 µL ligation mixture and incubated on ice for 30 min. Then the mixture was heat-shocked for 90 s at 42°C and immediately cooled on ice for 1 min. Finally, 350 µL of SOC-Medium were added and incubated for 45 min at 37°C shaking at 700 rpm. The transformation mixture was plated on agar plates containing ampicillin and was left to incubate in a 37°C incubator overnight. The resulting colonies were then transferred to 5 mL LB liquid medium supplemented with 100 µg /mL Ampicillin and were cultured overnight at 37°C shaking at 220 rpm. For a large scale plasmid preparation, 500 µL bacterial preparations were taken from the 5 mL LB culture and were used to inoculate 1 L LB broth containing 100 µg/mL Ampicillin, and were left to grow overnight at 37°C, shaking at 220 rpm. For making bacterial stock, 1.5 mL of bacterial suspension was mixed with 50% of glycerol and frozen at - 80°C.

2.2.1.3 Mini prep and Maxi prep

The QIAprep spin mini-prep Kit was used for preparing a small amount of plasmid DNAs according to the manufacturer's instructions. The EndoFree® Plasmid Maxi Kit was used for the large quantity of plasmid DNAs preparation according to the manufacturer's instructions.

2.2.2 DNA methods

2.2.2.1 DNA extraction and purification

Total DNA was extracted using the QIAamp DNA Mini Kit according to the manufacturer's instructions. Briefly, proteinase K digestion of the tissue samples was performed with lysis buffer overnight at 700 rpm at 56°C. The extracted DNAs were used for further detection or stored at - 20°C. The concentration and purity of the extracted DNAs were examined using the NanoDrop spectrophotometer. A ratio of absorbance at 260 nm and 280 nm was used to ensure the purity of DNA with a ratio close to 1.8 indicative of pure DNA. DNA concentrations were calculated by measuring absorption at 260 nm.

2.2.2.2 Normal PCR

Oligonucleotide primers for normal PCR were designed using online resources (http://www.ncbi.nlm.nih.gov/tools/primer-blast/). The primers with the highest scores were selected for commercial synthesis by the Life technologies™ company, Germany. For diagnoses, the GoTaq® polymerase and Green Master Mix was used for the PCR reaction according to the manufacturer's instructions. For gene cloning, the Pyrobest™ DNA-Polymerase was used for the PCR reaction due to its high accuracy during DNA replication. The PCR reactions were 50 µL in total volume, which composed of 2 µL of 10 mM dNTPs, 5 µL of 10× reaction buffers, 0.25 µL of Pyrobest™ DNA-Polymerase, 2 µL of primer sets, 2 µL of the template, and 36.75 µL ddH_2O. The PCR program was 94°C for 3 min, following 35 cycles of reactions: denaturing at 94°C for 30s; annealing at 56°C for 30 min; extension at 72°C for 30 s to 90 s. The extension time and annealing temperature varied according to the PCR product size and GC content, allowing 60 s of extension per 1000 bp product length. The PCR products were examined by 0.8 - 1.5% of agarose gel electrophoresis. Purification of PCR products was performed using QIAquick Gel Extraction Kit according to the manufacturer's instructions.

2.2.2.3 Real-time quantitative PCR (RT-qPCR)

SYBR Green I based RT-qPCR reactions were carried out using 20 µL reaction mixtures consisting of 10 µL of LightCycler 480 SYBR Green I Master, 50 ng of template, and 30 pmol of each forward and reverse primers. TaqMan probe based reactions were carried out using 20 µL reaction mixtures consisting of 10 µL PrimeTime® Gene Expression Master Mix, 1 µL of 20 mM primers and probes mix (Integrated DNA Technologies), and 50 ng of cDNA. All primers used in this study are listed in section 2.1.9. All RT-qPCR assays were performed using the LightCycler 480 instrument. Typically amplification for SYBR Green was performed using the following program: pre-incubation 95°C for 5 s following 45 cycles of amplification 95°C for 10 s, 56°C for 10 s, and 72°C for 5 s. The extension time and annealing temperature vary in terms of the PCR product size and GC content. At the end of the PCR run, a dissociation curve was generated. The melting curve program was performed: 95°C for 5 s, 65°C for 1 min, 40°C cooling for 10 s. The viral copy number was determined by a standard curve, which was generated by 10 fold dilutions of

standard plasmids containing the respective target sequence. The copy number of each standard concentration was calculated by the following equation:

$$copy\ number = \frac{6.02E23 \times (DNA)g/L \times (volume\ of\ DNA\ used\ in\ qPCR)}{MW\ of\ plasmid + MW\ of\ insert}$$

2.2.2.4 Rolling circle amplification (RCA)

RCAs were performed using the Illustra empliPhi100 Amplification Kit following the manufacturer's instructions with 5 mM extra dNTPs and 30 pmol CRPV E6, E2 primer pairs respectively. Digestions of the amplification products were performed using SmaI overnight at 25°C in a total volume of 20 µL. Digestion results were verified by 0.4% agarose gel electrophoresis (100 V, 1 h).

2.2.2.5 Bisulfite-based cytosine methylation analysis

Total DNA was extracted with the QIAamp DNA Mini Kit and was prepared for bisulfite conversion using EZ DNA Methylation™ Kit according to manufacturer's instructions. Bisulfite-treated DNA was amplified by nested PCR with reaction conditions as previously described (166) and adapted as follows: Denaturation (95°C 4 min), cycle 5 (95°C 45 s, 56°C 90 s, 72°C 4 min), cycle 35 (95°C 45 s, 60°C 90 s, 72°C 90 s), 72°C 4 min, hold 4°C. Methylation-specific primers for bisulfite PCR amplification were designed using the online resource from Zymo-research (http://www.zymoresearch.de/tools/bisulfite-primer-seeker) and were listed in section 2.1.9. PCR amplicons were then purified and cloned using CloneJET PCR Cloning Kit according to manufacturer's instructions, and at least 10 positive clones from each sample were sequenced. Only sequences with at least 90% conversion of cytosines outside CpGs were taken into account.

2.2.2.6 DNA sequencing

Sanger sequencing was carried out by GATC biotech AG, Constance, Germany. Sequences were analyzed using the Vector NIT® software.

2.2.3 RNA methods

To extract RNA, precautions were taken at all times to avoid the potential of RNA degradation by the ubiquitous presence of ribonuclease enzymes in cells, tissues or the environment. RNA was extracted using the RNeasy Miniprep Kit according to the

manufacturer's instructions. Briefly, for tissue RNA extraction, skin biopsies were cut into small pieces (approximately 10 - 40 mg) and were homogenized using the Ultra-Turrax T18. The homogenized lysates were centrifuged at 14,000 rpm for 10 min and subjected to the protocol for "RNA extraction from tissue" within the RNeasy Miniprep kit. The extracted RNA was quantified using the Nanodrop and stored at - 80°C. Complementary strand DNA synthesis was performed using the QuantiTect® Reverse Transcription Kit according to manufacturer's instructions.

Gene expression was quantified by RT-qPCR, see section 2.2.2.3. For relative quantification, target gene expression was normalized to the expression of the rabbit Glyceraldehyde 3-phosphate dehydrogenase (GAPDH) gene. The $2^{-\Delta\Delta cp}$ method was used for analyzing the results. SYBR Green I based RT-qPCR was performed using the following program: 95°C for 5 s following 40 cycles of amplification 95°C for 10 s, 60°C for 30 s. At the end of the PCR run, a dissociation curve was generated. The melting curve program was performed: 95°C for 5 s, 65°C for 1 min, 40°C cooling for 10 s. For quantitating quantification, a serial diluted standard plasmid containing target gene sequence was used. Taq-Man probe based RT-qPCRs were performed using the following program: 95°C for 5 s following 40 cycles of amplification 95°C for 10 s, 60°C for 30 s. All primers and probes were listed in the section 2.1.9.

2.2.4 *In vitro* cell culture methods

2.2.4.1 Normal cell line culture

Rabbit derived cell lines AVS, Vx2 were cultured in keratinocyte-SFM supplemented with human recombinant Epidermal Growth Factor and Bovine Pituitary Extract, and 1× antibiotics/antimycotics (1000 U per mL penicillin, 1 mg per mL streptomycin). At confluency, cells were subcultured by trypsinization and 3×10^4 cells per cm^2 were seeded in fresh collagen I coated or Primaria plates.

2.2.4.2 *Ex vivo* primary cell culture

Primary keratinocytes from NZW rabbits were isolated from rabbit skin biopsies using a modified protocol as previously described (167, 168). Rabbit skin punch biopsies were removed and incubated in a defined DMEM with 5 U per mL dispase II (10 mg per mL) and 10× antibiotics/antimycotics (1000 U per mL penicillin, 1 mg per mL streptomycin) at 4°C. The skin was then cut into pieces and trypsinized (0.25%/0.1%

trypsin-EDTA) for 20 min. Cells were filtered using 100 µm filter and seeded at a density of 3× 10^4 cells per cm^2 in each 6 cm collagen coated plate. The cells were cultured in keratinocyte-SFM, supplemented with human recombinant Epidermal Growth Factor (EGF) and Bovine Pituitary Extract (BPE), and 1× antibiotics/antimycotics. At confluency, cells were subcultured by trypsinization and 3×10^4 cells per cm^2 were seeded in fresh collagen I coated plates.

2.2.4.3 Transfection of Eukaryotic cell

The FuGENE® HD Transfection Reagent was used for eukaryotic cell transfection. The ratio of FuGENE transfection reagent to DNA was 5:2. The adherent cells were plated one day before transfection so that cells are approximately 80% confluent on the day of transfection. In general, 1 - 2×10^4 adherent cells were plated in 2 mL per well of a 6-well plate. The FuGENE® HD Transfection reagent/DNA mixture was incubated for 15 minutes at room temperature. The mixture was then added to the 6-well plate and mixed by pipetting. The cells plate was returned to the incubator for 48 hours.

2.2.4.4 Cell proliferation WST-1 assay

The quantification of cell proliferation and cytotoxicity was determined by WST-1 based assay according to institutional guidelines. Briefly, cells were seeded at a concentration of 5× 10^3 cells/well in 100 µL KSFM culture medium with EGF and BPE in 96 wells Primaria plate. Cells were incubated for 24 h at 37°C and 5% CO_2, and the culture medium was replaced by KSFM medium with different concentrations of immunosuppressant drugs. Cells were incubated for 4 to 5 days at 37°C and 5% CO_2. And 10 µL/well Cell Proliferation Reagent WST-1 was added and incubated for 4 h at 37°C and 5% CO_2. After thoroughly shaking for 1 min on a shaker, the absorbance of the samples against a background controls as blank was measured using a microplate (ELISA) reader. The wavelength for measuring the absorbance of the formazan product was 440 nm. The reference wavelength was 600 nm. The results were analyzed by Gen5™ software.

2.2.4.5 Immunofluorescence staining

The primarily expanded rabbit keratinocytes were seeded in 24-well collagen I coated plates and were cultured for 2 days in KSFM medium. Cells were fixed with acetone

for 5 min at room temperature and were washed in 1× PBS three times for 5 min. After incubation with 1% BSA in 1× PBST for 30 min to block unspecific binding of the antibodies, cells were incubated with the primary cytokeratin 15 antibody (1:50) for 1 h at room temperature. After three times wash in 1× PBS, cellular DNA was stained with DAPI for 1 min. Images were obtained with a Zeiss Axiovert 200 microscope.

2.3 Animal experiments

2.3.1 Ethical approval and project license application

All animal experimental procedures were approved (Permit Number: H2/13) by the responsible authority (Regierungspraesidium Tuebingen, Baden-Wuerttemberg, Germany) according to the German Animal Welfare Act (*TierSchG § Abs. 1*) and were performed according to institutional guidelines.

2.3.2 Helios® Gene Gun infection

2.3.2.1 Precipitation of CRPV DNA to gold particles

For the infection of rabbit skin, CRPV DNA was purified with the EndoFree® Plasmid Maxi Kit and adjusted to approx. 1 µg/µL. Each DNA was mixed with 50 mg gold particles, 100 µL of 0.05 M spermidine. Samples were then sonicated (4× 10 sec), incubated with 100 µg CRPV DNA and precipitated with 100 µL of 1 M $CaCl_2$ at room temperature for 10 min. The DNA-coated gold particles were washed 3 times with 100% ethanol and were stored in 6 mL of 100% ethanol at - 20°C.

For dilutions of CRPV DNA, the start concentration of CRPV DNA was 1 µg/µL followed by different dilutions. Four different concentrations of CRPV DNA from 1 µg/µL to 10 ng/µL were generated and gold particles were coated. In order to have a high gold-coating efficiency, CRPV DNAs were diluted using pUC19 plasmids to keep the final concentration of 100 µg/100 µL for each dilution according to the manufacturer's instructions of the Helios® Gene Gun system.

2.3.2.2 Preparation of cartridges for Helios® Gene Gun System

Cartridges were prepared using the Tubing Prep Station according to the manufacturer's instructions. Briefly, the Tefzel® tube was flushed with nitrogen gas. 3 mL of the CRPV coated gold particles in ethanol were injected into the tube. After

precipitation of the gold particles, the ethanol was removed. By suction and rotating the hose, the gold particles were uniformly distributed on the inner tube surface. The tube was dried for 5 minutes and was cut into 1 cm long cartridges using the Tubing Cutter. The cartridges were then stored at 4°C.

2.3.2.3 Delivering of CRPV DNA by Helios® Gene Gun System

NZW outbred rabbits were anesthetized with a mixture of Ketamine and Sedator®. The fur on the rabbits' back was trimmed with an electric clipper and wet-shaved with a razor blade. All sites to be infected were marked with black tattoo ink. For each site, sandpaper treatment was conducted to disrupt the upper layer of the skin, and then 10 cartridges were delivered to the wounded tattoo marked site using the Helios® Gene Gun System with 350 psi injected pressure.

2.3.3 Sample collection from rabbits

A collection of a skin punch biopsy was performed under general anesthesia described above. Standard 3 mm and 6 mm biopsy punches and a sterile disposable scalpel were used to remove the skin tissue. Suturing of the wound was performed when using 6 mm biopsy punches. Hemostasis was achieved by applying pressure for several minutes with a sterile swab. Once the skin tissue biopsy was removed, it was wrapped in aluminum foil and was snap-frozen in liquid nitrogen, then stored at -80°C.

Rabbits were euthanized at the end of experiments via administering 200 mg/mL solution of potassium chloride directly to the heart. Following confirmation of death, the lymph nodes and important organs such as lung, liver, and spleen were collected and snap-frozen in liquid nitrogen, then stored at - 80°C.

2.3.4 Drug-induced immunosuppression in NZW rabbits

Cyclosporin A (CsA) (Sandimmun® 50 mg/mL) and Dexamethasone (Dex) (Dexadreson® sodium, 2 mg/mL) were injected subcutaneously into the neck fold of the rabbits. The treatment was previously described (106). The optimized doses for immunosuppressive drug administration in this study were 7.5 mg/kg CsA three times per week (Monday, Wednesday, and Friday) and 0.15 mg/kg Dex twice per week (Tuesday and Thursday). The physical condition was vigorously monitored at each treatment to ensure rabbits were maintaining body weight, as well as food and water

intake. Immunosuppressed rabbits were kept in individual cages in a separate SPF (Specific-pathogen-free) room and were fed with autoclaved water.

2.3.5 Flow cytometry (FACS)

Flow cytometry used for quantification of peripheral blood lymphocytes has been previously described (106, 169). In brief, at least 1 mL of whole peripheral blood was collected from the rabbit's ear vein using heparin coated syringes. 500 µL blood was diluted with 4.5 mL FACS buffer and centrifuged at 300×g for 5 min at room temperature. After removal of the supernatant, red blood cells were lysed in 10 mL standard Ammonium-Chloride-Potassium (ACK) buffer for 10 min at room temperature with gentle agitation. The lysed red blood cells were separated by centrifugation at 300× g for 5 min. leucocytes were re-suspended in the FACS buffer and were distributed into 200 µL for each reaction. The sample was incubated with 10 µL of each FITC-conjugated mAb: mouse anti-rabbit T lymphocytes (TLC, also known as CD5), CD4+ and CD8+, mouse IgG1 negative control, and mouse IgG2a negative control at 4°C for 30 min. After 3 times wash (300× g for 5 min) in FACS buffer, the leucocytes were resuspended in 800 µL FACS buffer. The stained T-lymphocytes membrane markers were determined by one color flow cytometry, which was performed using an FACSCalibur. For each FACS measuring, 100,000 cells were sorted. FACS data was analyzed using CellQuest Pro software (FIG 2.3.1). The concentration of T-cells in PBMCs was calculated by the following equation:

$$T-cells\ /mL = \frac{\left[\frac{T\ cell counts - Control counts}{Volume for FACS}\right] \times Total\ volume\ (800\ \mu L)}{Total\ volume\ of\ blood\ (500\ \mu L)} \times 1000\ (mL)$$

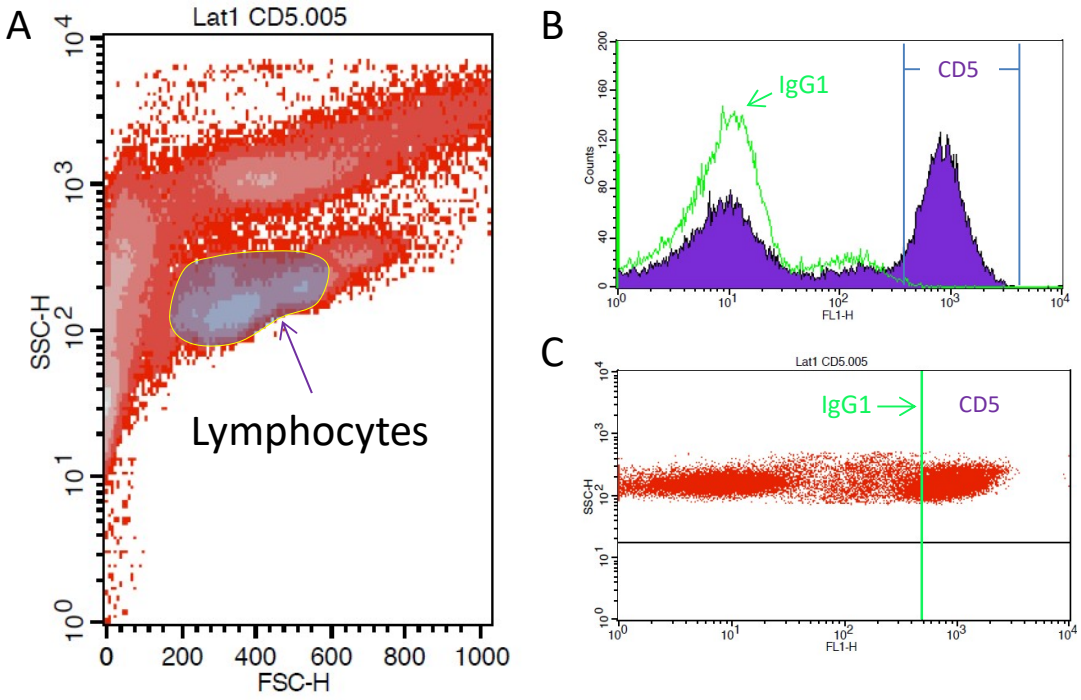

D

Quadrant Statistics

File: Lat1 CD5.005
Sample ID: Lat1 CD5
Tube: Untitled
Acquisition Date: 13-May-14
Gated Events: 26761
X Parameter: FL1-H (Log)
Quad Location: 491, 17

Log Data Units: Linear Values
Patient ID:
Panel: Untitled Acquisition Tube List
Gate: G1
Total Events: 100000
Y Parameter: SSC-H (Log)

Quad	Events	% Gated	% Total	X Mean	X Geo Mean	Y Mean	Y Geo Mean
UL	15939	59.56	15.94	64.70	15.50	163.04	155.47
CD5 UR	10822	40.44	10.82	968.89	903.07	154.61	147.94
LL	0	0.00	0.00	***	***	***	***
LR	0	0.00	0.00	***	***	***	***

FIG 2.3.1 Example of the FACS analysis of rabbit CD5 cells (T lymphocyte, TLC). Red blood cells were lysed in whole blood samples and subjected to FACS analysis using anti- rabbit CD5 and control IgG1. A: Lymphocytes were gated following examination of density plots. B, C, D: For each detection, 100,000 cells were sorted. The stained T cell population was determined and normalized to IgG1 controls.

2.3.6 Ultra Violet light treatment

Rabbits were anesthetized and shaved, then were placed under the UV source at a distance of 15 cm from side back skin. The intensity of UV was measured by a UVX radiometer sensor and calculated by the equation, $J = W.s$ with respect to the light source. The non-irradiated skin was covered by photoresist plastic sheeting. A UVB lamp (312 nm, 15 W VL-115.M) which stably emitted light at 1000 μW/cm^2 at a distance 15 cm was used. The doses of UVB treatment were from 10 to 800 mJ/cm^2 and were calculated by the exposure times ranging from 10 to 800 seconds. A UVA lamp (365 nm, 30 W VL-215.L) which stably emitted light at 2300 μW/cm^2 at a distance 15 cm was used. The dose of 5 mJ/cm^2 UVA treatment were calculated by the exposure time 36 min 14 s, and the dose of 1 mJ/cm^2 UVB treatment were calculated by the exposure time 16 min 40s.

2.4 Collection of clinical data and Statistical analysis

At each examination, the number, location and dimensions (length, width, height) of each papilloma were recorded. The data were used to calculate the papilloma volume (V), V= 4π/3× length/ 2× width/ 2× height/2 (170) and the papilloma specific growth rate (SGR), SGR = ln (V2/V1) /(t2 - t1) (171). Statistical analyses were conducted using GraphPad Prism 5 software (La Jolla, USA). If the data sets were not normally distributed, the Mann-Whitney *t*-test was used to determine significant differences ($p < 0.05$). If the data sets can be transformed to a normal distribution model then the logarithmic transformation was used for the justification, and the unpaired Student's *t*-test was conducted to determine significant differences ($p < 0.05$).

2.5 Overview of the animal experiment

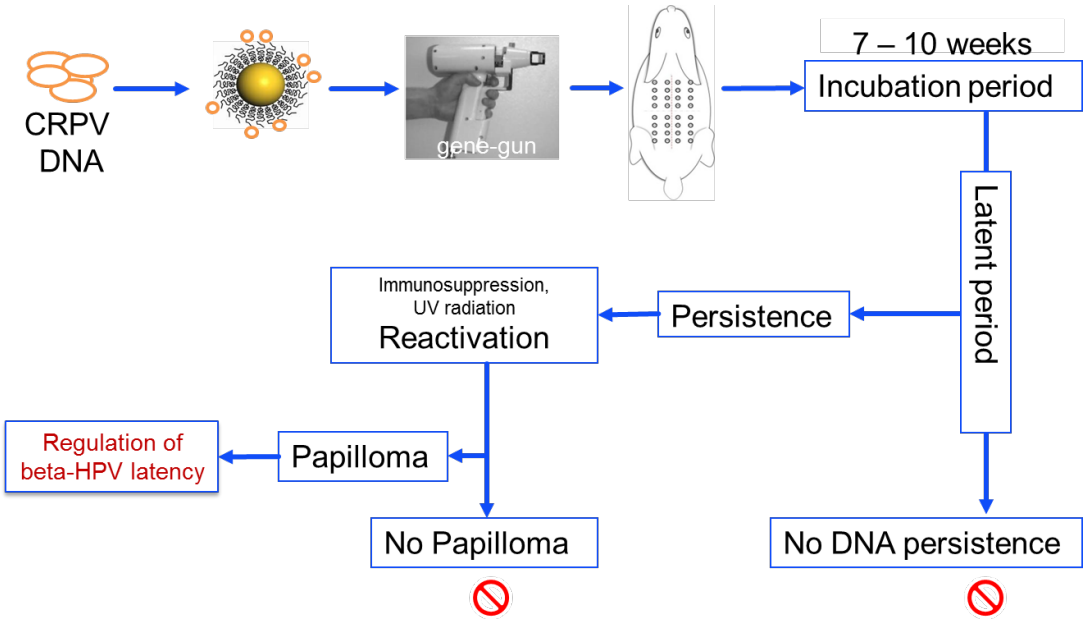

3 RESULTS

3.1 CRPV latent infection animal model

3.1.1 Development of RT-qPCRs for the quantification of latent CRPV genome and transcripts

Highly sensitive SYBR Green I based RT-qPCRs targeting various viral genes were established and evaluated for the detection of a minimum of 1 copy of CRPV genome per reaction. Primers were designed to specifically target CRPV gene sequences. The melting curves of each RT-qPCR showed that all primers were specific to CRPV. Detection of serially diluted standard CRPV plasmids showed that these RT-qPCRs were able to detect at least 4 copies of CRPV DNA per reaction (**Table 3.1.1**). The primer set SE6/LE6 showed the highest specificity among the primer sets in rabbit skin biopsies, which was then used for CRPV DNA quantification in the following experiments.

Table 3.1.1 Summary of the sensitivities of the RT-qPCR

Primers	Standard curve	Efficiency value	Cycles to detect of one copy DNA	One copy detect rate[a]	Limit of detection [b] (copies)
SE6/LE6	Y = -3.34x + 38.3	- 3.34	39	60%	4
LE6	Y = -3.57x + 39.7	- 3.57	40	50%	4
E1^E4	Y = - 3.37x + 41.8	- 3.37	42	30%	10
GAPDH	Y = - 3.64 + 40.5	- 3.64	41	30%	6

Note: [a] successful detection of one copy DNA standard plasmid in 10 repeats.

[b] 90% successful detection of certain copy numbers of DNA standard plasmid in 10 repeats.

The CRPV E1^E4 primers, which have been shown to detect all viral early mRNAs as previously described (161) were used for the quantification of viral transcripts. As tested in this study, this TaqMan probe based CRPV E1^E4 RT-qPCR showed high sensitivity in detecting viral transcripts as low as 1 viral mRNA copy per reaction.

The ratio of CRPV DNA copy to cell number was determined by RT-qPCR using the SE6/LE6 primer set and CP values were normalized to the rabbit GAPDH gene copy number per cell. The average rabbit GAPDH gene copy number per cell was determined by quantifying GAPDH genes in the rabbit-derived AVS cell line. The

results showed that the GAPDH primer pair used in this study detected approximately 17 ± 4 (Median ± SD) copies of GAPDH “homologous” sequences per rabbit cell. Therefore, 17 copies of GAPDH per rabbit cell were used for the normalization of viral DNA copy number to cell number in the following experiments.

3.1.2 Development of a rabbit model for CRPV latent infection

It has been shown that CRPV DNA can persist either after low-titer virus infection or after lesion regression (109, 111). In this study, a low dose of viral DNA infection was used to establish an *in vivo* CRPV latent infection model in NZW rabbit.

We first defined a CRPV DNA dose which consistently induces asymptomatic infections at the majority of the infected sites. Three NZW rabbits were cutaneously infected with serially diluted CPRV DNA (**FIG 3.1.1 A**) via the Bio-rad Helio Gene Gun system. Rabbits were anesthetized and were shaved before infection. All sites to be infected were marked with black tattoo ink. Ten weeks p.i. – which is the time frame by which papilloma formation is generally completed, we found that 40 ng CRPV DNA resulted in 29.2% (7/24) papilloma formation (**FIG 3.1.1 B**). Infection of the skin with CRPV was very well tolerated by all NZW rabbits with no apparent adverse effects on their health and weight gain.

To investigate whether the viral DNA was retained in the asymptomatic infected site, skin biopsies were taken from asymptomatic tattoo ink-marked areas 15 weeks post infection and after euthanization (up to 14 months p.i., **Table S1**). CRPV DNA was quantified using highly sensitive RT-qPCR. We determined that a median of 7 copies of CRPV DNA per 1000 cells were present at the asymptomatic sites 15 weeks post infection and 14 copies of CRPV DNA per 1000 cells after euthanization. However, there is no significant increase between 15 weeks post infection and after euthanization. The level of viral DNA detected in skin biopsies was approximately 3 to 5 log-folds lower compared to the median viral DNA copies in papillomas, which are approximately 68 copies per cell. No viral DNA was detected in normal uninfected skin biopsies (**FIG 3.1.1 C**)

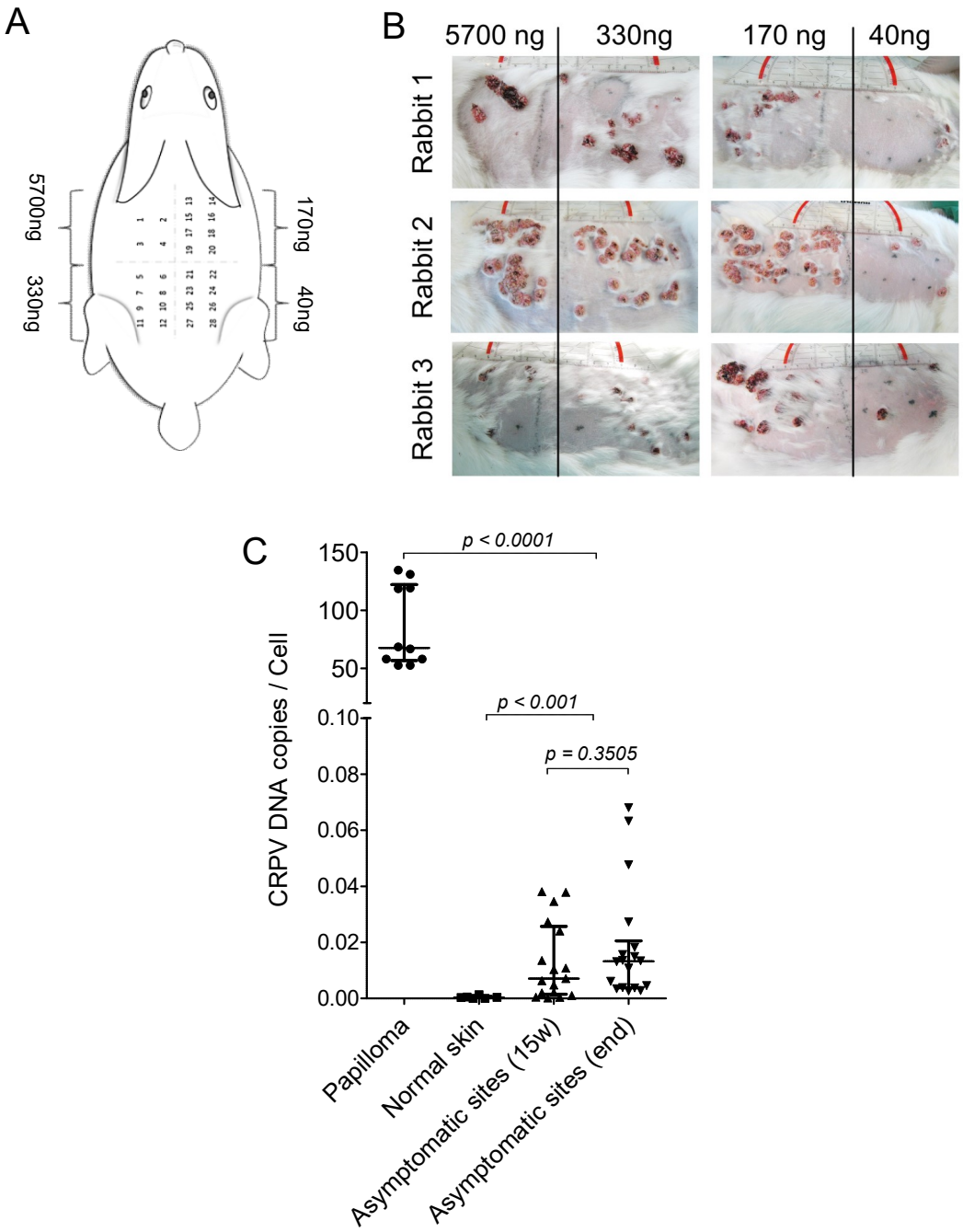

FIG 3.1.1 Low-dose CRPV infection leads to reduced papilloma induction and latent infection. (A) Schematic of the infection pattern on a NZW rabbit's back skin. Each number in the drawing represents one site of infection. (B) Papilloma formation at 10 weeks p.i.. Visible papillomas occurred within 10 weeks p.i.. There was no formation of new papilloma after 10 weeks. (C) Persistence of CRPV DNA copy number following latent infection. Papilloma samples were taken from rabbit 1, 2, 3 after euthanization. Skin biopsies were taken from rabbit 1, 2 and 3. Each dot in the graph represents one sample. Papilloma n=10, normal skin n=6, asymptomatic sites (15w) n=17, asymptomatic sites (end) n=18. The Mann-Whitney test was conducted for the statistical significant test.

3.1.3 Persistence of CRPV genomes in latently infected sites

To determine for how long the viral DNA persists in latently infected skin sites, skin biopsies were taken sequentially from asymptomatic infected sites from 6 rabbits (rabbit 1, 2, 3, 14, 15, and LAT4; see **Table S1)**, and were subjected to RT-qPCR quantification. Collectively, one-month p.i. we detected a median viral copy number of approximately 10 copies per 1000 cells. This number did not significantly change (p >0.05) during the following sequential measurements spanning a total of 14 months (15 copies per 1000 cells). No viral DNA was detected in normal skin biopsies (**FIG 3.1.2**).

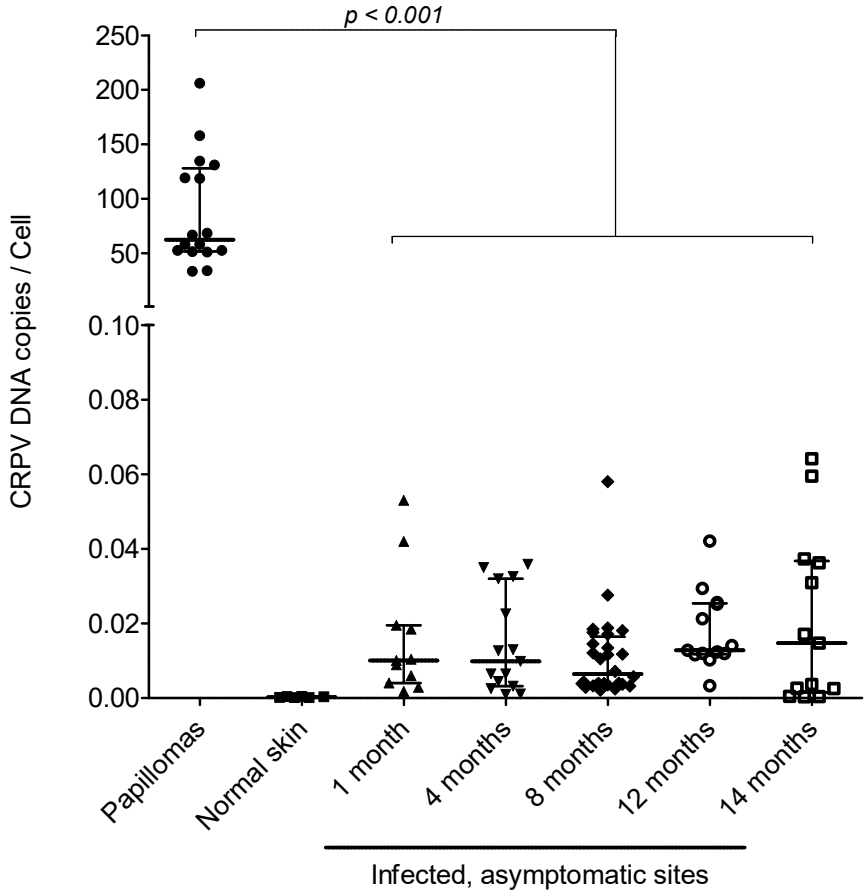

FIG 3.1.2 CRPV DNAs persisted long post infection in asymptomatic low dose infected site. CRPV DNA copy numbers were normalized to 17 copies of GAPDH copy number per cell. Each dot in the graph represents one sample. Papillomas n =16 (Median = 62 copies/cell), normal skin n =10, 1 month n =11 (Median =10 copies/ 1000 cells), 4 months n = 15 (Median= 9 copies/1000 cells), 8 months n =28 (Median = 6 copies/1000 cells), 12 months n=13 (Median = 12 copies/1000 cells), 14 months n=13 (Median = 15 copies/1000 cells). The Mann-Whitney test was conducted for the statistical significant test.

In this study, 21 rabbits were infected with various doses of CRPV DNA see **Table S1**. The CRPV DNA concentration delivered by the Gene Gun correlates with the efficiency of papilloma induction (**FIG 3.1.3**). In total, 223 of infected asymptomatic skin biopsies were obtained from 20 rabbits, except for rabbit 10 which developed 100% of papillomas at all infected sites (**Table S1**). Altogether, 88% (198/223) of the sites were found containing CRPV DNA up to 24 months p.i. (**Table 3.1.2**). The average median level of the CRPV DNA in the asymptomatic site was 13 copies per 1000 cells (**FIG 3.1.4**).

In addition, low levels of CRPV E1^E4 transcripts were detectable at an average of one copy per 10,000 GAPDH mRNAs only in 32% (17/53) of the skin biopsies (**Table 3.1.2**).

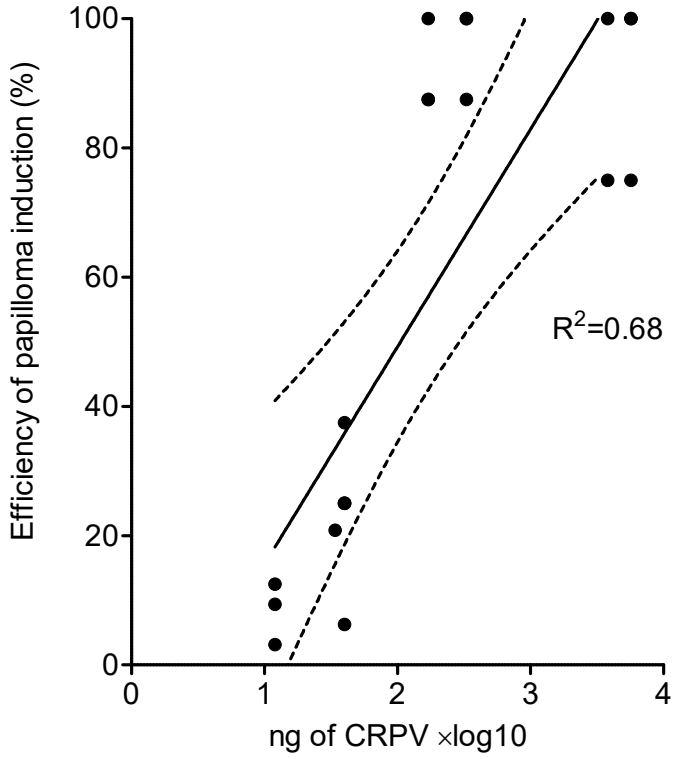

FIG 3.1.3 The amount of CRPV DNA correlates with papilloma induction. The original data are shown in Table S1. The dashed lines represent the 95% Confidence Intervals. The R^2 represents the regression coefficient of determination, meaning 68% of the variance in the response variable can be explained by the explanatory variables, and the remaining 32% can be attributed to unknown, lurking variables or inherent variability.

Table 3.1.2 Summary of samples detected in this study

Sample	Viral DNA			Viral transcripts		
	Total	Positive*	Percentage	Total	Positive	Percentage
Normal skin	58	0	0	21	0	0
Latently infected skin	223	198	88%	53	17	32%

*A sample was considered positive only when the Tm value of the qPCR was the same as the positive control and the Cp value was < 37.

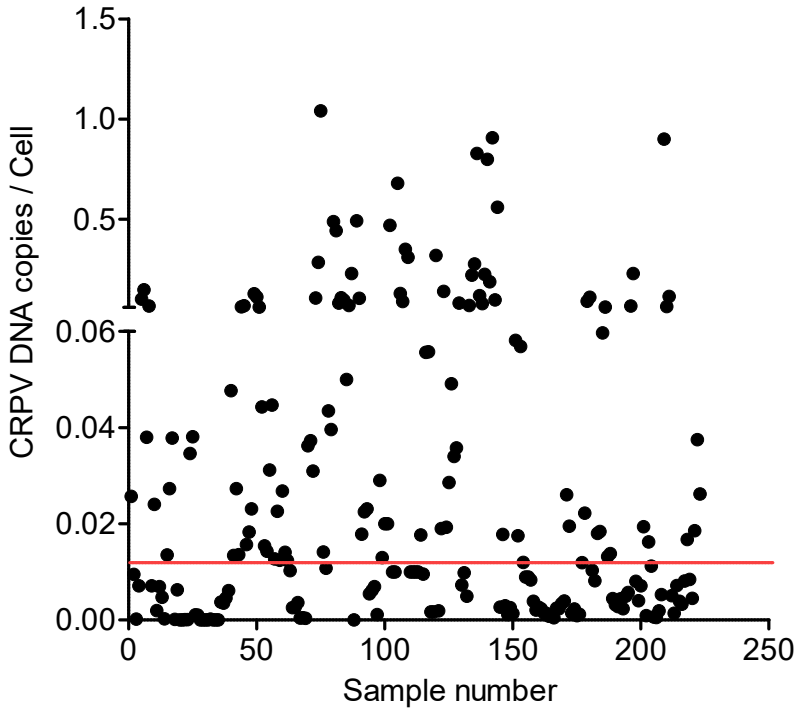

FIG 3.1.4 CRPV DNA persisted in 223 asymptomatic infected sites of 20 rabbits. CRPV DNA copy numbers were normalized to 17 copies of GAPDH copy number per cell. Each dot in the graph represents one sample. The red line indicates the average median level of CRPV copies, which is 0.01323. The viral DNA copy numbers of 49 samples are above 6 copies per 100 cells.

3.1.4 *Ex vivo* expansion of latently infected cells

We isolated primary rabbit skin cells from 16 CRPV latently infected sites and 6 normal skin sites of 3 rabbits. To isolate both the epithelial cells and hair follicle cells, the whole skin tissue was subjected to primary cell isolation (**FIG 3.1.5A**). After the second passage, CRPV DNA was detected in 12 out of 16 latently infected skin

cultures, with 5 copies/cell in average (**FIG 3.1.5 B**). Viral DNA was not found in the 6 sets of normal skin expanded cells. Three of the CRPV DNA positive primary cell cultures had been found to express low levels of E1^E4 transcripts. However, we were unable to culture these primary cells beyond passage 6 (**FIG 3.1.5 C**). The expanded primary rabbit cell populations did undergo very slow cell division. In order to find out which type of rabbit epithelial stem cells that survived during the *ex vivo* expanding, we tried to look for potential markers that might identify the type of cells. Previously, we have shown that during productive infection, the primary target cells of CRPV are located in self-renewable HF stem cells (78). Therefore, we used one of the potential biomarkers - the cytokeratin 15 (K15) protein which is used as a marker of stem cells of the hair-follicle bulge to identify the stem cells (172). Using immunofluorescence staining, we found 24% of the expanded cells express K15 in the expanded cell culture (**FIG 3.1.6**).

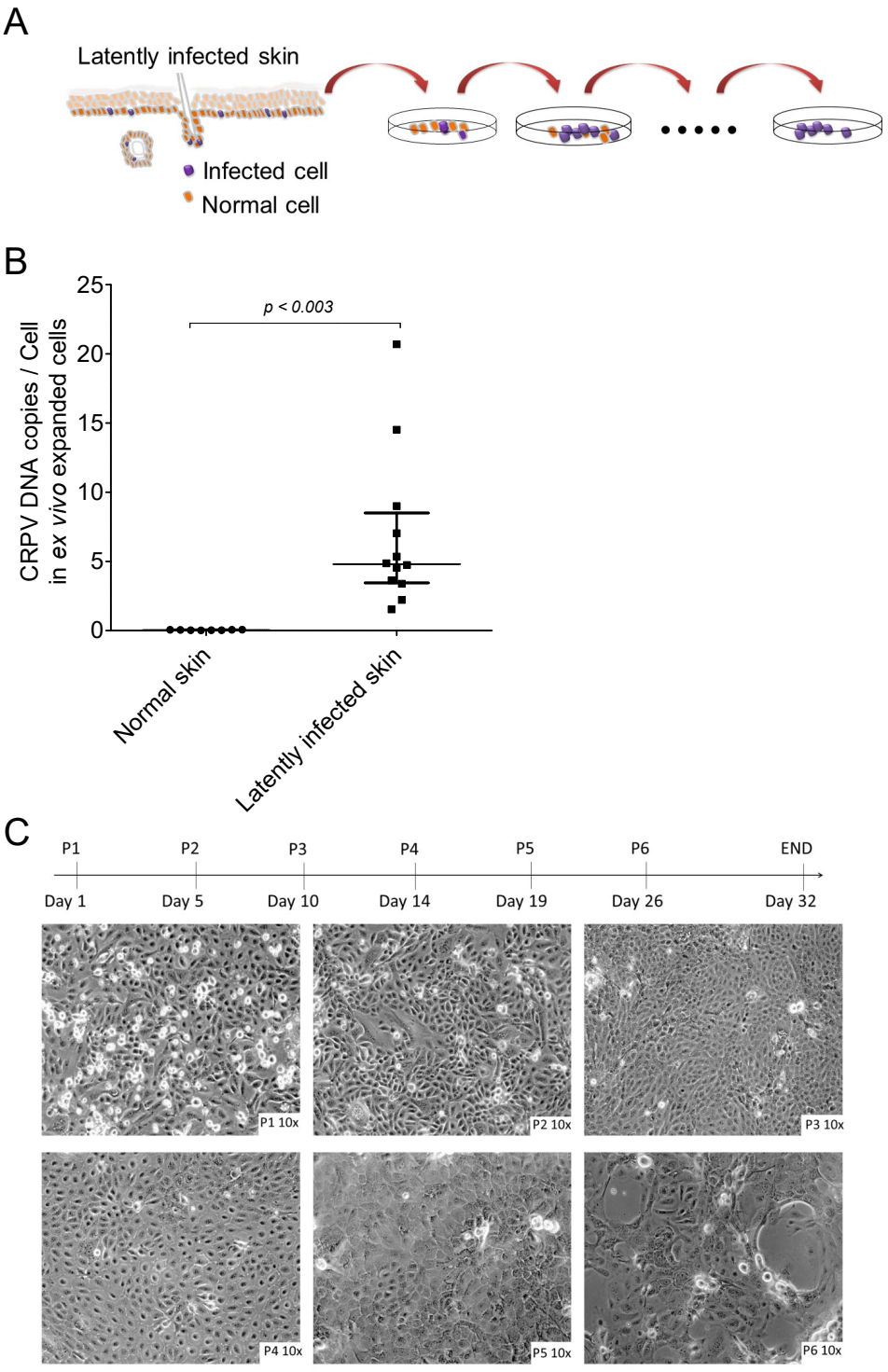

FIG 3.1.5 *Ex vivo* culture of infected cells. (A) Experimental set up of expanding latently infected skin cells *ex vivo*. (B) RT-qPCR quantification of CRPV DNA in the normal skin cell culture (n= 8) or latently infected skin cell culture (n= 12) passage 3, 10 days after explantation. (C) Representative example of an *ex vivo* culture of latently infected skin tissue #7 which was taken 18 months p.i. from rabbit LAT4 during autopsy (Table S1).

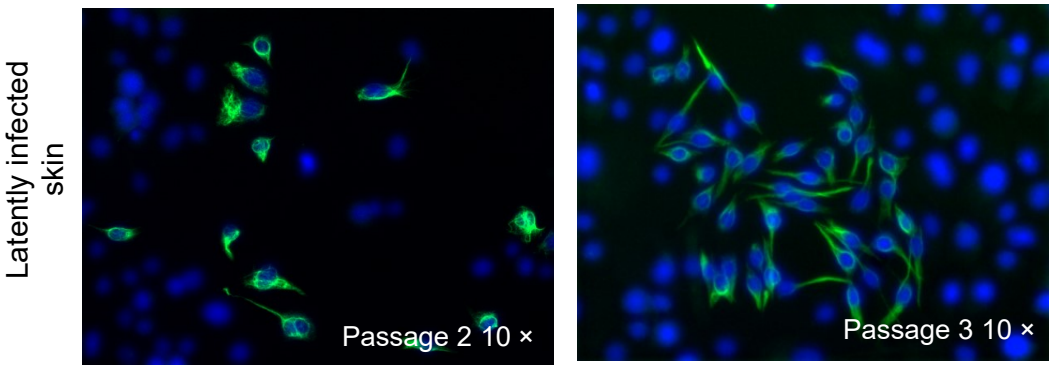

FIG 3.1.6 Immunofluorescence staining of *ex vivo* expanded cells from latently infected skin sites with K15 antibody.

3.1.5 Determination of the methylation status of latent viral genomes

To investigate whether latent viral gene expression is regulated by levels of DNA CpG methylation during PV latency, we performed bisulfite-mediated methylation PCR amplification and sequencing to detect potential CpG methylation in latent viral DNAs. We first designed three methylation specific nested primer sets that cover the entire region of the CRPV URR (Methprimer 1 and 2, **FIG 3.1.7**) as well as the early promoter region of CRPV E6 (Methprimer 3, **FIG 3.1.7**). The inner PCR amplicons were then cloned, and at least 10 positive clones were sent for sequencing. In total, we analyzed five latently infected skin sites taken from the tattoo marked skin of 5 rabbits (rabbit 1, 2, 3, 4 and 5, see Table S1), as well as samples from one papilloma and the pLAII-CRPV recombinant plasmid. The results of the sequence alignments showed that 99% of cytosines were converted to thymines. However, no CpG methylation site was found in any of the clones.

Interestingly, two bacterial DNA methylase (*dcm ,CCAGG)* methylated sites (position: 7795^7799 and 115^119) have been found in 48% (24/50) and 34% (17/50) of the above sequenced clones, respectively (**Table 3.1.3**), which originates from DH5α *E. coli* used for amplification of the viral genome plasmid pLAII-CRPV before inoculation of rabbit skin. The *dcm* methylations were lost completely in sequenced clones of rabbit 3 and LAT 4 fourteen months p.i. (**Table 3.1.3**). CpG methylations, as well as dcm methylations, were not detected in papillomas. In contrast, the two *dcm* sites were found 100% methylated in the original pLAII-CRPV plasmid preparation (**Table 3.1.3**).

In addition, by sequence analysis, we found that a total of eleven *CCAGG* and twelve *CCTGG* sequences exist in the pLAII-CRPV genome. It is known that almost all commonly used cloning strains such as DH5α *E. coli* are *dcm*$^+$. As it is unclear whether bacterial DNA methylation affects viral infection, we therefore looked for *E. coli* strains that do not methylate dcm. We found one strain - SCS110 competent cells which is ideal for preparing plasmid-free of *dam* or *dcm* methylation(173). We compared the methylation status of a CRPV DNA preparation from the *dcm*$^+$ DH5a strain to a preparation from the *dcm*$^-$ SCS110 strain. Indeed, the pLAII-CPRV produced in DH5a *E. coli* were completely methylated by *dcm* DNA methylases (**FIG 3.1.8**). In contrast, the DNA produced by the SCS110 strain was not methylated (**FIG 3.1.8**).Therefore, the SCS110 competent cells were used for the production of viral DNA in the following experiments.

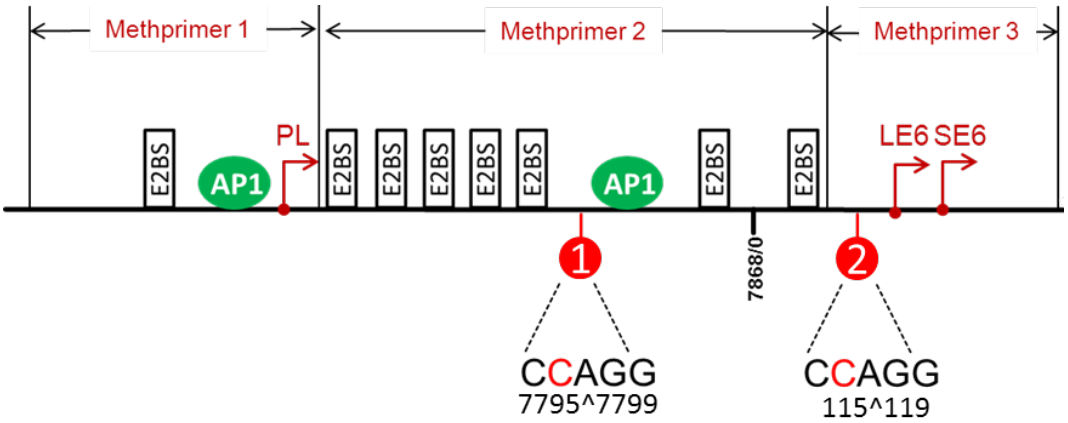

FIG 3.1.7 Cartoon of the motifs of CRPV URR-LE6 region and methylation primers amplification. Two *dcm* sites (CCAGG) were observed in some of the clones. E2BS: E2 binding site, PL: late promoter, AP1: Activator protein 1, LE6: long E6, SE6: short E6.

Table 3.1.3 Two dcm methylations in latently infected samples

Rabbit	Latent skin methylated clone/total clones (Percentage of *dcm* methylations)	
	7795^7799	115^119
Rabbit 1	5/10 (50%)	0/10 (0)
Rabbit 2	9/10 (90%)	10/10 (100%)
Rabbit 3	0/10 (0)	0/10 (0)
Rabbit LAT 4	1/10 (10%)	0/10 (0)
Rabbit 5	9/10 (90%)	7/10 (70%)
pLAII-CRPV	10/10 (100%)	10/10 (100%)
Papilloma	0/10 (0)	0/10 (0)

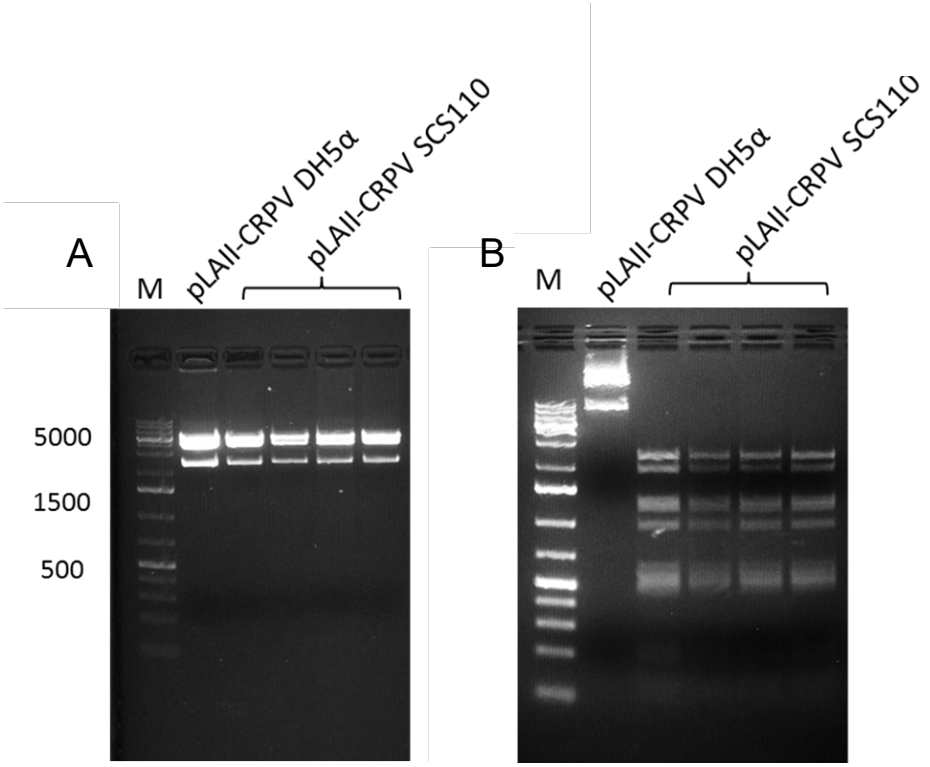

FIG 3.1.8 The methylation status of CRPV DNAs in the *dcm*$^+$ DH5a strain SCS110 strain. (A) Digested by BamH1 which cuts the viral genome without preference of any methylations. (B) Digested by PspGI which specifically cuts the non-methylated *dcm (CCA/TGG)* sites.

3.1.6 Determination of the physical status of latent CRPV DNAs

To further determine the physical status of the persistent viral DNA, we performed rolling circle amplification (RCA) experiments. The RCA can specifically amplify circular DNAs (174) (**FIG 3.1.9 A**). The RCA experiment was initially performed

according to the manufactures' instruction of TempliPhi 100 Amplification Kit. However, the sensitivity was low, which is why we optimized the protocol by adding an additional specific viral primer set for SE6/LE6 into the reaction. After optimizations, the RCA detects at least 0.1 pg of pLAII-CRPV pure plasmid DNA (**FIG 3.1.9 B**). Additionally, the RCA method showed no amplification of CRPV genomes, which are "head-to-tail" integrated into the host genome in Vx2 cells (**FIG 3.1.9 B**).

The RCA method was applied to amplify viral DNA, which was extracted from latently infected skin biopsies. The results showed that RCA amplified CRPV DNA in one of the latent samples (**FIG 3.1.9 C**) indicating that complete episomal CRPV genomes were present in at least in one of the latently infected skin tissues. However, due to the low sensitivity of RCA per se, only samples with higher copy numbers of CRPV DNA (above one copy per cell) were detected. The majority of the viral DNA in latent samples was undetectable (**FIG. S1)**.

In addition, full-length CRPV E1 and E2 were detected in latently infected skin samples containing high viral DNA loads (**FIG 3.1.10**). Sequencing results of the positive bands of E1 and E2 showed 100% matches to the CRPV sequences.

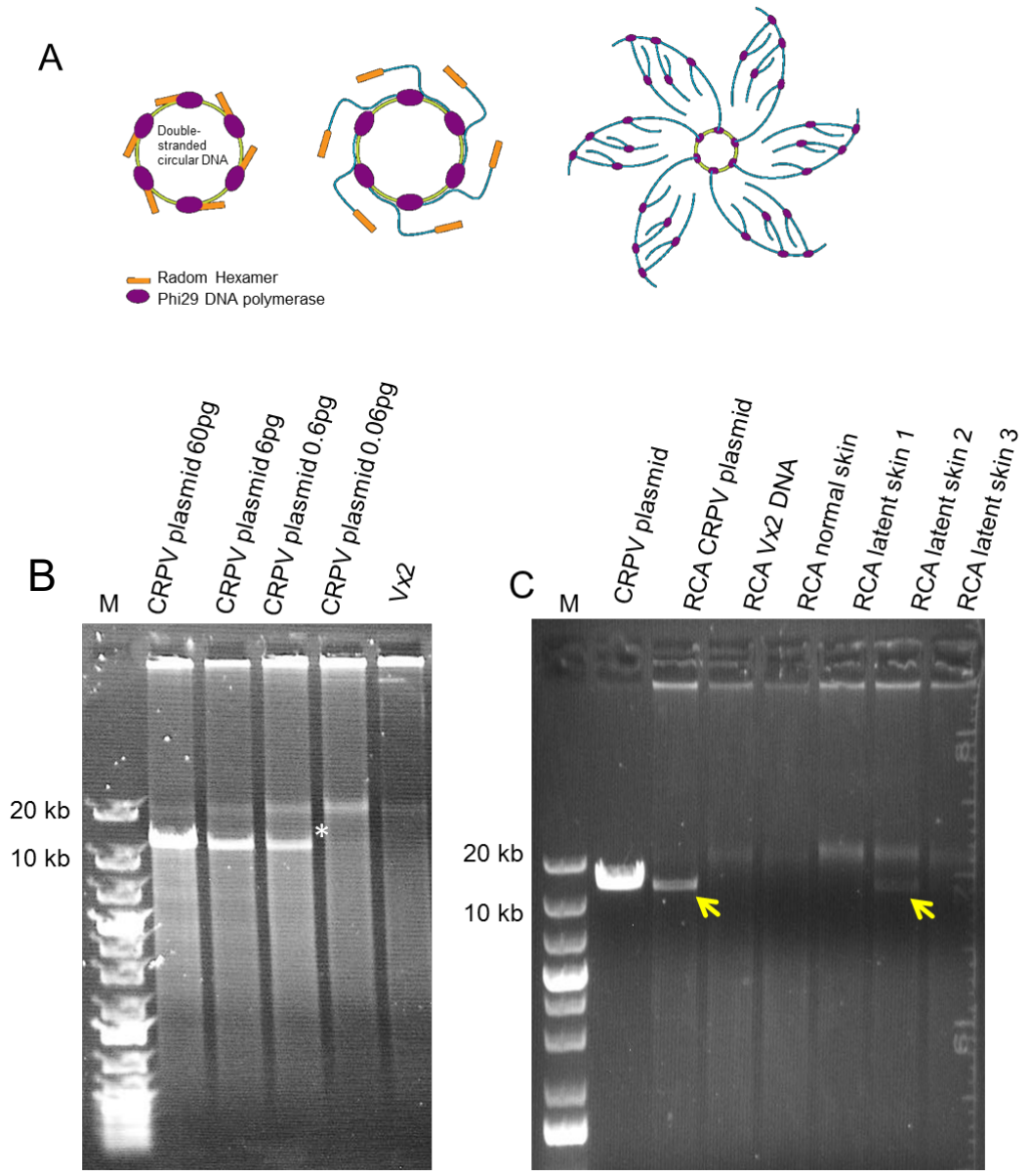

FIG 3.1.9 RCA amplified latent viral DNA. (A) The principle of RCA amplification, adapted from http://www.mclab.com/RCA-DNA-Amplification-Kit.html. (B) Test of the sensitivity and specificity of RCA amplification using serial diluted standard pLAII-CRPV plasmid. M: GeneRuler 1 kb plus DNA lander. (C) RCA amplifed DNA in high viral copy samples. M: 1 kb maker, a: CRPV-pLAII plasmid control, b: RCA amplified CRPV-pLAII plasmid, c: RCA amplified DNAs from Vx2 cells, d-g: RCA amplified DNAs from latently infected skin biopsies. The arrows indicate the positive band.

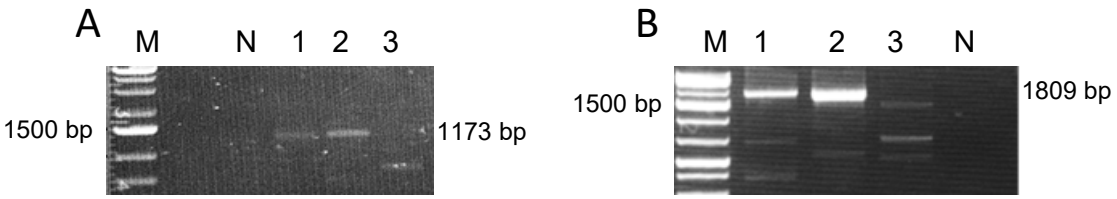

FIG 3.1.10 Detection of full length CRPV E1 and E2 in viral latency. (A) E2 full length detection. M: 1 kb maker, N: negative control, 1 to 3 were latently infected samples from rabbit 9. (B) E1 full length detection. M: 1 kb maker, N: negative control, 1 to 3 were latently infected samples from rabbit 12. The viral copy numbers of the 3 samples were determined by RT-qPCR, which was 119 copies/100 cells, 143 copes/ 100 cells, and 18 copies/ 1000 cells, respectively.

3.2 The effect of ultraviolet (UV) light on CRPV latent infection

It has previously been reported that low-dose CRPV infection could be facilitated by UVB light in domestic Dutch-Belted rabbit model system shortly after injection (110). Other latent viruses, for example, herpes simplex virus can also be activated by UV light (175). We have demonstrated that CRPV DNA persisted in the infected sites for more than 14 months without causing papillomas (**Table 3.1.2**). We, therefore, asked whether UVB light affects the persistent infection of CRPV infection.

3.2.1 Establish UV light irradiation conditions for NZW rabbit model

To initially determine a suitable UVB intensity for the treatment of rabbit skin, we first established a model for UVB radiation of normal NZW rabbit skin (**FIG 3.2.1 A**) by using different UVB light intensities ranging from 120 mJ/cm^2 to 800 mJ/cm^2 (**FIG 3.2.1 B**). The results showed that an intensity of 450 mJ/cm^2 causes the normal rabbit skin sunburn symptoms such as reddening and peeling of the skin 3-day post radiation (**FIG 3.2.1 B**), but no severe symptoms such as blistering or edema. As UV radiation alone is a casual risk factor of skin tumor and to reduce the strong side effect of UV radiation, we selected an intensity of 200 mJ/cm^2 for the following experiments.

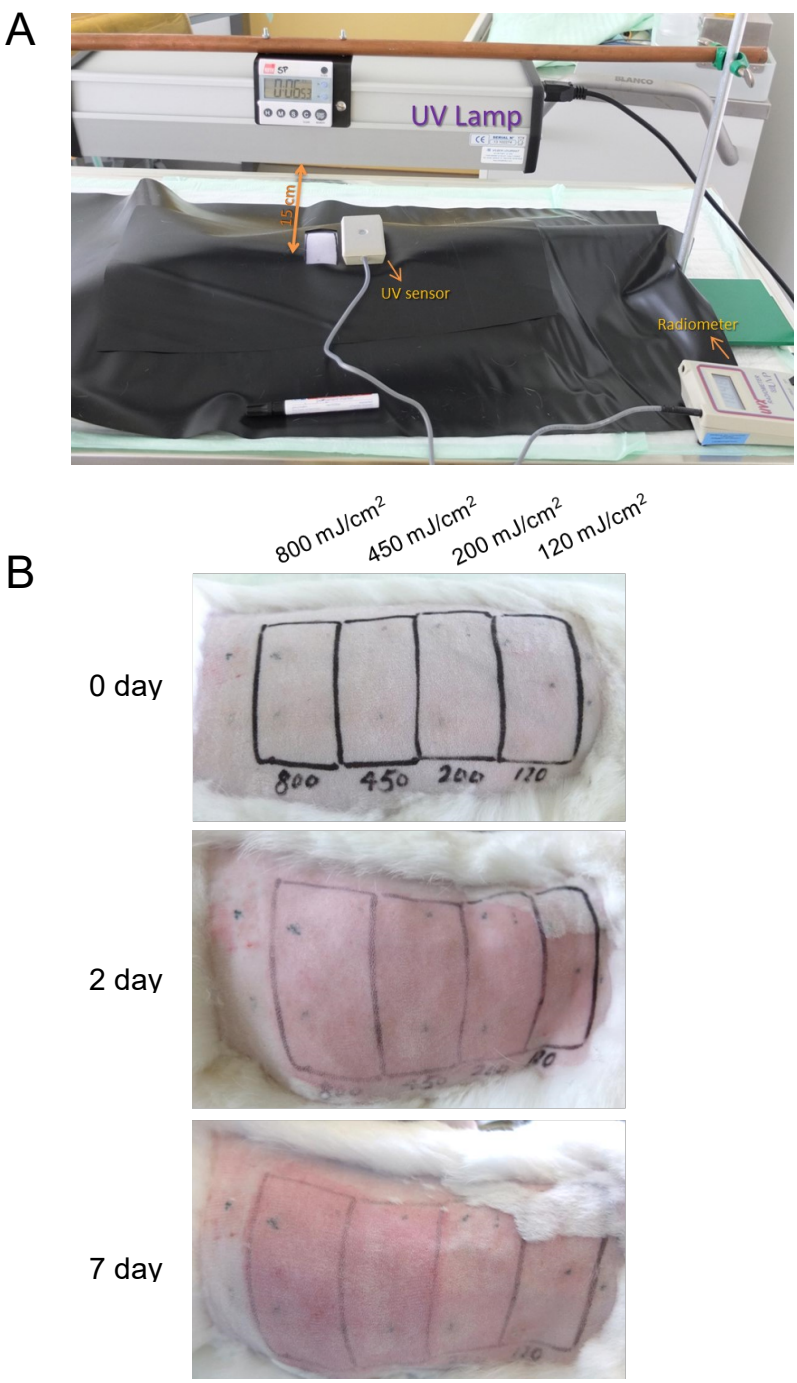

FIG 3.2.1 Effect of UVB on normal rabbit skin. A, UVB lamp construction. The black plastic was tested to completely prevent UVB radiation from passing through, and was used to cover the other parts of the skin. The UV sensor was directly placed near the radiated area to measure the radiation intensity. The measurement results can be read on the radiometer. The distance between UVB lamp and the skin was 15 cm, which results in 1000 μW/cm^2. The intensity of UVB was calculated by the equation: J=Ws. B, Effect of the four intensities of UVB on normal rabbit skin within one week.

3.2.2 The role of UVB light radiation on papilloma formations induced by low dose CRPV infection

In this experiment, four rabbits were infected with 34 ng of CRPV per site with the infection pattern shown in **FIG 3.2.2 A**. Additionally, the cutaneous injection of the pUC19 plasmid was used as a mock control for UVB treatment. UVB light was applied to three of four latently infected rabbits at days 12 and 15 (**FIG 3.2.2 B**). Biopsies were taken at different time points to monitor the amount of viral DNA. We found that the CRPV DNA persisted and observed a slight but insignificant increase after the second UVB irradiation (**FIG 3.2.2 C**). Visible papillomas appeared within 8 weeks post infection on all four latently infected rabbits. Papilloma formation rate was slightly increased and with high variability, but not significant in the UVB-treated group (27.78% UVB-treated sites versus 20.08% untreated site). Despite the same treatments, rabbit LAT2 developed fewer papillomas (2/24) compared to rabbits LAT 1 (10/24), LAT3 (8/24) and LAT4 (8/24) (**Table 3.2.1, FIG 3.2.2 D**). No papilloma appeared at pUC19 mock inoculated sites.

Table 3.2.1 Summary of papilloma formation within 8 weeks post-infection. (++ indicates two UVB treatments)

Rabbit ID	Treatment	Number of positive sites/ number of infected sites		Efficiency of CRPV inducing papilloma
		CRPV	pUC 19	
LAT 1	UVB ++	10/24	0/8	41.67%
LAT 2	UVB ++	2/24	0/8	8.33%
LAT 3	UVB ++	8/24	0/8	33.33%
LAT 4	UVB -	5/24	0/8	20.08%

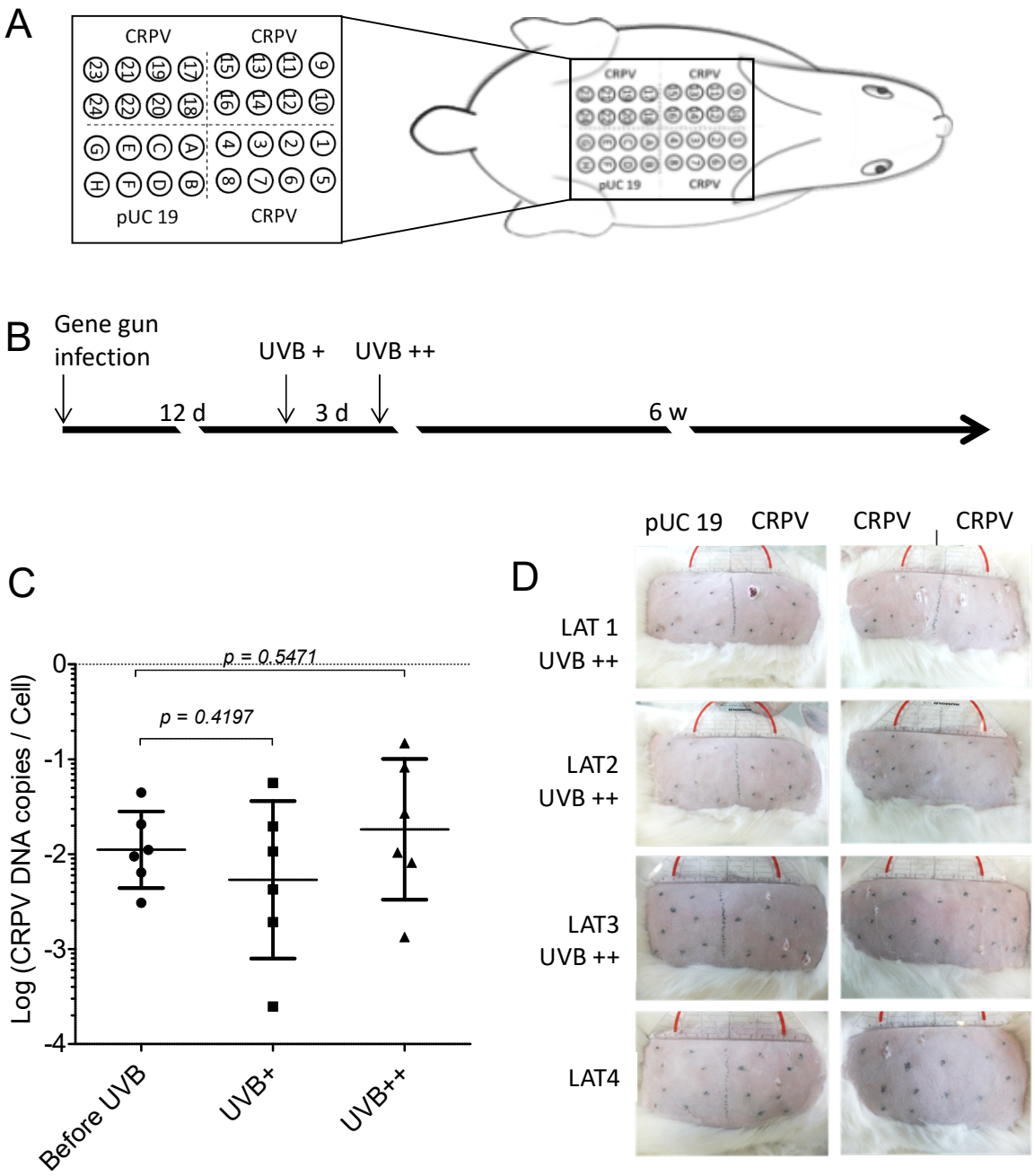

FIG 3.2.2 UVB irradiation of latently infected sites. (A) The infection pattern on the back of rabbits. (B) Schematic overview of the study design. (C) Copy number of CPRV DNA following infection. Each dot represents one sample. Six samples were analysis from each group. The data was log-transformed, and then the unpaired *t*-test was conducted for the statistical significant test. (D) Papilloma formation within 8 weeks post-infection. + indicates one UVB treatment.

3.2.3 The effect of UVB light radiation on CRPV latent infection

In general, spontaneous formation of visible CRPV induced papillomas is completed within 8 to 10 weeks p.i (107). The sites, which harbor viral DNAs without lesions after 8 to 10 weeks post infection, were considered latently infected. The third UVB irradiation was applied to all four rabbits at the 8th-week post infection (**FIG 3.2.3 A**). We observed no new papilloma formation on all four rabbits in the following 8 weeks observation. Instead, two papillomas regressed on rabbit LAT 1 (**FIG 3.3.5** and **Table 3.2.2**). No papilloma appeared at pUC19 mock inoculated sites.

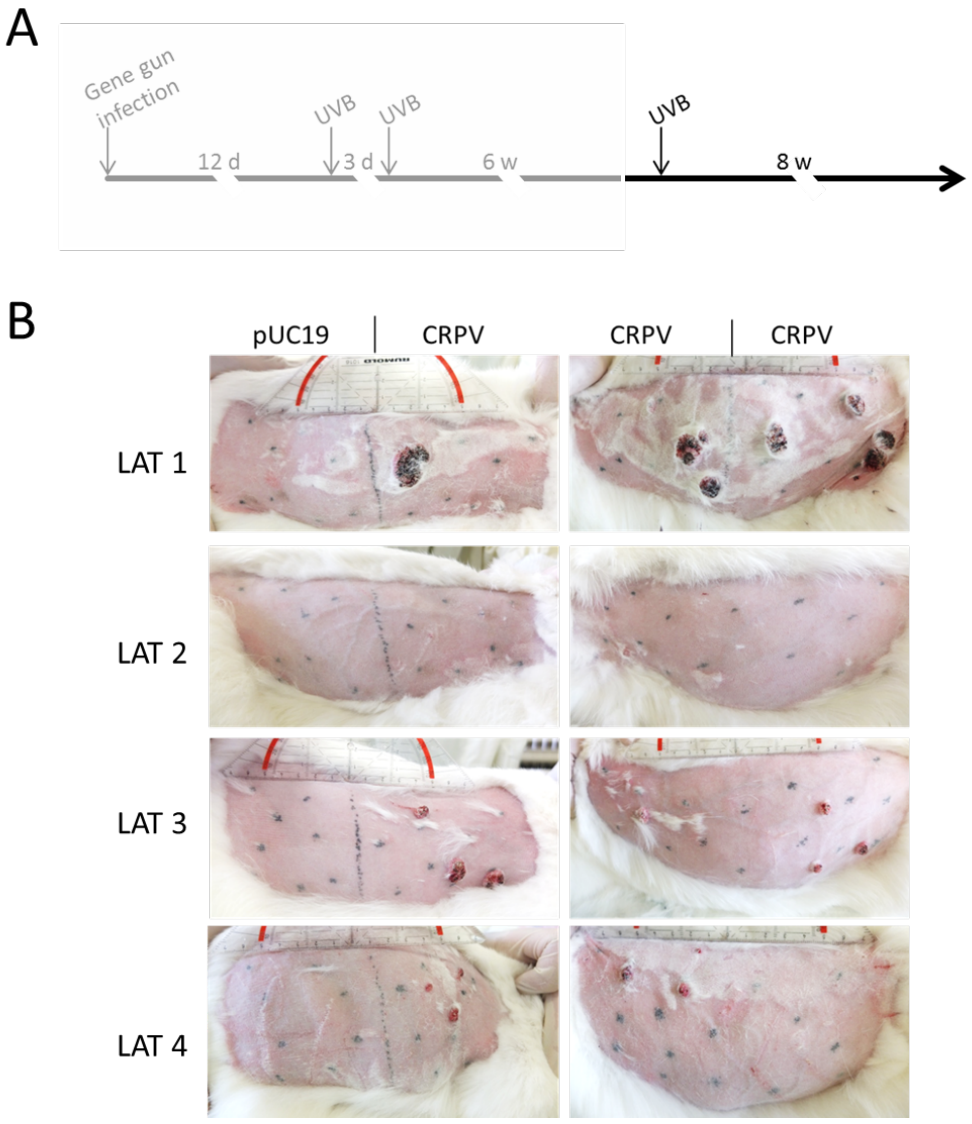

FIG 3.2.3 Papilloma formation within 9 weeks post-infection. All four rabbits were treated with 200 mJ/cm^2 UVB (UVB+). Photographs were taken after two weeks of the late UVB treatment.

Table 3.2.2 Summary of papilloma formation within 16 weeks post-infection. (+++ indicates three UVB treatments, + indicates one UVB treatment)

Rabbit ID	Treatment	Number of positive sites/ number of infected sites		Efficiency of CRPV inducing papilloma
		CRPV	pUC 19	
LAT 1	UVB +++	8/24	0/8	33.33%
LAT 2	UVB +++	2/24	0/8	8.33%
LAT 3	UVB +++	8/24	0/8	33.33%
LAT 4	UVB +	5/24	0/8	20.08%

3.3 Reactivation of latent viral infection by wound healing

Mechanical irritation of rabbit skin prior to infection with CRPV virions or genomes enhanced infectivity, but it is not clear whether or not such treatment has an effect on latent CRPV reactivation (176). For this experiment, we irritated the asymptomatic sites which were infected with 40 ng CRPV DNA (**FIG 3.1.1**). The glass sand paper was used for scraping the infected site until the skin showed some redness. The irritations were performed directly on the tattoo ink marked areas where the viral DNA was inoculated. Irritation treatment was started 7 weeks p.i.. However, we observed a trend but not significant increasing of latent viral copy numbers and no appearance of new papillomas during six weeks of irritation treatment (**FIG S2**).

3.4 Immunosuppression on CRPV latent infection

Drug-induced immunosuppression has been proposed to be one of the risk factors for the reactivation of latent PV infection in OTRs (9, 83). This experiment was designed to test this hypothesis.

3.4.1 Establishment of drug-induced immunosuppression on NZW rabbits

To establish drug-induced immunosuppression conditions on domestic NZW rabbits, we first administered triweekly CsA (15 mg/kg) and bi-weekly Dex (0.5 mg/kg) to two normal rabbits as previously described (106). The body weight of the rabbits was meticulously monitored daily to ensure that animals are maintaining their body weight, as well as food and water intake. The peripheral blood mononuclear cells (PBMCs) were taken from the ear vein of the rabbit every other week post-

immunosuppression, and were subjected to FACS analysis. We found that the rabbits' body weight decreased sharply after four weeks of drug administrations, and one rabbit had to be euthanized because it lost more than 20% of its body weight (**FIG 3.4.1 A**). According to our animal experiment approval, the experiment had to be terminated due to over 20% of weight loss. T-cells of both rabbits were significantly reduced two weeks post-immunosuppression (**FIG 3.4.1 B, C**).

Hence, we reduced the drug dosages by half to 7.5 mg/kg CsA three times per week (Monday, Wednesday, and Friday) and 0.15 mg/kg Dex twice per week (Tuesday and Thursday). Three of four rabbits were administered with CsA and Dex. The health status of all rabbits was closely monitored at each treatment. The PBMCs were subjected to FACS analysis of T-cell populations using the T-cell markers TLC, CD4+ and CD8+. After 10 weeks of immunosuppression, we observed that the rabbits' body weight maintained at a relatively constant level (**FIG 3.4.2 C**). We still found significant reductions of T-cell counts starting two weeks post-immunosuppression. No significant difference in T-cell counts between the lower dosages and the initial high-dose treatment was found (**FIG 3.4.2 C, FIG 3.4.2 B**).

In addition, rabbit LAT2 died with unexpected lung infections. To avoid further complications, we specified our protocol for the drug-induced immunosuppression of NZW rabbit as follows:

Rabbits to be immunosuppressed need to be kept in a separate SPF immunosuppression room and fed with autoclaved water and irradiated hay.

To avoid cross contamination, the experimenter has to change lab coat, gloves, foot and head cover, and disinfect when entering the immunosuppression room.

The body weight, food and water intake of immunosuppressed rabbits need to be checked before each treatment.

7.5 mg/kg CsA three times per week (Monday, Wednesday, and Friday) and 0.15 mg/kg Dex twice per week (Tuesday and Thursday) are multi-point injected subcutaneously into the nuchal fold of the rabbits.

During the course of immunosuppression, when the rabbit lost body weight ≥10% in 5 days, the administration of the drugs should be reduced (e.g, 3.5 mg/kg CsA and

0.07 mg/kg Dex). If the body weight was still decreasing, the treatment had to stop until the rabbit regains 10% weight. The treatment had to be terminated once the rabbit loses over 20% of its initial baseline weight.

Approximately 1 ml of PBMCs was taken via the rabbit's ear vein without anesthesia every two weeks after immunosuppression and then is processed for FACS analysis within 18 hrs.

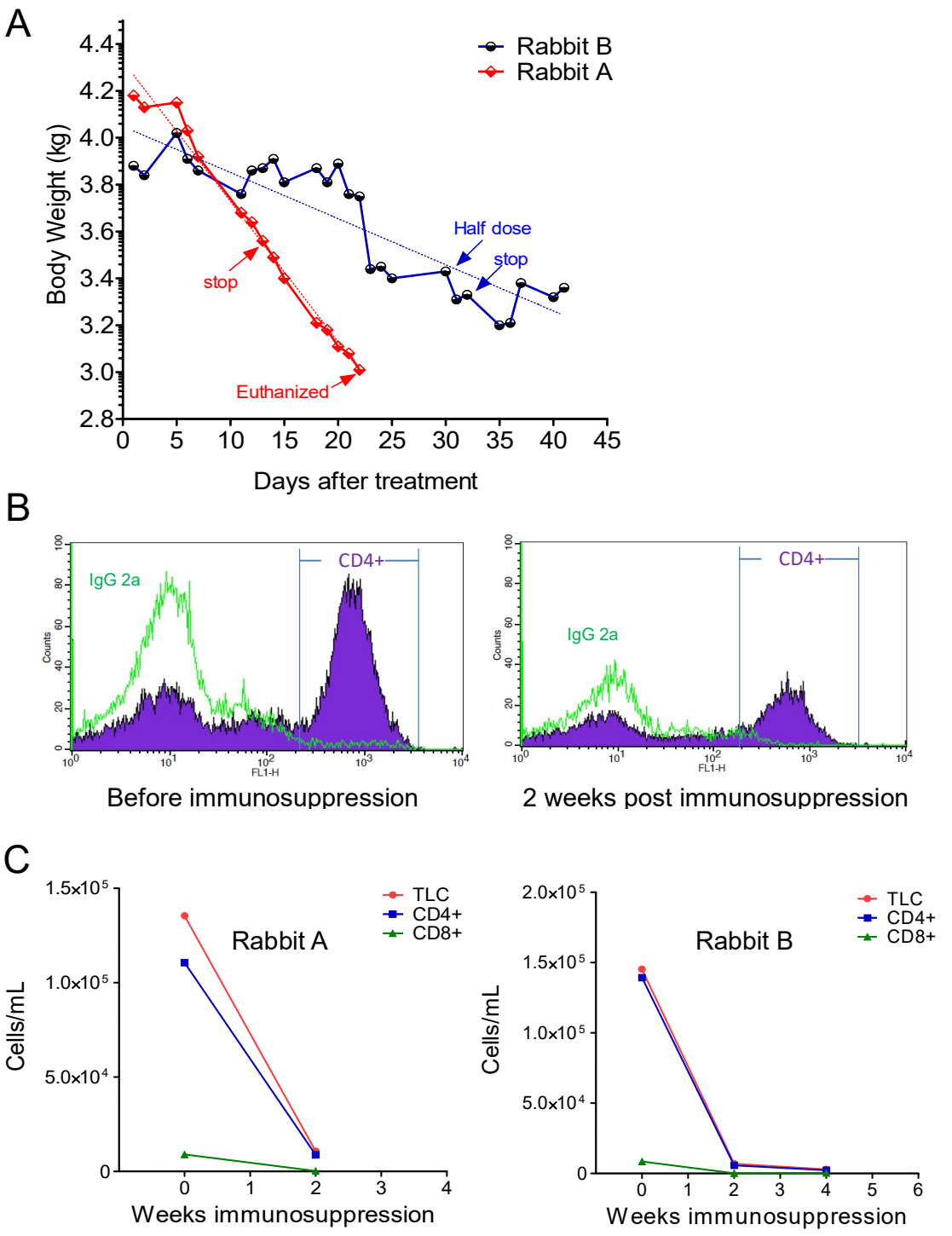

FIG 3.4.1 Drug-induced immunosuppression on NZW rabbits. (A) Body weight of immunosuppressed rabbits. (B) Representative FACS analysis results. IgG 2a is negative/isotype control. (C) FACS analysis of T cells in PBMCs of immunosuppressed rabbits. The week 0 means the PBMCs were taken one day before the immunosuppression.

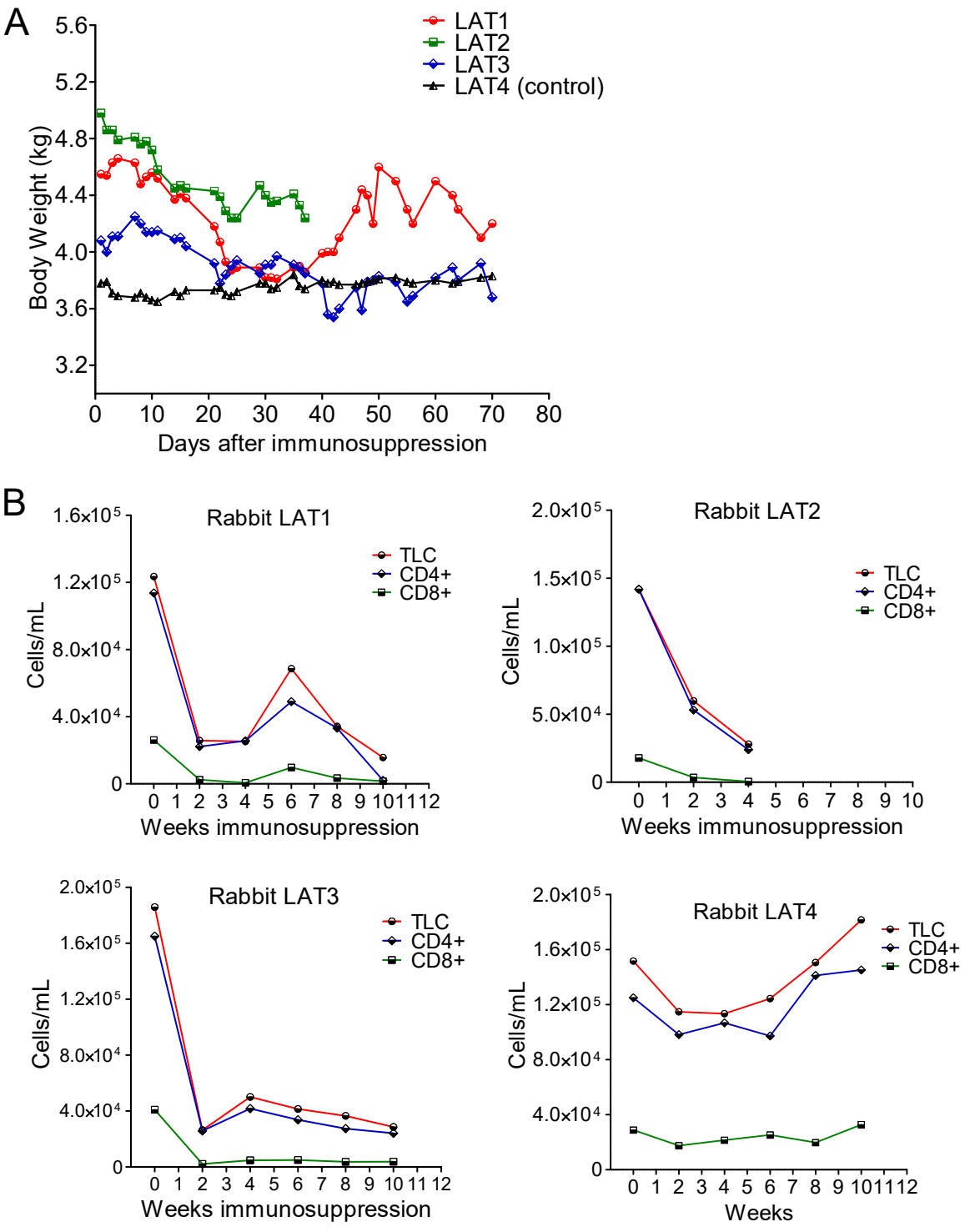

FIG 3.4.2 Establishment of drug-induced immunosuppression on NZW rabbit model. (A) Body weight of immunosuppressed rabbits. Rabbit LAT2 died due to unexpected lung infection. (B) FACS analysis of T cells in PBMCs of immunosuppressed rabbit LAT1, LAT2, and LAT3, and non-immunosuppressed rabbit LAT4. The week 0 means the PBMCs were taken one day before the immunosuppression.

3.4.2 The effect of immunosuppression on CRPV latent infection

After establishing the immunosuppressive treatment conditions, we investigated whether CRPV infections were controlled by decreased immunological control. We infected 4 rabbits with low dose 12 ng CRPV DNA and then administered rabbit 7 and 8 with immunosuppressive drug CsA and Dex one week p.i., and with the rabbit 5 and 6 seven weeks p.i. (**Table 3.4.1**). The immunosuppressed rabbits slowly gained weight (**FIG 3.4.3 A**). T-cell counts were significantly decreased after 2 weeks of immunosuppressive treatment and were maintained at a low level (**FIG 3.4.3 B**). Skin biopsies were taken 6 weeks, 11 weeks and 17 weeks post-immunosuppression. We found that the viral DNA copy number of samples from 11 weeks and 17 weeks post-immunosuppression showed a significant increase compared to that of 6 weeks after immunosuppression (**FIG 3.4.3 C**). There were two samples both from rabbit 8 that had no increase of viral copy number 6 weeks post immunosuppression but showed significant higher viral DNA copy number (> 1 copy/cell) above the average (7 copies/100 cells) 11 weeks and 17 weeks post immunosuppression respectively (**FIG 3.4.3 C**). The papilloma formation on all 4 rabbits was completed within 8 weeks. There was no difference in terms of papilloma formation whether the immunosuppression started one-week p.i. or 7 weeks p.i. (**Table 3.4.1**). Furthermore, there was no appearance of new papillomas during 5 months after the cessation of immunosuppression (**Table 3.4.1**).

Table 3.4.1 Papilloma counts following low viral dose infection and immune-suppression

Rabbit	Infected dose	Immunosuppression start		Treatment duration (weeks)	Papilloma positive/total infected spots (Weeks p.i.)	
		2 weeks p.i.	7 weeks p.i.		Week 10	Week 20
Rabbit 5	12 ng		+	11	1/32 (3.13%)	1/32 (3.13%)
Rabbit 6	12 ng		+	11	3/32 (9.38%)	3/32 (9.38%)
Rabbit 7	12 ng	+		17	3/32 (9.38%)	3/32 (9.38%)
Rabbit 8	12 ng	+		17	1/32 (3.13%)	1/32 (3.13%)

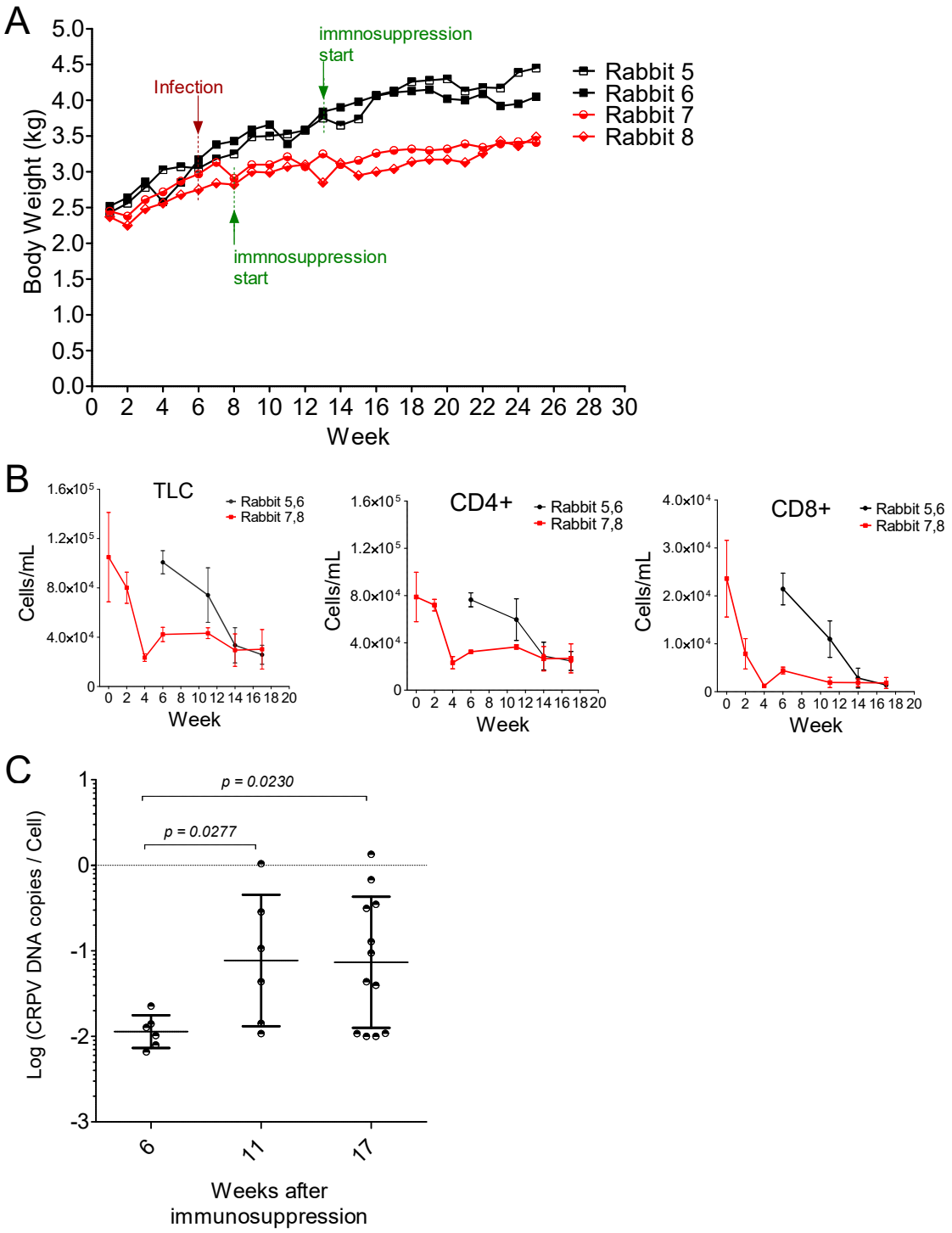

FIG 3.4.3 Drug-induced immunosuppression elevates latent viral DNA copy number. (A) The body weight during treatment of the rabbits. (B) FACS analysis of TLC, CD4+ and CD8+ populations of the PBMCs of immunosuppressed rabbits. (C) The quantification of CRPV DNA copy numbers in latently infected skin following immunosuppression. Each dot represents one sample. The data was log-transformed, and then the unpaired *t*-test was conducted for the statistical significant test.

3.4.3 The effect of CsA based immunosuppression on papillomas formation

CRPV induced papillomas follow a highly predictable development. Papillomas appear earliest 3 - 5 weeks after inoculation, and the formation is virtually complete by 8 to 10 weeks (107). Ten weeks after infections, the infected sites without visible lesions are considered latent infection. In this experiment, we infected 5 rabbits with a high dose (3.8 µg/ site) of CRPV DNA and immunosuppressed 3 of these rabbits starting 2 weeks p.i. (**Table 3.4.2**). The body weight of all immunosuppressed rabbits was constantly growing but slower compared to controls. The efficiency of papilloma formation in the immunesuppressed group is highly variable, but not significantly different from the control group (p = 0.1836). Interestingly, during the latent period, the appearance of 2 new papillomas (Papilloma 1 and 2) 15 weeks p.i. (13 weeks after immunosuppression) and the papilloma #3 appeared 18 weeks p.i. (16 weeks after immunosuppression) on the rabbit 11 in the immunosuppressed group was highly unusual (**FIG 3.4.4 A, Table 3.4.2**), which was not observed in control rabbits. As shown by FACS analysis, T-cells were significantly decreased after 2 weeks of immunosuppression and were maintained at a low level (**FIG 3.4.4 B**). The quantification of the viral DNA in latently infected biopsies from all 3 immunosuppressed rabbits showed higher viral copy numbers (> 1 copy/ cell) in 4 out of 18 biopsies above the average (4 copies/ 100 cells) 16 weeks post-immunosuppression (**FIG 3.4.4 C**). The total number of latently infected sites, which harbor increased viral DNAs in the immunosuppressed group was significantly higher compared to the controls (**FIG 3.4.4 C**). There was no formation of new papillomas within the following 5 months of observation.

Table 3.4.2 Papilloma counts following high viral dose infection and immuno-suppression

Rabbit	Immunosuppression treatment	Infected dose of CRPV DNA	Papilloma positive/total infected spots (Weeks post infection)	
			Week 10	Week 20
Rabbit 9	-	3.8 µg	13/16 (81.25%)	13/16 (81.25%)
Rabbit 10	-	3.8 µg	16/16 (100%)	16/16 (100%)
Rabbit 11	+	3.8 µg	7/16 (43.75%)	9/16 (56.25%)
Rabbit 12	+	3.8 µg	13/16 (81.25%)	13/16 (81.25%)
Rabbit 13	+	3.8 µg	6/16 (37.5%)	6/16 (37.5%)

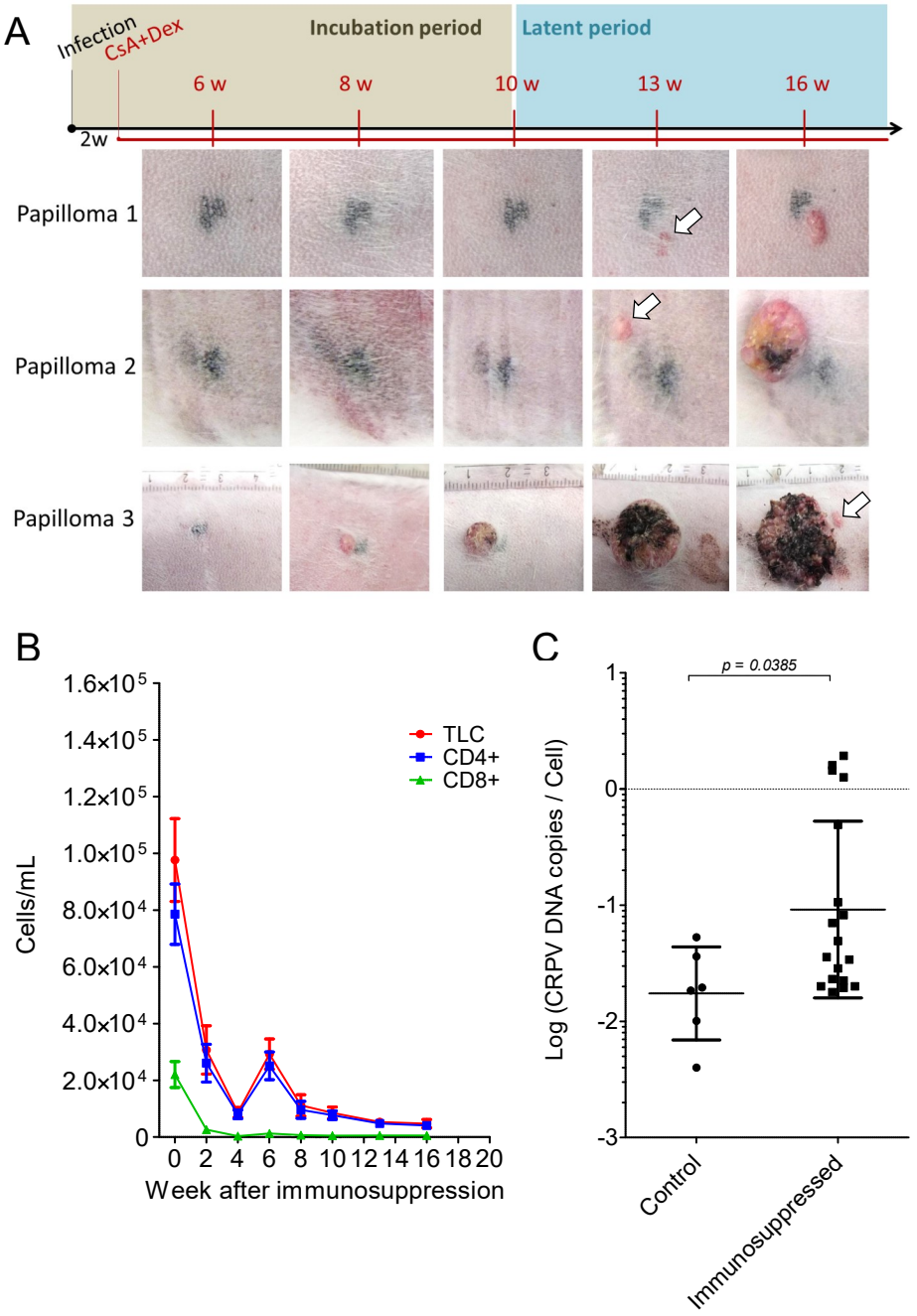

FIG 3.4.4 Drug-induced immunosuppression facilitates the onset of papilloma development and elevates viral copy numbers in high viral dose infection. (A) Three papillomas appeared during the latent period following 13 weeks immunosuppression (papilloma 1, 2) and 16 weeks immunosuppression (papilloma #3) on rabbit 11. (B) FACS analysis of the TLC, CD4+ and CD8+ T-cell populations in the peripheral blood of all three immunosuppressed rabbits. The mean ± SDs of T-cell populations at each time point were showed in the graph. (C) The quantification of CRPV DNA copy numbers in latently infected skin following 16 weeks immunosuppression. Each dot represents one sample. The data was log-transformed, and then the unpaired *t*-test was conducted for the statistical significant test.

3.4.4 The effect of immunosuppression on the susceptibility of low-dose CRPV infection

We have shown that CsA-based immunosuppression had no effect on the papillomavirus infection whether the immunosuppression starts one-week p.i. or 7 weeks p.i. (**Table 3.4.1**). In this experiment, we tested the effect of immunosuppression prior infection on the papilloma formation induced by low-dose CRPV infection. Five rabbits were infected with 10 ng CRPV DNA, of which three were immunosuppressed 2 weeks prior infection (**FIG 3.4.5 A**). The immunosuppression period lasted 16 weeks. T-cells were significantly decreased 2 weeks after drug-induced immunosuppression and were maintained at a low level (**FIG 3.4.5 B**). The body weight of all immunosuppressed rabbits was constantly growing. The formation of all papillomas was virtually completed by week 10 p.i.. No new papilloma appeared within 20 weeks p.i.. The efficiency of papilloma formation 10 weeks p.i. is highly variable, but not significantly different between the immunosuppressed group and the controls (p = 0.522) (**Table 3.4.3**).

Table 3.4.3. Papilloma formation following immunosuppression and low viral dose infection.

Rabbit	Infected dose of CRPV DNA	Immunosuppression 2 weeks prior infection	Papilloma positive/ total infected spots (weeks post infection)	
			Week 10	Week 20
Rabbit 14	42 ng	-	1/16 (6.25%)	1/16 (6.25%)
Rabbit 15	42 ng	-	4/16 (25%)	4/16 (25%)
Rabbit 16	42 ng	+	0/16 (0)	0/16 (0)
Rabbit 17	42 ng	+	1/16 (6.25%)	1/16 (6.25%)
Rabbit 18	42 ng	+	2/16 (12.5%)	2/16 (12.5%)

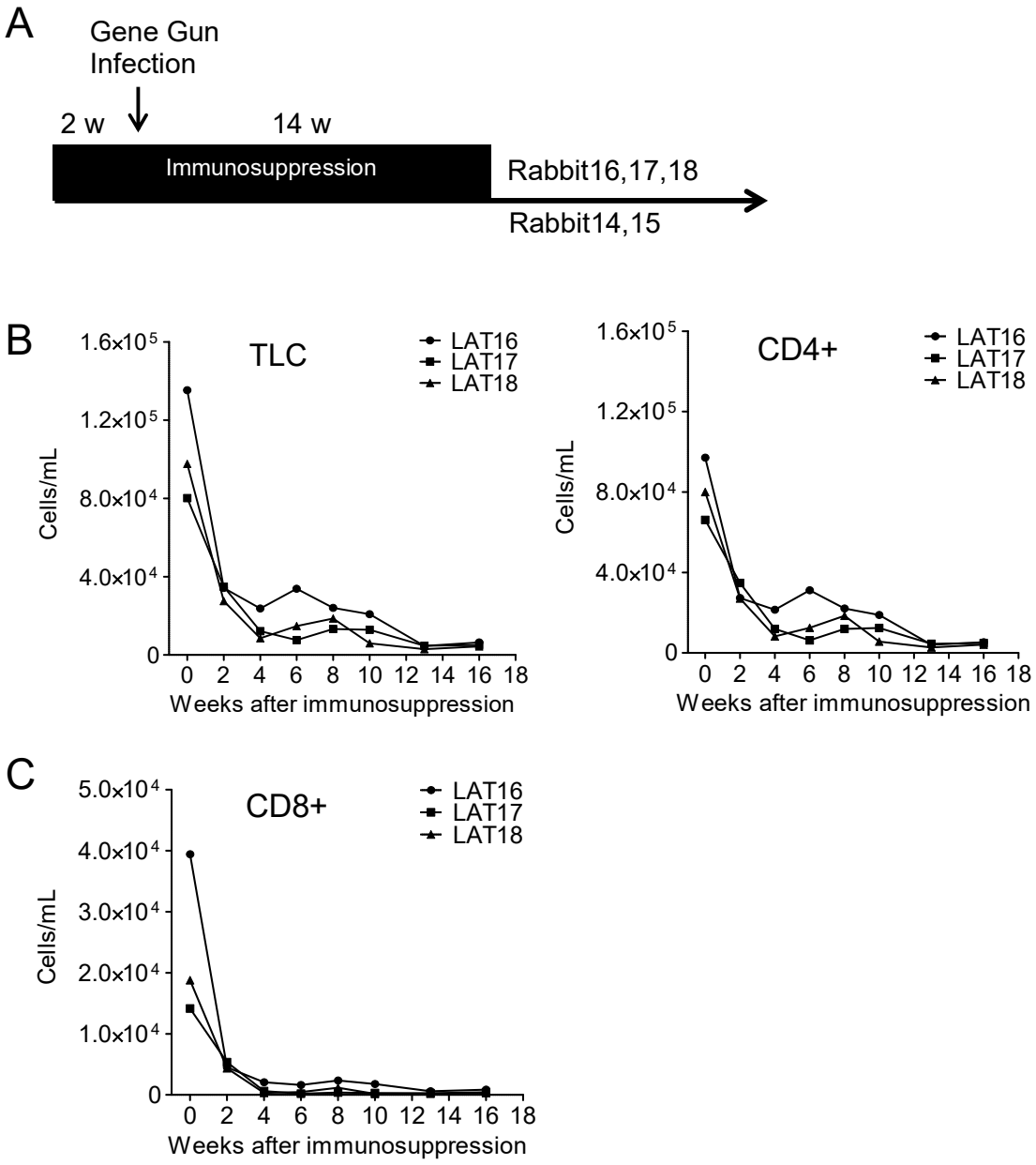

FIG 3.4.5 The effect of immunosuppression on the susceptibility of low-dose CRPV infection. (A) Schedule of the CsA-based immunosuppression. (B) FACS analysis of the TLC, CD4+ and CD8+ T-cell populations in the peripheral blood of immunosuppressed rabbits

3.5 The effect of immunosuppression and UV light radiation on CRPV latent infection

We have shown in **Chapter 3.2** that irradiation using 200 mJ/cm^2 of UVB light had no effect on latent CRPV infection, and in **Chapter 3.4** we observed no increased tumor formation, but an increase of viral DNA copy numbers in latently infected skin sites upon immunosuppression. In this experiment, we intended to investigate the effect of the combination of the immunosuppression and the UV light radiation on the viral latent infection.

3.5.1 Establish UVA/B light radiation conditions on NZW rabbit model

As shown the low intensity of UVB (200 mJ/cm^2) did not significantly affect CRPV latent infection. We then asked whether the UV-mediated sunburn effect might be required for the activation of latent viral infection. Therefore, as previously published (177) we applied a combination of UVB (1 J/cm^2) and UVA (5 J/cm^2) to two rabbits to test the sunburn effect. Indeed the UVA/B treatment caused severe reddening of the rabbits' skin after 3 days, and peeling of the dead skin 2 weeks post radiation, but no severe symptoms such as blistering, or edema (**FIG 3.5.1**).

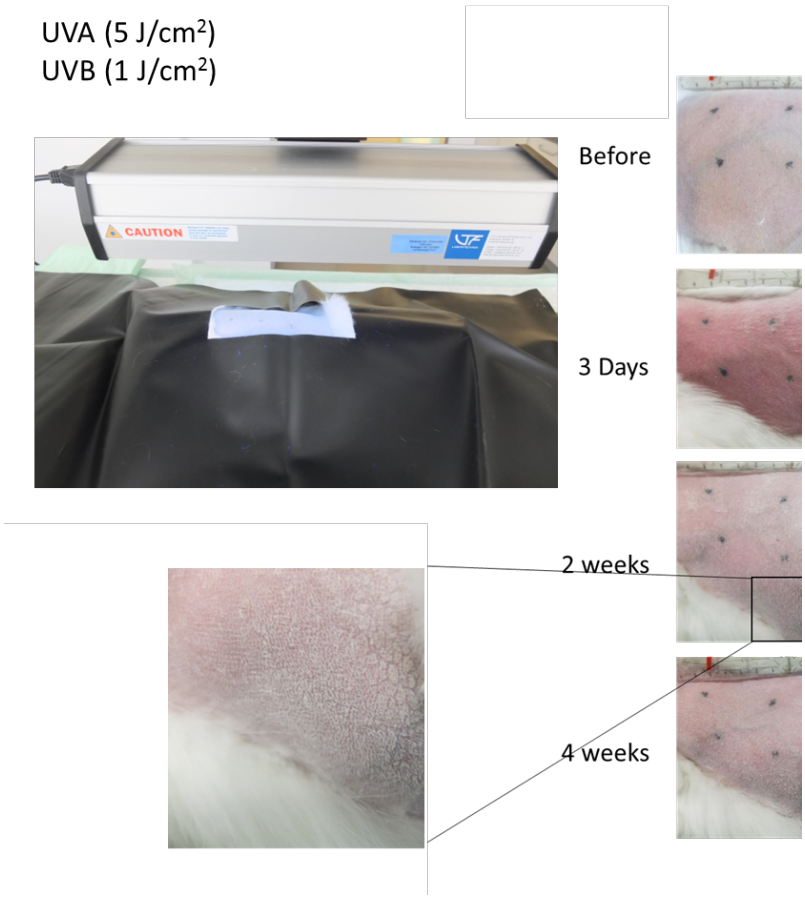

FIG 3.5.1 Sun-burn effects on the NZW rabbit's back skin under 5 J/cm^2 of UVA and 1 J/cm^2 of UVB.

3.5.2 The effect of immunosuppression combined with UVA/B light on CRPV latent infection

To address whether latent viral infection benefits from decreased immunological control and UV radiation, a combination of drug-induced immunosuppression and UV radiation was performed. The five rabbits used in this experiment were infected with 42 ng CRPV (**Table 3.4.3**). The immunosuppressive drugs were applied to three of the five infected rabbits 20 weeks p.i. (**FIG 3.5.2 A**). The UVA/B radiation was then performed 2 weeks after immunosuppression (22 weeks p.i.) (**FIG 3.5.2 A)**. The immunosuppression period lasted 16 weeks. The FACS analysis showed that the T-cell counts were significantly reduced by drug treatment and were controlled at a low level during the experiment (**FIG 3.5.2 B**). Latently infected skin biopsies were taken

16 weeks post-immunosuppression for analysis. As shown by RT-qPCR, the latent viral copy numbers were elevated in latently infected skin biopsies compared with the controls (**FIG 3.5.2 C**). No new papilloma appeared during or after the immunosuppression period (**Table 3.5.1**).

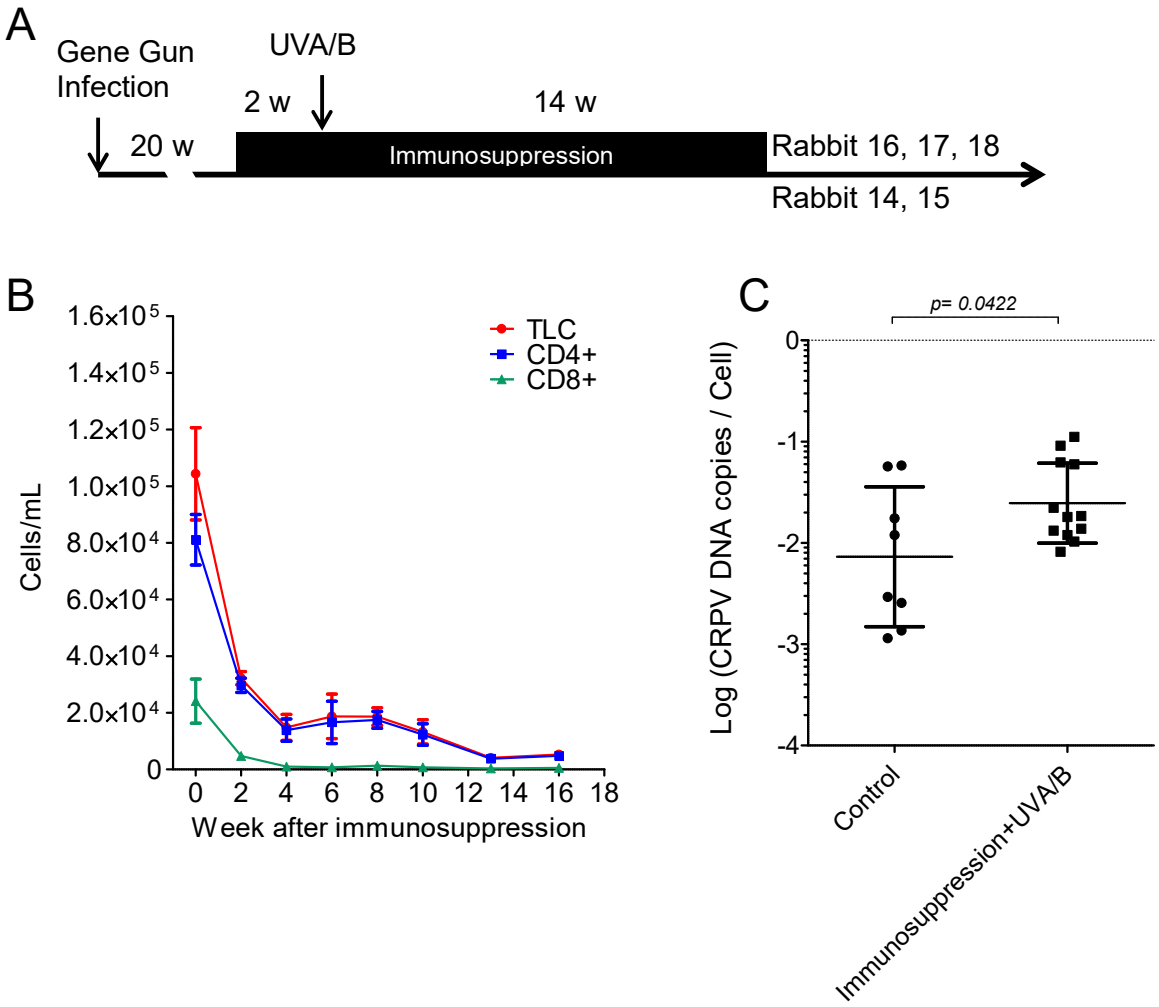

FIG 3.5.2 The role of drug-induced immunosuppression and UV radiation in viral latent infection. (A) Schedule of the CsA-based immunosuppression and UV radiation. (B) FACS analysis of the TLC, CD4+ and CD8+ T-cell populations in the peripheral blood of all three immunosuppressed rabbits. The mean ± SDs of T-cell populations at each time point were showed in the graph. (C) The quantification of CRPV DNA copy numbers in biopsies of latently infected skin sites at 16 weeks of immunosuppression. Each dot represents one sample. The data was log-transformed, and then the unpaired *t*-test was conducted for the statistical significant test.

Table 3.5.1. Papilloma formation following low viral dose infection, immune-suppression and UVA/B radiation.

Rabbit	Infected dose of CRPV DNA	Immuno-suppression treatment	UVA(5J/cm^2) UVB (1J/cm^2)	Papilloma positive/total infected spots (weeks post infection)	
				Week 20	Week 36
Rabbit 14	42 ng	-	-	1/16 (6.25%)	1/16 (6.25%)
Rabbit 15	42 ng	-	-	4/16 (25%)	4/16 (25%)
Rabbit 16	42 ng	+	+	0/16 (0)	0/16 (0)
Rabbit 17	42 ng	+	+	1/16 (6.25%)	1/16 (6.25%)
Rabbit 18	42 ng	+	+	2/16 (12.5%)	2/16 (12.5%)

Four weeks after the first UVA/B radiation, we repeated the treatment (**FIG 3.5.3 A**). Unfortunately, one of the immunosuppressed rabbit 18 suddenly lost more than 20 % of body weight in one week after the UVA/B radiation for unknown reasons; therefore it was excluded from the experiment. Skin biopsies were taken 16 weeks post-immunosuppression at latently infected sites and were analyzed by RT-qPCR. The results showed that there were 2 samples with higher viral copies (>1 copy/ cell) above the average (1 copy/ 500 cells). However, overall the viral DNA copy number in the taken samples showed no significant increase in the treated group compared to the controls (**FIG 3.5.3 B**). No papillomas appeared during the immunosuppression periods and following 5 months after cessation of immunosuppression.

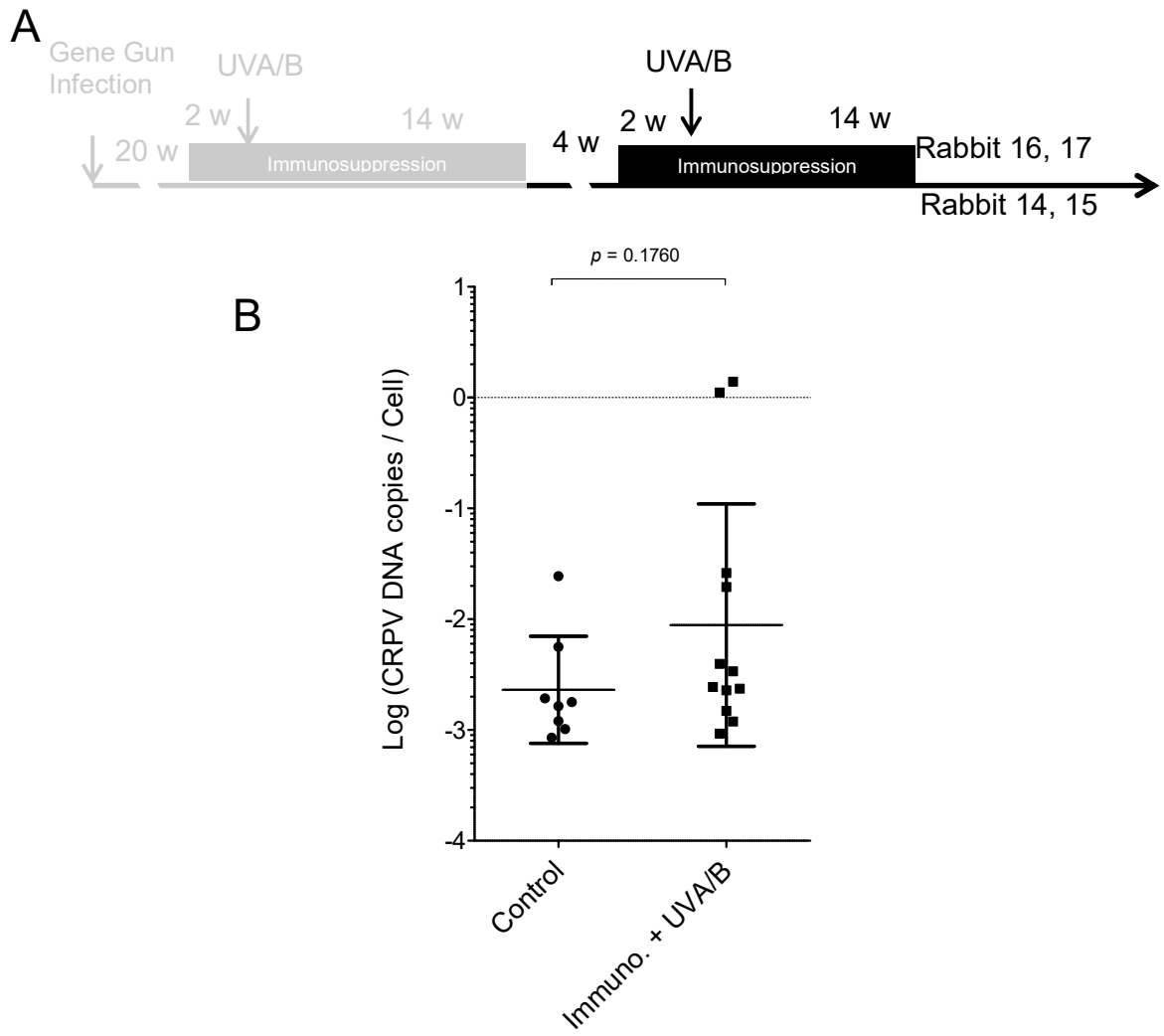

FIG 3.5.3 Repeated treatment of CsA-based immunosuppression and UV radiation. (A) Schematic illustration of the experiment. (B) The quantification of CRPV DNA copy numbers in latently infected skin biopsies 16 weeks post immunosuppression. Each dot represents one sample. The data was log-transformed, and then the unpaired *t*-test was conducted for the statistical significant test.

3.6 The effect of immunosuppression on pre-existing papilloma growth

3.6.1 The effect of immunosuppression on pre-existing papilloma growth

During our pilot experiments of finding the optimal immunosuppression conditions, we observed that pre-existing papillomas grew much faster under CsA-based immunosuppressive treatment than the untreated controls (**FIG S3**). To confirm the observation, we carefully followed and measured the volume of single papillomas at

all infected sites (**Table 3.4.2**). Papilloma sizes were measured weekly for 10 weeks. We observed that the dynamic growth of papillomas at all infected sites of the 3 immunosuppressed rabbits (rabbit 11, 12 and 13) was significantly faster (**FIG 3.6.1**) compared to the non-immunosuppressed controls (rabbit 9 and 10). Despite under the same treatment, the papillomas on rabbit 13 appeared to have a slower growth rate compared to rabbit 12 and 11, but still significant faster compared to control rabbits (**FIG 3.6.1 C**). Rabbit 12 had to be euthanized in week 13 post-immunosuppression due to an overburden of large papillomas (**FIG 3.6.1 A, C**). Furthermore, after the cessation of immunosuppression of rabbit 11 and 13, we observed the average volume of papillomas declined 25% within 8 weeks, then following constant normal growth speed (SGR: 4%/day) in the following 7 months of observation. When we reverted the experiment and immunosuppressed one of the control rabbit 9, we observed a significant increase in the volume of all papillomas within 8 weeks. The size of papillomas on the remaining control rabbit 10 showed no significant increase in the same period (**FIG 3.6.2**).

The figure is on the next page

FIG 3.6.1 Drug-induced immunosuppression facilitates papilloma growth. (A) The growth curve of the average papilloma volume in the immunosuppressed group (rabbit 11, 12 and 13) and control group (rabbit 9 and 10). The numbers of papilloma measured for each rabbit were: 12 papillomas from rabbit 9 and 10; 7 papillomas from rabbit 11; 13 papillomas from rabbit 12; 5 papillomas from rabbit 13. Rabbit 12 had to be euthanized after 13 weeks of immunosuppression due to the large sizes of papillomas. (B) The specific growth rate (SGR) of a single papilloma. Each dot in the graph represents the average SGR of one papilloma. The Mann-Whitney test was conducted for the statistical significant test. (C) The growth speed of papillomas in each rabbit. (D) Represent photos of non-immunosuppressed rabbit (rabbit 9) and immunosuppressed rabbit (rabbit 12) after 13 weeks immunosuppression.

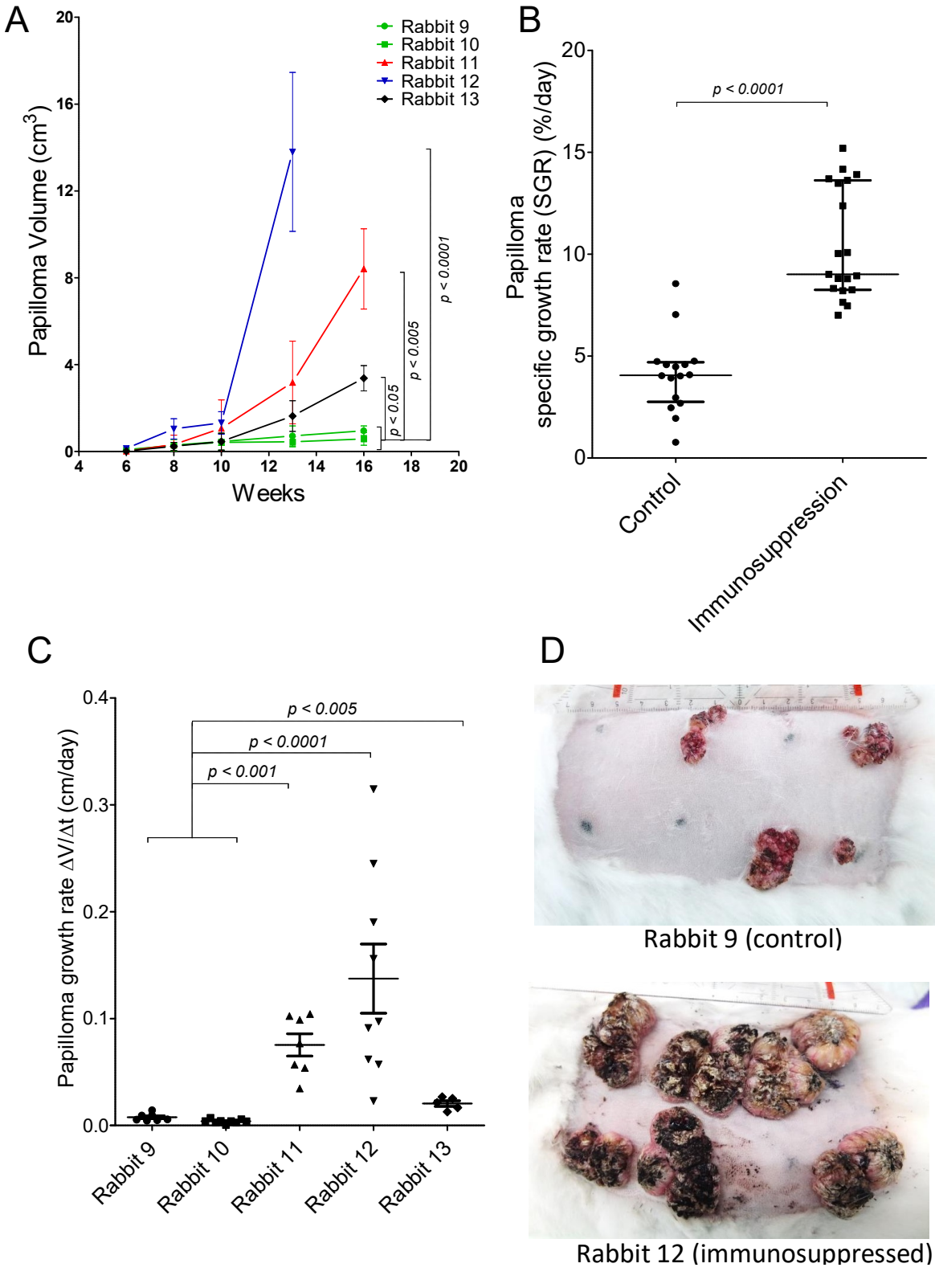
A
Papilloma Volume (cm3)
Weeks
Rabbit 9
Rabbit 10
Rabbit 11
Rabbit 12
Rabbit 13
p < 0.0001
p < 0.005
p < 0.05
B
Papilloma specific growth rate (SGR) (%/day)
p < 0.0001
Control
Immunosuppression
C
Papilloma growth rate ΔV/Δt (cm/day)
p < 0.005
p < 0.0001
p < 0.001
Rabbit 9
Rabbit 10
Rabbit 11
Rabbit 12
Rabbit 13
D
Rabbit 9 (control)
Rabbit 12 (immunosuppressed)

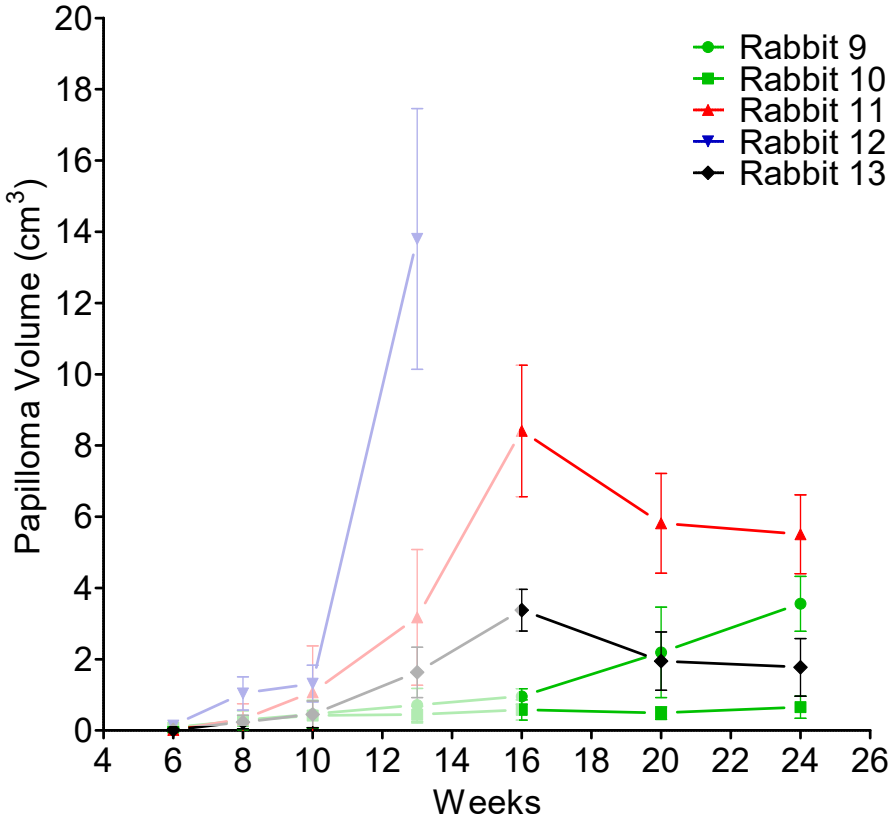

FIG 3.6.2 Reverse effect of immunosuppression or cessation of immunosuppression. After the cessation of the immunosuppression on rabbit 11 and 13, we observed a decreased volume of the papillomas within 8 weeks, and vice versa. When we started to immunosuppression on one of the control rabbit 9, we observed significant increase volume of papilloma in all infected sites.

3.6.2 The effect of immunosuppression on viral DNA copies and E1^E4 transcripts in papillomas.

To determine whether immunosuppressant treatment contributes to viral infection, we quantified viral DNA copies and E1^E4 transcripts in papillomas. To do so, papillomas were surgically removed at 13 weeks post-immunosuppression (15 weeks p.i.) from both the immunosuppressed and the control rabbits, and subjected them to RT-qPCR analysis, the results showed that there were no significant differences in either the viral genome copy numbers (**FIG 3.6.3 A**) or E1^E4 expressions (**FIG 3.6.3 B**) between the two groups.

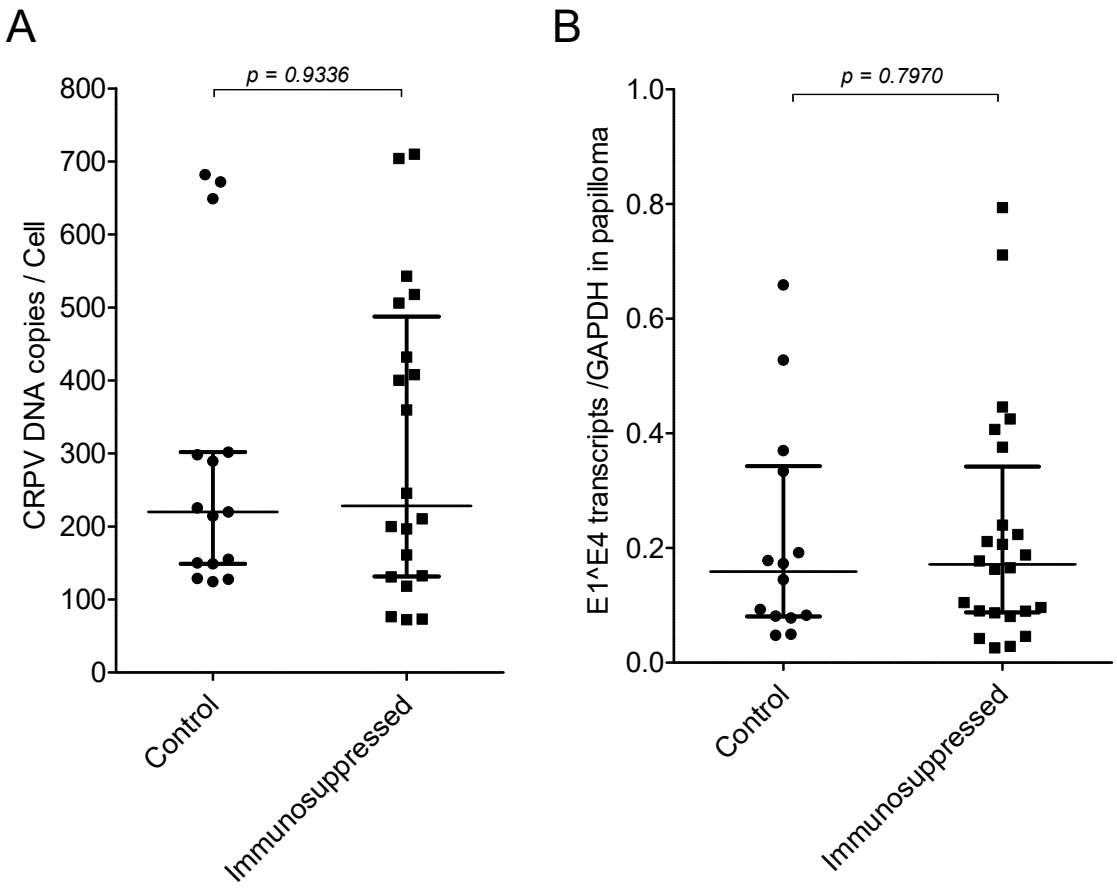

FIG 3.6.3 Drug-induced immunosuppression does not influence viral genome copy numbers and viral gene expression within papillomas. (A) CRPV DNA copy numbers in papillomas of the control group (rabbit 9, 10) and in the immunosuppressed group (Rabbit 11, 12 and 13). There is no significant difference between these two groups. (B) The level of CRPV E1^E4 transcripts in papillomas of the control group and the immunosuppressed group. No significant difference was observed between these two groups. The Mann-Whitney test was conducted for the statistical significant test.

3.6.3 The role of immunosuppression on immune response and T-cell cytotoxicity

By FACS analysis, we found that the TLC, CD4+, and CD8+ cells were significantly decreased in PBMCs of rabbits that were immunosuppressed for 13 weeks (**FIG 3.6.4 A**). In order to obtain a more detailed overview of the immune situation in immunosuppressed rabbits, we analyzed the expression of immune response-associated cytokines both in the PBMCs and papillomas. Total RNA was isolated from PBMCs and papillomas 13 weeks after immunosuppression for the analysis of expression levels of cytokines associated with T-cells and cytotoxicity: Transforming

growth factor beta (TGF-β), interleukin 10 (IL-10), interferon γ (IFN- γ), interleukin 6 (IL-6), interleukin 8 (IL-8), interleukin 17a (IL-17a), interleukin-1 beta (IL-1β), Chemokine (C-C motif) ligand 4 (CCL4), FAS-ligand (Fas-l), perforin 1 (Pfr-1), Tumor necrosis factor alpha (TNFα). The $2^{-\Delta\Delta cp}$ method was used for RT-qPCR relative quantification. We found that the drug-induced immunosuppression broadly down-regulated cytokines associated with T-cell response and cytotoxicity in both the PBMCs and in papillomas (**FIG 3.6.4 B**). However, there are exceptions, for instance, the expression of genes including IL8 and IL-1β, which were specifically up-regulated only in papilloma samples (**FIG 3.6.4 B**).

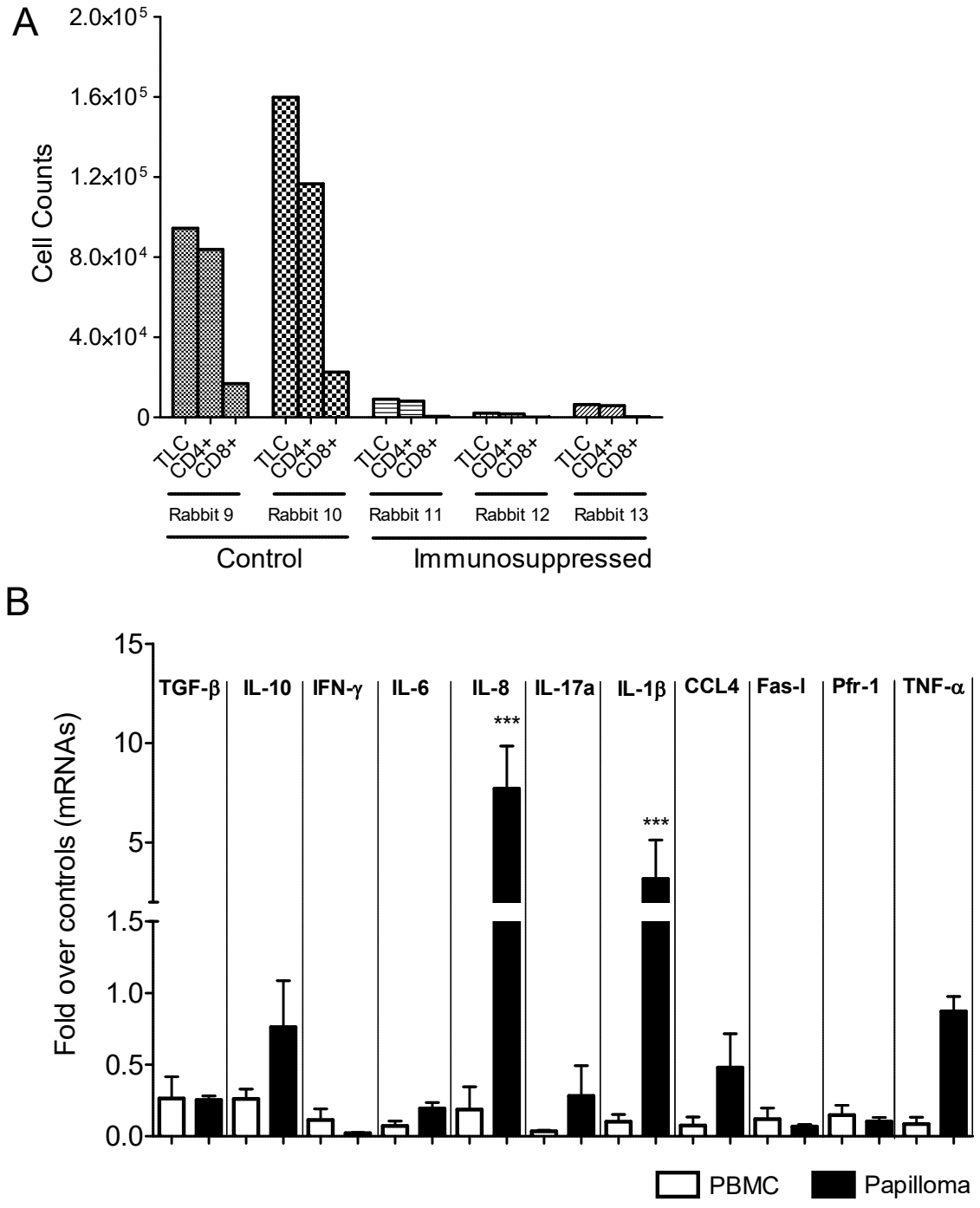

FIG 3.6.4 Gene expression profiles associated with T-cells and cytotoxicity. (A) FACS analysis of T cells in the PBMCs 13 weeks post immunosuppression. (B) The expression of cytokines in PBMCs versus papillomas 13 weeks post immunosuppression. The gene expression of cytokines of immunosuppressed group (rabbit 11, 12 and 13) was normalized to that of the non-immunosuppressed control group (rabbit 9 and 10), respectively. $P < 0.001$: ***.

3.6.4 The effect of the immunosuppresive drugs on the rabbit cell proliferation *in vitro.*

It has been shown that the immunosuppressant drugs such as CsA can induce *in vitro* cell proliferation and tumorigenesis independent of the immune system in different human-derived cells (178, 179). This experiment was designed to investigate the possible effect of immunosuppressant drugs on cell proliferation of rabbit-derived cell lines such as AVS cell line and Vx2 cell line. The immunosuppressant Sirolimus (SRL), known as an inhibitor of the mammalian target of rapamycin (mTOR), was used as a control.

We first tested a therapeutic concentration 250 nM (0.3 ng/μL) CsA, 100nM (0.04 ng/μL) Dex, and 100 nM (0.1 ng/μL) Sir on AVS cells growth, respectively as previously described (178, 180, 181). To do so, 5000 AVS cells in 100 μL KSFM with EGF and BPE were seeded in 24 well collagen I coated plates. Twenty-four hours after seeding, the culture medium was replaced by KSFM medium without BPE, or with BPE containing EGF, CsA, Dex, or SRL, respectively (**FIG 3.6.5**). Five days after treatment, cells were harvested and counted. The results showed that the treatment of CsA increased the AVS cells number compared to the treatment of EGF, Dex or SRL (**FIG 3.6.5**, **FIG S4**).

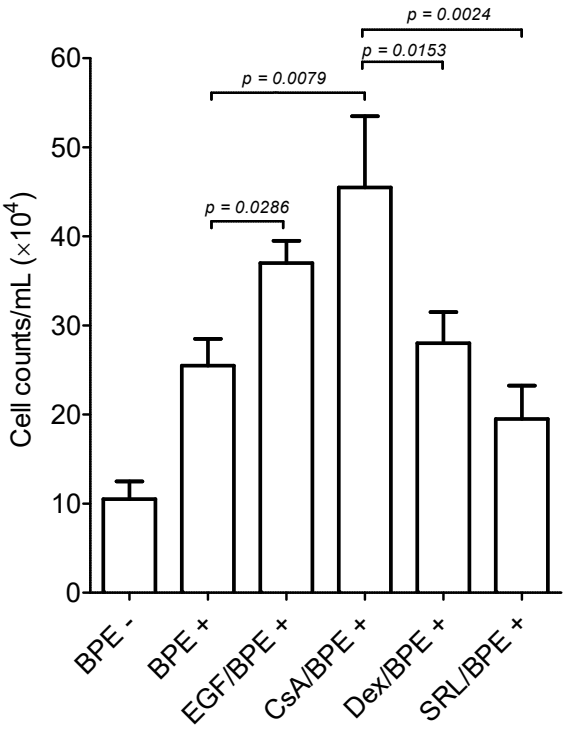

FIG 3.6.5 The effect of BPE, EGF, CsA, Dex, and SRL on rabbit derived cells (AVS) growth. BPE: Bovine Pituitary Extract; EGF: human recombinant Epidermal Growth Factor; CsA: Cyclosporine A; Dex: Dexmethasone; SRL: Sirolimus.

We next investigated the effect of the three immunosuppressants on cell proliferation using WST-1 assay. The results showed that CsA showed growth enhance effects on Vx2 cells at a concentration ranging from 0.1 ng/μL (83 nM) to 1 μg/μL (0.83 mM), whereas Dex and Sir showed no significant effect on Vx2 cell growth (**FIG 3.6.6 A**). In addition, CsA showed an enhanced effect on AVS cell growth at a concentration ranging from 0.1 ng/μL (83 nM) to 10 ng/μL (8.3 μM), whereas Dex and SRL showed growth inhibit effects (**FIG 3.6.6 B**).

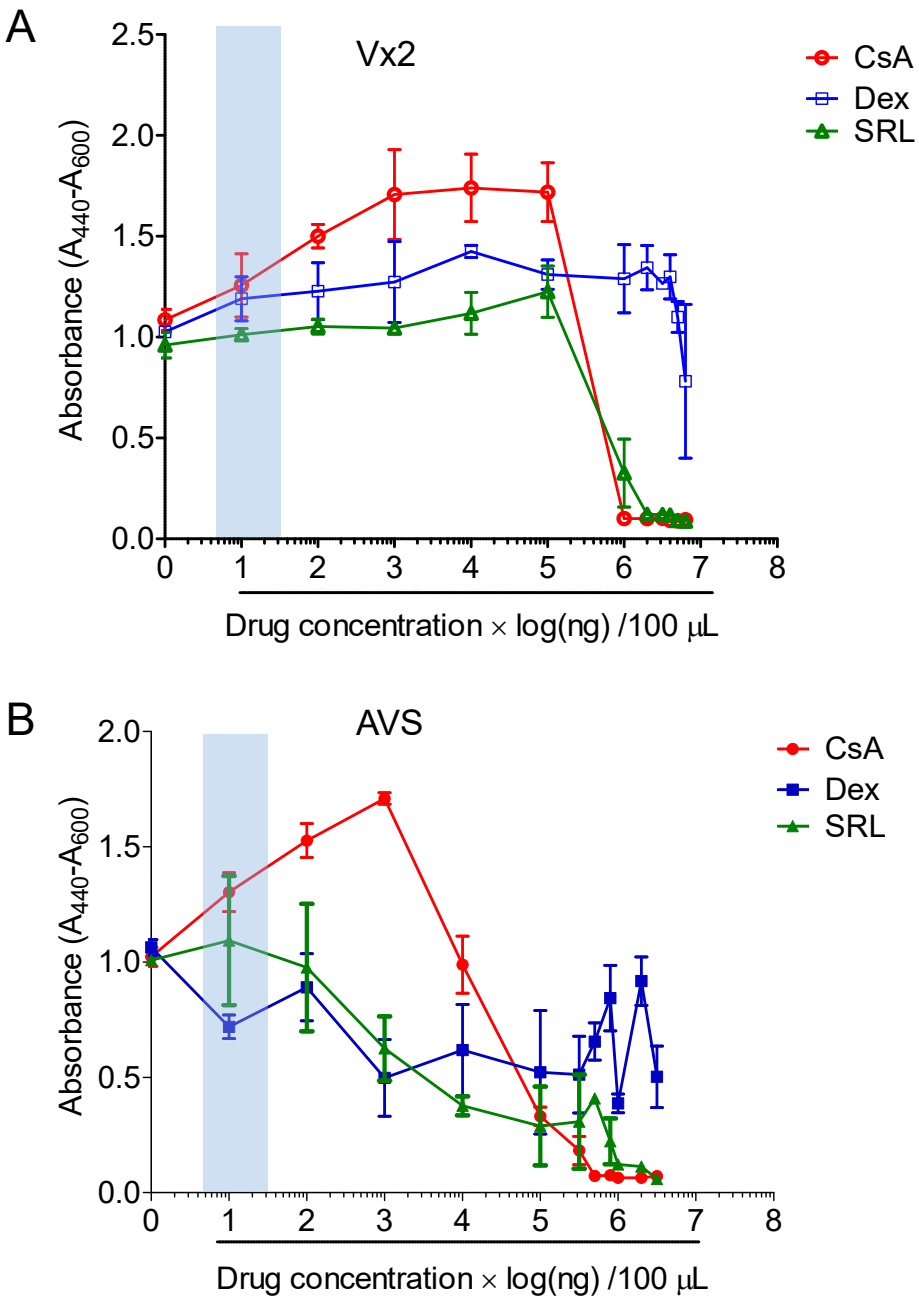

FIG 3.6.6 The effect of immunosuppressive drugs on rabbit derived cells growth. (A) Cell proliferation of Vx2 cells. (B) Cell proliferation of AVS cells. The light blue bar marks the range of therapeutic blood and drug concentrations in rabbits.

4 DISCUSSION

In this study, we established an outbred CRPV/rabbit model to investigate whether latent cuHPVs infections are controlled by the immune system and/or UV radiation. We observed that a level of one viral DNA copy per 200 to 1000 cells can be detected in 88% of the latently infected skin sites more than 14 months p.i.. Viral copy numbers dramatically increased, when latent skin samples were explanted in tissue culture. We also observed an increase in viral genome copy numbers in latently infected skin sites remaining in the animal upon immunosuppression, but no increased tumor formation. Surprisingly, the combination of immunosuppression and UVA + UVB radiation showed no significant difference compared to immunosuppression alone. However, a dramatic increase of pre-existing papilloma growth was observed upon CsA-based immunosuppression. T-cell counts and T-cell associated cytokines were significantly decreased by immunosuppression. Interestingly, the pro-inflammatory cytokines such as IL-8 and IL-1β were significantly upregulated specifically in the fast growing papillomas. Furthermore, our results indicate that the proliferation of rabbit-derived cells was increased upon CsA treatment *in vitro*.

4.1 A CRPV/rabbit model for cuHPV latency study

The aim of this project was to optimize the CRPV model system in order to allow us to study the latent state of the cuHPV life cycle. The CRPV infection of domestic rabbits is the best model for studying cuHPV-associated disease (182), latent infections (109, 110), as well as malignant progression and testing immunotherapeutic strategies (107, 108). In a CRPV/rabbit model, the formation of papillomas is virtually completed by 10 weeks, and invasive malignant progression after 6 - 12 months post-infection (78, 134).

The infection induced by either CRPV virions or viral DNAs in domestic NWZ rabbits is abortive (107). This has the advantage that the risk of new infections or reinfections during reactivation due to virus production and spread is eliminated. Moreover, we used tattoo ink for easy identification of previously infected tissues. We were subsequently able to harvest these sites and study them specifically in more detail. The highest efficiency of papilloma formation is obtained using a gene-gun

system for CRPV DNA inoculation (107). By using this system, we were able to quantify the exact amount of viral DNA being delivered using RT-qPCR and thus are able to evaluate the efficacy of the experiment (**FIG 3.1.1A, Table S1**). The infection of rabbits with CRPV is highly reproducible with almost all rabbits forming visible papillomas within 10 weeks. We used the out-bred NZW rabbits with different genetic background in this study to mimic the real situation in humans.

Previous studies of CRPV infection of domestic Dutch-Belted rabbits demonstrated that a low-titer vrial infection (approximately 10^5 viral particles/1-cm^2 site) resulted in asymptomatic infection with minimal spontaneous activation. Viral DNA could still be detected one-year p.i. (109, 110). In our studies of CRPV latent infection in domestic NZW rabbits, we observed similar results. Inoculation of low-dose CRPV DNA per site resulted in asymptomatic infection at the majority infected site (**FIG 3.1.1B**). Using our highly sensitive RT-qPCR method, we were able to examine CRPV DNA copy number at infected asymptomatic sites and in apparent papillomas. During a latent infection, there appeared to be no significant amplification of viral DNA (**FIG 3.1.2**) and limited viral gene expression (**Table 3.1.2**), which is similar to that was found in the ROPV latent infection model (105). We also observed that the level of viral DNA detected at latently infected sites of our model system is relevant to that was found in the eyebrow hair of immunocompetent people (1 copy per 60 to 600 cells) (68, 183).

4.2 Possible factors that contribute to CRPV latent infection

The skin cells are composed of multiple complex cell compartments such as cells of intermolecular epidermis, hair follicles (HF), sebaceous gland and immune system (76, 184). During the viral latency, most of the skin cells were uninfected, which may dilute out the latently infected cells. The low levels of latent viral copy number per cell in clinical rabbit skin biopsies may therefore not represent the true viral DNA copies per infected cell. However, when the infected skin biopsies were explanted *ex vivo* in suitable conditions, a higher copy number of viral DNAs was observed in the explanted cells (**FIG 3.1.5**). Although it is not clear which type of cells harbor latent viral DNAs in the skin, it is most likely that the CRPV latently infected cells are also present in HFs, as we have previously shown that during productive infection, the primary target cells of CRPV are located in self-renewable HF stem cells (78).

Additionally, we observed that a quarter of the explanted cells express one of the potential HF stem cell markers K15 (**FIG 3.1.6**). It has been shown that cells present in the bulge region of HFs can be quiescent for up to one year (185). It is possible that some viral DNA establishes long-term latent infection in the slow cycling quiescent stem cells. These cells are likely to be activated and undergo cell division or differentiation during normal homeostasis or wound repair resulting in an elevation of viral DNA copy numbers. Accordingly, cells harboring latent viral genome were likely to be activated from their quiescent state when explanted *ex vivo* resulting in a dramatic increase of viral copy numbers (**FIG 3.1.5B**).

It is clearly shown in this study that unlike the latent infection with EBV and HIV (186, 187), the latent CRPVs were not strictly regulated by levels of DNA CpG methylation in the host cells, since no CpG methylation has been found in the promoter region of CRPV latent viral genome (**FIG 3.1.7**). In addition, it is likely that some of the latent viral genomes stay episomal, as circular episomal viral DNA forms can be found and full-length E1 and E2 genes can be detected (**FIG 3.1.9, 3.1.10**). However, we cannot rule out the existence of potential integrated forms in the latently infected cells.

Interestingly, one unexpected finding led us to identify whether the CRPV DNA was replicating in host cells. The *dcm* methylations are known in almost all commonly used cloning bacterial strains such as DH5α *E. coli*, which specifically methylates sequences which contain CCA/TGG (*dcm*) (173). In this study, the original CRPV DNA were amplified using DH5α *E. coli*, and we showed that the *dcm*s of viral plasmid DNA were completely methylated (**Table 3.1.3, FIG 3.1.8**). Those *dcm* methylations were retained only in some of the sequenced clones from latently infected skin sites. However, most of the sequenced clones lost *dcm* methylations indicating that the viral DNAs were newly synthesized in the infected cells, which strongly argues that the latent viral genomes were replicating in the host cells. However, the results also showed that 34% to 48% of the original viral plasmid DNAs with *dcm* methylation were still retained for such long time in an unreplicated form more than 14 months p.i. (**Table 3.1.3**). The exact reason is unclear. As discussed previously, one possible explanation is that these original viral plasmid DNAs were maintained in the slow-cycling quiescent epidermal stem cells.

4.3 Low-dose UVB radiation showed no significant effect on papilloma formation and viral copy numbers

UV light is believed to be an important risk factor for the development of beta-HPV associated cutaneous warts in immunocompetent general population (13, 69). The first evidence is shown by Zhang *et al*., (110) where UV radiation may facilitate low-dose papillomavirus particle induced infection via induction of E6/E7 oncogenes expression. However, it is worth noting that in this previous study the UV treatment was performed two weeks after infection, which was during the incubation period of the development of a visible papilloma (usually take 7 to 10 weeks). From this data, it is not clear whether UV irradiation activates latent viral infection or facilitates the appearance of low-dose viral infections resulting in an increased formation of papillomas. Most recently, Uberoi *et al*., (75) demonstrated that UVB induces immunosuppression in immunocompetent mice that strongly correlates with the MmuPV1 induced papilloma formation.

It is known that the E6 protein of cuHPV 8, 20, 22, 38, 76, 92 and 96 can inhibit apoptosis in response to UV-mediated damage *in vitro* (45, 58, 188). Several *in vivo* experiments have shown that the expression of the viral gene E2 (189), E6 (177) or all early genes (190) in K14HPV8 transgenic mice and E6 and E7 (191) in K14HPV38 transgenic mice contribute to the development of skin tumors following UV radiation. However, these observations remain controversial, because in these studies the viral genes are under the control of a heterologous UV-responsive keratin-14 promoter in the context of these transgenic mouse models, the physiological relevance of this observation is more related to an increase of viral transcription after UV radiation than to the effect of UV irradiation (75).

On the contrary, using the outbred CRPV/rabbit system we observed a trend but no significant increasing of viral copy number after incubation period, and no significant effect on papilloma formation upon UV irradiation (**FIG 3.2.2 and Table 3.2.1**), as well as no effect on papilloma formation in latent stage (**FIG 3.2.3 and Table 3.2.2**). Though, it is possible that the intensity of UVB light we applied here was too low, or the reactivation of latent viral infection requires more repeated doses of UVB radiation.

In addition, It has been reported that latent PV DNA infections could be activated by mechanical irritations in a rodent *Mastomys Natalensis* laboratory animal model, which naturally carries an endogenous latent MnPV (192). However, our attempts to use mechanical irritation to reactivate CRPV latent infection were unsuccessful (**FIG S2**). Some possible explanations include, firstly, the mechanical irritation cannot be standardized, and the period of the treatment may have been too short compared to the MnPV experiment (67 weeks). Secondly, the number of reactivated latent infected sites may have been too small, which reduced the possibility of inducing new papillomas. Therefore, we are unable to make a clear statement as to whether the mechanical irritation could reactivate the latent CRPV infection or not. A further study should be designed to address this question.

4.4 No increased tumor formation, but an increase of viral DNA copy numbers in latently infected skin sites upon immunosuppression

Beta-HPV infections are common and mostly asymptomatic in the general population (12, 90, 91). Drug-induced immunosuppression post-transplantation led to the elevation of beta-HPV viral loads in most OTRs (68, 92, 93), which suggests that either reactivation of latent infection or increased susceptibility to new infections took place. Studies of ROPV infection in rabbits hint to the point that latent viral DNA can persist in the epithelial basal layer up to one year with limited viral transcriptions (105). However, drug-induced systematic immunosuppression showed an increase in latent viral copy numbers, but not significant effect on the ROPV latent infection in papilloma formation (only one papilloma appeared) (106). In addition, ROPV causes mucosotropic lesions in the back side tongue of rabbits, which regress in 100% with 8 weeks p.i.. The results of the ROPV model may therefore not be applicable for the study of latent infections of cutaneous PVs.

Most recently, in a MmuPV1 mouse model, the infection of the virus is species-specific to individual mouse strains and the depletion of CD3+ cells permits efficient infection of non-susceptible mice. Neither the depletion of CD4+ nor CD8+ cells alone increased the susceptibility of MmuPV1 infections (121). Remarkably, Wang, *et al*., (122) also showed no appearance of papillomas in CD4+ or CD8+ depleted mice

upon MmuPV1 infection, but the viral DNA can still be detected 5 weeks p.i.. When the either CD4+ or CD8+ depleted mice were treated with anti-CD3 antibody, papillomas significantly appeared in only the CD4+ depleted group (14/15) within ten weeks, but not in the CD8+ depleted group (1/15). Although the reason was not clear, the new appearance of papillomas is an indication of reactivation of latent infection from asymptomatic sites.

In this study, we employed the outbred CRPV/rabbit model and administered immunosuppressive regimen to the latently infected rabbits, which is the closest system to the infection of cuHPV in OTRs. Using this latent model system we observed no increased tumor formation (**FIG 3.4.3, Table 3.4.1**), but an increase of viral DNA copy numbers in latently infected skin sites upon immunosuppression (**FIG 3.4.3 C)**. It is possible that reactivation of the latent infection may need longer-term of immunosuppression. Under chemical immunosuppression, we observed surprisingly three new papillomas that appeared more than 15 weeks p.i. (**FIG 3.4.4**), which might indicate that immunosuppression treatment could activate latent viral infection in some cases. Because CRPV infection of NZW rabbits does not result in virus production, we can rule out that, the new papillomas occurred due to an increased susceptibility to new infections. However, all three papillomas that appeared under immunosuppression were found only in one rabbit; and as out-bred rabbits were used in this CRPV-infection model, we cannot exclude that rabbit leukocyte antigen types may contribute to this effect.

We also observed that the viral DNA mediated infection using Gene gun method showed no increased susceptibility upon immunosuppression either started 2 weeks prior infection or 2 weeks p.i. (**Table 3.4.1, 3.4.2 and 3.4.3**). One possible explanation is that the infection using viral DNA can be inhibited only by the cell-mediated immune response because infection bypasses any effect of neutralizing antibodies, which are induced by primary infections with viral particles (107). At an early stage, the systematic immunosuppression might not increase the susceptibility of the viral DNA induced infection.

4.5 The combination of immunosuppression and UVA/B radiation showed no significant difference compared to immunosuppression alone

In clinical observations, the presence of cuHPV associated warts appeared in 15% of renal transplant recipients (RTR) during the first year post-transplantation, 25% – 42% within 3 years post transplantation, and 77% – 92% in 5 years post transplantation (62). UV light is believed to be an important risk factor for the development of cuHPV associated warts in RTRs, as most lesions appeared in sun-exposed areas (13, 61). In addition, the cumulative incidence of SCCs steadily increased in RTRs over the years after the start of immunosuppression, e.g, it reaches 60% at 20 years in Australia with a high sunlight exposure (51, 193, 194), and only 20% in Norway with much less sunny climate (195). These observations indicate that systemic immunosuppression and UV light might work in synergy for reactivation of latent HPV infections. Therefore, we performed both immunosuppression and UVA/B irradiation to reactivate CRPV induced latent infections. Surprisingly, we observed no significant effect in terms of viral load or papilloma formations compared to immunosuppression alone (**FIG 3.5.2, FIG 3.5.3, and FIG S5**). The reason why the combination of these two factors had no significant effect is still unclear. One possibility is that the reactivation of latent viral infections may require prolonged immunosuppression (years) and multiple UV exposures. However, due to side effects of immunosuppressant drugs and UV radiations, it is difficult to achieve a long-term treatment using this animal model.

4.6 CsA-based immunosuppression promotes pre-existing papilloma growth

CsA, a well-known calcineurin inhibitor (CNI) that acts selectively on T cell activity, has long been used to prevent solid organ rejection in OTRs (196). In addition, it has also been approved for the treatment of diseases in dermatology such as psoriasis, atopic dermatitis, and blistering disorder by the US Food and Drug Administration in 1997 (197, 198). For the immunosuppressive effect, “CsA forms a complex with cyclophilin, which inactivates calcineurin phosphorylase, preventing the

phosphorylation of NFATs and, therefore the transcription of interleukin-2 (IL-2). IL-2 is required for full activation and proliferation of T-lymphocytes" (196, 197).

It has been shown that the use of CsA in NZW rabbit not only led to immunosuppressive effect, but also cause many side effects such as loss of weight, reduced food and water consumption, and reduced movement (199). Reduction of CsA dose reduced toxicity, but at the expense of reduced immunosuppression (199). However, with a combination of corticosteroids drugs such as Dex resulted in effective immunosuppression effect and reduction of toxicity in a domestic rabbit (106). Systematic immunosuppression using CsA alone or combined with Dex delayed the spontaneous regression of papillomas induced either by CRPV or ROPV (106, 157).

In this study, we observed that CsA combined with Dex treatment significantly facilitated the growth of pre-existing papillomas induced by CRPV in outbred NZW rabbits (**FIG 3.6.1**). Interestingly, cessation of immunosuppression resulted in shrinking of the fast growing papillomas but did not cause complete regression (**FIG 3.6.2**). Our data shows that the fast-growing papillomas were not associated with the levels of viral DNA copies or viral gene expressions (**FIG 3.6.3**). We showed that that the reduction of cytotoxic CD8+ cells and downregulation of the expression of cytokines in papillomas might contribute to the increased growth of papilloma (**FIG 3.6.1**). One possibility is that the reduction of cytotoxic CD8+ cells promotes papillomas growth, whereas the cessation of immunosuppression lead to the recovery of T-cells, which eliminated highly immunogenic tumor cells and left the low immunogenic tumor cells to grow at a normal speed (**FIG 3.6.2, and 3.6.4**). The broad downregulation of cytokines is another indication of significantly suppressed activity of T lymphocytes parallel to FACS analysis (**FIG 3.6.4**).

Interestingly, of the cytokines examined in this study, the expression of IL-8 and IL-1β was specifically upregulated only locally in papillomas of immunosuppressed animals (**FIG 3.6.4 B**). It is known that IL-8 and IL-1β are type Th2 pro-inflammatory mediators, and their upregulation indicates severe chronic host inflammatory responses. IL-8 is a chemokine mainly produced by macrophages and other cell types such as keratinocytes. IL-8 function as a primary cytokine recruits neutrophils to the site of infection during the acute phase of inflammation. Increased expression

of IL-8 has been demonstrated in cancer cells, tumor-associated macrophages, endothelial cells, and infiltrating neutrophils, suggesting that IL-8 may function as a significant regulator factor within the tumor microenvironment. The expression of IL-8 has also been correlated with angiogenesis, tumorigenicity, and metastasis of tumors in numerous xenograft and orthotopic *in vivo* models (reviewed in (200)). Accordingly, IL-1β, an important mediator of the inflammatory response, that is mainly produced by activated macrophages as a proprotein is involved in a variety of cellular activities such as cell proliferation, differentiation, and apoptosis. It has also been shown that IL-1β is abundant at tumor sites, where it may affect the process of carcinogenesis, tumor growth and invasiveness, as well as the patterns of tumor-host interaction (reviewed in (201)). It has been shown recently that increased local expression of IL-8 and IL-1β in the cervical region indicates the progression of cervical intraepithelial neoplasia lesions in Japanese patients (202). In contrast, most recently Martin Kast's group reported that patients with "Treeman disease" have significantly reduced expression levels of IL-8 and IL-1β (HPV 2017 - Papillomavirus Conference, unpublished data). The Treemen disease is a condition associated with infection of HPV types 1 or 2 results in an uncontrolled "tree bark-like" growth and proliferation of infected keratinized epithelium in the hands and feet. It has been proposed that the causes of Treemen disease arises from a genetic defect that causes a potential immune deficiency related to Langerhans cell and innate skin immunity against HPV infection. However, this situation might differ from drug-induced systematic immunosuppression, whereas T-cells were suppressed.

Therefore, the increasing expression of IL-8 and IL-1β in papillomas of immunosuppressed animals might indicate the increasing activities of tumor associated marcrophages, which might be also an indicative of ongoing inflammation in the tumor microenvironment and possibly one of the causes of the fast growing papillomas.

4.7 CsA treatment induce cell proliferation independent of immunosuppression

It is believed that immunosuppression alone is not sufficient to promote SCC of the skin. For instance, it is well recognized that HIV-infected patients with profound

immune depletion, show a significantly lower incidence (4.11 fold) of SCC of the skin compared to OTRs (28.62 fold), arguing against a direct role of the immune system in malignant transformation of epidermal cells to cancer (203). OTRs treated with Tacrolimus, another CNI inhibitor, for immunosuppression had a lower incidence of SCCs post-transplantation than patients on CsA (204). There is compelling evidence that CsA causes increases in metastases of carcinoma in laboratory animals lacking an immune system (205). Additionally, immunosuppressant Sirolimus (SRL) inhibits the tumor promoting effects of CsA in such mice (206). On the other hand, it has been reported by numerous studies that CsA has pro carcinogenic effects, e.g. treatment of CsA lead to the activation of the proto-oncogene Ras (179), oncogene ATF3 (207, 208), TAK1/TAB1 pathway (209), AKT pathway (210), and mitochondrial reactive oxygen species (ROS) (178). Using a microarray analysis, Tiu *et al*., (211) demonstrated that the treatment of CsA in a cell line of SCC activates or inhibits a variety of genes important for cell-cycle regulation, apoptosis, and oncogene/ tumor-suppressor activation. Above all, these studies indicate that CsA not only functions as an immunosuppressant on the immune system but also potentiates carcinogenesis independent of the immune system. However, the CsA-based immunosuppression has been used in all previous PV-related studies (106, 121, 157, 212), and the direct effect of this immunosuppressant on PV-induced tumorigenesis has not been investigated. Here we demonstrated that CsA induces proliferations in rabbit-derived cells indicating a role that CsA might play in the direct tumorigenesis.

Taken together, the fast growth of pre-existing papillomas may result from the involvement of multiple factors such as reduction of immune surveillance, upregulation of pro-inflammatory cytokines such as IL8 and IL-1β, and maybe CsA supported tumorigenesis.

4.8 Outlook

We established an outbred CRPV/rabbit model to investigate cutaneous PV latent infection. Our work not only has provided insights into the virus life cycle, but also opened avenues for further exploration that will help to answer some remained important questions.

4.8.1 Target epithelial stem cells of latent papillomavirus infection

As discussed in section 4.2, based on our preliminary data we hypothesized that cells harboring latent CRPV genomes are a group of quiescent epithelial HF stem cells. However, it needs further investigation, e.g. identifying the direct association between latent viral genome and target stem cells. One approach is to use immunofluorescence combined with a LCM method to identify epithelial stem cells. A panel of antibodies should be used to detect the presence or absence of cellular proteins. In using such antibodies on rabbit skin dissections, it will be possible to identify cells that display these markers such as Lgr-5, K14, K15, CD34, CD200, or β1 integrin, and are therefore likely to be stem cells. Dissection of these cells by LCM followed by extraction of viral DNA and analysis by RT-qPCR will determine if CRPV DNA is present in these cells, but absent in cells lacking these markers. By targeting the infected cells, it will help us to investigate the viral life cycle under the latent state. However, during the course of this study these experiments could not be performed, due to lack of functional commercial primary antibodies against rabbits.

4.8.2 Alternative long-term immunosuppression regimens

We have observed that administration of CsA in NZW rabbit not only led to immunosuppressive effect, but also cause many side effects including loss of weight, reduced food and water intake. Although combination of Dex reduced such side effects, to achieve long-term (e.g. one year) immunosuppression remains a challenge. As we discussed in 4.5, accumulation of long-term immunosuppression might be required for reactivation of latent viral infections. Therefore, finding an alternative immunosuppression strategy is essential to answer the question. Possible immunosuppressant candidates such as SRL and Tacrolimus which are increasingly used in human transplant patients undergoing long-term immunosuppression as an alternative to CsA as it is less toxic and reduction of the incidence of carcinogenesis (196). Although, there is little research being done in rabbits in this regard, success has been achieved in mice (213).

4.8.3 Investigate factors that contribute to pre-existing papilloma growth *in vivo*

We observed that CsA-based immunosuppression led to fast-growing papillomas, and our results indicate that the proliferation of rabbit-derived cells was increased upon CsA treatment. Future studies should be designed to investigate whether the

fast growing papillomas are associated with the suppression of immune system and/or the drug-dependent manner *in vivo*. Evidences have been shown that immunosuppressant SRL reduces the incidence and progression of skin cancer, whereas CsA promote tumor growth and skin cancer in OTRs (214), as well as in mouse model (215). Studying the effect of immunosuppression induced by SRL or CsA on the pre-existing papilloma growth will help to answer the question.

5 CONCLUSION

We have established an outbred CRPV/rabbit model for the study of latent infections with cutaneous papillomavirus which allows investigating factors controlling the latent state.

We demonstrated that short-term immunosuppression increased latent viral genome copy numbers, but did not lead to new papilloma formation. Low-dose UV alone showed no significant effect on viral latency. The combination of short-term immunosuppression and UV radiation showed no significant difference compared to immunosuppression alone. However, it is still possible that the reactivation of latent viral infection may require longer-term systematic immunosuppression or multiple UV radiations.

In addition, CsA-based immunosuppression facilitates pre-existing papilloma growth likely via reduction of immune surveillances, upregulation of pro-inflammatory cytokines such as IL8 and IL-1β, and maybe CsA related tumorigenesis

Our findings here may provide implications for the clinic treatment of CsA-based immunosuppression of OTRs associated with cuHPV infection.

6 REFERENCES

1. Knipe DM, Howley PM. 2007. Fields Virology, 5th ed. Lippincott Williams and Wilkins, Philadelphia.
2. Rector A, Van Ranst M. 2013. Animal papillomaviruses. Virology.
3. Tse H, Tsang AK, Tsoi H-W, Leung AS, Ho C-C, Lau SK, Woo PC, Yuen K-Y. 2012. Identification of a novel bat papillomavirus by metagenomics. PLoS One 7:e43986.
4. ICTV 2015, posting date. Virus Taxonomy: http://www.ictvonline.org/virustaxonomy.asp. [Online.]
5. Van Doorslaer K. 2013. Evolution of the *Papillomaviridae*. Virology.
6. de Villiers E-M. 2013. Cross-roads in the classification of papillomaviruses. Virology.
7. Bouvard V, Baan R, Straif K, Grosse Y, Secretan B, El Ghissassi F, Benbrahim-Tallaa L, Guha N, Freeman C, Galichet L. 2009. A review of human carcinogens—Part B: biological agents. Elsevier.
8. IARC 2012, posting date. Human Papillomaviruses: http://monographs.iarc.fr/ENG/Monographs/vol100B/. [Online.]
9. Doorbar J, Quint W, Banks L, Bravo IG, Stoler M, Broker TR, Stanley MA. 2012. The biology and life-cycle of human papillomaviruses. Vaccine 30:F55-70.
10. Bzhalava D, Guan P, Franceschi S, Dillner J, Clifford G. 2013. A systematic review of the prevalence of mucosal and cutaneous human papillomavirus types. Virology.
11. Hazard K, Karlsson A, Andersson K, Ekberg H, Dillner J, Forslund O. 2007. Cutaneous human papillomaviruses persist on healthy skin. J Invest Dermatol 127:116-119.
12. Ma YF, Madupu R, Karaoz U, Nossa CW, Yang LY, Yooseph S, Yachimski PS, Brodie EL, Nelson KE, Pei ZH. 2014. Human Papillomavirus Community in Healthy Persons, Defined by Metagenomics Analysis of Human Microbiome Project Shotgun Sequencing Data Sets. J Virol 88:4786-4797.
13. Asgari MM, Kiviat NB, Critchlow CW, Stern JE, Argenyi ZB, Raugi GJ, Berg D, Odland PB, Hawes SE, de Villiers E-M. 2008. Detection of human papillomavirus DNA in cutaneous squamous cell carcinoma among immunocompetent individuals. J Invest Dermatol 128:1409-1417.
14. Bavinck JNB, Plasmeijer EI, Feltkamp MC. 2008. β-Papillomavirus infection and skin cancer. J Invest Dermatol 128:1355-1358.
15. Akgül B, Cooke JC, Storey A. 2006. HPV-associated skin disease. J Pathol 208:165-175.
16. de Villiers EM, Fauquet C, Broker TR, Bernard HU, zur Hausen H. 2004. Classification of papillomaviruses. Virology 324:17-27.
17. Münger K, Howley PM. 2002. Human papillomavirus immortalization and transformation functions. Virus Res 89:213-228.

18. Chen Z, Schiffman M, Herrero R, DeSalle R, Burk RD. 2007. Human papillomavirus (HPV) types 101 and 103 isolated from cervicovaginal cells lack an E6 open reading frame (ORF) and are related to gamma-papillomaviruses. Virology 360:447-453.

19. Nobre RJ, Herráez-Hernández E, Fei J-W, Langbein L, Kaden S, Gröne H-J, de Villiers E-M. 2009. E7 oncoprotein of novel human papillomavirus type 108 lacking the E6 gene induces dysplasia in organotypic keratinocyte cultures. J Virol 83:2907-2916.

20. Venuti A, Paolini F, Nasir L, Corteggio A, Roperto S, Campo MS, Borzacchiello G. 2011. Papillomavirus E5: the smallest oncoprotein with many functions. Molecular cancer 10:140.

21. Trus BL, Roden RB, Greenstone HL, Vrhel M, Schiller JT, Booy FP. 1997. Novel structural features of bovine papillomavirus capsid revealed by a three-dimensional reconstruction to 9 Å resolution. Nat Struct Mol Biol 4:413-420.

22. Belnap DM, Olson NH, Cladel NM, Newcomb WW, Brown JC, Kreider JW, Christensen ND, Baker TS. 1996. Conserved features in papillomavirus and polyomavirus capsids. J Mol Biol 259:249-263.

23. Scheffer KD, Gawlitza A, Spoden GA, Zhang XA, Lambert C, Berditchevski F, Florin L. 2013. Tetraspanin CD151 mediates papillomavirus type 16 endocytosis. J Virol 87:3435-3446.

24. Johansson C, Schwartz S. 2013. Regulation of human papillomavirus gene expression by splicing and polyadenylation. Nature Rev Microbiol.

25. Pyeon D, Pearce SM, Lank SM, Ahlquist P, Lambert PF. 2009. Establishment of human papillomavirus infection requires cell cycle progression. PLoS Pathog 5:e1000318.

26. Sapp MJ. 2013. HPV virions hitchhike a ride on retromer complexes. Proc Natl Acad Sci USA 110:7116-7117.

27. Spoden G, Kuhling L, Cordes N, Frenzel B, Sapp M, Boller K, Florin L, Schelhaas M. 2013. Human papillomavirus types 16, 18, and 31 share similar endocytic requirements for entry. J Virol 87:7765-7773.

28. McBride AA. 2013. The Papillomavirus E2 proteins. Virology.

29. Wu S-Y, Chiang C-M. 2007. The double bromodomain-containing chromatin adaptor Brd4 and transcriptional regulation. J Biol Chem 282:13141-13145.

30. Iftner T, Haedicke-Jarboui J, Wu S-Y, Chiang C-M. 2016. Involvement of Brd4 in different steps of the papillomavirus life cycle. Virus Res.

31. Chow LT, Broker TR, Steinberg BM. 2010. The natural history of human papillomavirus infections of the mucosal epithelia. APMIS : acta pathologica, microbiologica, et immunologica Scandinavica 118:422-449.

32. Maglennon GA, Doorbar J. 2012. The biology of papillomavirus latency. Open Virol J 6:190-197.

33. Bergvall M, Melendy T, Archambault J. 2013. The E1 proteins. Virology 445:35-56.

34. Dreer M, van de Poel S, Stubenrauch F. 2017. Control of viral replication and transcription by the papillomavirus E8^ E2 protein. Virus Res 231:96-102.

35. Roman A, Munger K. 2013. The papillomavirus E7 proteins. Virology.

36. DiMaio D, Petti LM. 2013. The E5 proteins. Virology.

37. Doorbar J. 2013. The E4 protein; structure, function and patterns of expression. Virology 445:80-98.

38. Accardi R, Gheit T. 2014. Cutaneous HPV and skin cancer. La Presse Médicale 43:e435-e443.

39. Elbel M, Carl S, Spaderna S, Iftner T. 1997. A comparative analysis of the interactions of the E6 proteins from cutaneous and genital papillomaviruses with p53 and E6AP in correlation to their transforming potential. Virology 239:132-149.

40. Yamashita T, Segawa K, Fujinaga Y, Nishikawa T, Fujinaga K. 1993. Biological and biochemical activity of E7 genes of the cutaneous human papillomavirus type 5 and 8. Oncogene 8:2433-2441.

41. Schmitt A, Harry JB, Rapp B, Wettstein FO, Iftner T. 1994. Comparison of the properties of the E6 and E7 genes of low- and high-risk cutaneous papillomaviruses reveals strongly transforming and high Rb-binding activity for the E7 protein of the low-risk human papillomavirus type 1. J Virol 68:7051-7059.

42. Caldeira S, Zehbe I, Accardi R, Malanchi I, Dong W, Giarrè M, de Villiers E-M, Filotico R, Boukamp P, Tommasino M. 2003. The E6 and E7 proteins of the cutaneous human papillomavirus type 38 display transforming properties. J Virol 77:2195-2206.

43. Muench P, Probst S, Schuetz J, Leiprecht N, Busch M, Wesselborg S, Stubenrauch F, Iftner T. 2010. Cutaneous papillomavirus E6 proteins must interact with p300 and block p53-mediated apoptosis for cellular immortalization and tumorigenesis. Cancer Res 70:6913-6924.

44. Wallace NA, Robinson K, Howie HL, Galloway DA. 2015. β-HPV 5 and 8 E6 disrupt homology dependent double strand break repair by attenuating BRCA1 and BRCA2 expression and foci formation. PLoS Pathog 11:e1004687.

45. Underbrink MP, Howie HL, Bedard KM, Koop JI, Galloway DA. 2008. E6 proteins from multiple human betapapillomavirus types degrade Bak and protect keratinocytes from apoptosis after UVB irradiation. J Virol 82:10408-10417.

46. Jabłonska S, Majewski S, Obalek S, Orth G. 1997. Cutaneous warts. Clin Dermatol 15:309-319.

47. Andersson K, Michael K, Luostarinen T, Waterboer T, Gislefoss R, Hakulinen T, Forslund O, Pawlita M, Dillner J. 2012. Prospective study of human papillomavirus seropositivity and risk of nonmelanoma skin cancer. American journal of epidemiology 175:685-695.

48. Mudigonda T, Pearce DJ, Yentzer BA, Williford P, Feldman SR. 2010. The economic impact of non-melanoma skin cancer: a review. J Natl Compr Canc Netw 8:888-896.

49. Madan V, Lear JT, Szeimies R-M. 2010. Non-melanoma skin cancer. The Lancet 375:673-685.

50. Lewandowsky F, Lutz W. 1922. Ein Fall einer bisher nicht beschriebenen Hauterkrankung (Epidermodysplasia verruciformis). Arch Dermatol Res 141:193-203.

51. Bavinck JNB, Feltkamp M, Struijk L, ter Schegget J. 2001. Human papillomavirus infection and skin cancer risk in organ transplant recipients. J Investig Dermatol Symp Proc 6:207-211.

52. Jablonska S, Dabrowski J, Jakubowicz K. 1972. Epidermodysplasia verruciformis as a model in studies on the role of papovaviruses in oncogenesis. Cancer Res 32:583-589.

53. Orth G. 1987. Epidermodysplasia verruciformis, p. 199-243, The papovaviridae. Springer.

54. Ramoz N, Rueda L-A, Bouadjar B, Montoya L-S, Orth G, Favre M. 2002. Mutations in two adjacent novel genes are associated with epidermodysplasia verruciformis. Nat Genet 32:579-581.

55. Orth G. 2006, p 362-374. Seminars in immunology.

56. Kalińska-Bienias A, Kowalewski C, Majewski S. 2016. The EVER genes – the genetic etiology of carcinogenesis in epidermodysplasia verruciformis and a possible role in non-epidermodysplasia verruciformis patients. Postep Derm Alergol 33:75-80.

57. Majewski S, Jabłońska S. 1995. Epidermodysplasia verruciformis as a model of human papillomavirus-induced genetic cancer of the skin. Arch Dermatol 131:1312-1318.

58. Jackson S, Storey A. 2000. E6 proteins from diverse cutaneous HPV types inhibit apoptosis in response to UV damage. Oncogene 19:592.

59. Euvrard S, Kanitakis J, Claudy A. 2003. Skin cancers after organ transplantation. The New England journal of medicine 348:1681-1691.

60. Stockfleth E, Nindl I, Sterry W, Ulrich C, Schmook T, Meyer T. 2004. Human Papillomaviruses in Transplant-Associated Skin Cancers. Dermatol Surg 30:604-609.

61. Wieland U, Kreuter A, Pfister H. 2014. Human papillomavirus and immunosuppression, p. 154-165, Human Papillomavirus, vol. 45. Karger Publishers.

62. Martelli-Marzagão F, Santos Junior G, Ogawa M, Enokihara M, Porro A, Tomimori J. 2016. Human papillomavirus detected in viral warts of renal transplant recipients. Transplant infectious disease : an official journal of the Transplantation Society 18:37-43.

63. Howley PM, Pfister HJ. 2015. Beta genus papillomaviruses and skin cancer. Virology 479:290-296.

64. Arron ST, Ruby JG, Dybbro E, Ganem D, DeRisi JL. 2011. Transcriptome sequencing demonstrates that human papillomavirus is not active in cutaneous squamous cell carcinoma. J Invest Dermatol 131:1745-1753.

65. Schiller JT, Buck CB. 2011. Cutaneous squamous cell carcinoma: a smoking gun but still no suspects. J Invest Dermatol 131:1595-1596.

66. Fisher M, Kripke M. 2002. Systemic alteration induced in mice by ultraviolet light irradiation and its relationship to ultraviolet carcinogenisis. Bulletin of the World Health Organization 80:908-912.

67. Rebel H, Bodmann C, van de Glind G, de Gruijl F. 2012. UV-induced ablation of the epidermal basal layer including p53-mutant clones resets UV carcinogenesis showing squamous cell carcinomas to originate from interfollicular epidermis. Carcinogenesis 33:714-720.

68. Weissenborn S, Neale RE, Waterboer T, Abeni D, Bavinck JNB, Green AC, Harwood CA, Euvrard S, Feltkamp MC, de Koning MN. 2012. Beta-papillomavirus DNA loads in hair follicles of immunocompetent people and organ transplant recipients. Med Microbiol Immun 201:117-125.

69. Forslund O, Iftner T, Andersson K, Lindelof B, Hradil E, Nordin P, Stenquist B, Kirnbauer R, Dillner J, de Villiers EM. 2007. Cutaneous human papillomaviruses found in sun-exposed skin: Beta-papillomavirus species 2 predominates in squamous cell carcinoma. J Infect Dis 196:876-883.

70. Wallace NA, Robinson K, Howie HL, Galloway DA. 2012. HPV 5 and 8 E6 abrogate ATR activity resulting in increased persistence of UVB induced DNA damage. PLoS pathogens 8:e1002807.

71. Wallace NA, Gasior SL, Faber ZJ, Howie HL, Deininger PL, Galloway DA. 2013. HPV 5 and 8 E6 expression reduces ATM protein levels and attenuates LINE-1 retrotransposition. Virology 443:69-79.

72. Poon TS, Barnetson RSC, Halliday GM. 2005. Sunlight-induced immunosuppression in humans is initially because of UVB, then UVA, followed by interactive effects. Journal of Investigative Dermatology 125:840-846.

73. Kripke ML. 1984. Immunological unresponsiveness induced by ultraviolet radiation. Immunol Rev 80:87-102.

74. Rana S, Byrne SN, MacDonald LJ, Chan CY-Y, Halliday GM. 2008. Ultraviolet B suppresses immunity by inhibiting effector and memory T cells. The American journal of pathology 172:993-1004.

75. Uberoi A, Yoshida S, Frazer IH, Pitot HC, Lambert PF. 2016. Role of Ultraviolet Radiation in Papillomavirus-Induced Disease. PLoS Pathog 12:e1005664.

76. Watt FM, Jensen KB. 2009. Epidermal stem cell diversity and quiescence. EMBO molecular medicine 1:260-267.

77. Blanpain C, Fuchs E. 2006. Epidermal stem cells of the skin. Annu Rev Cell Dev Biol 22:339.

78. Schmitt A, Rochat A, Zeltner R, Borenstein L, Barrandon Y, Wettstein FO, Iftner T. 1996. The primary target cells of the high-risk cottontail rabbit papillomavirus colocalize with hair follicle stem cells. J Virol 70:1912-1922.

79. Struijk L, ter Schegget J, Bouwes Bavinck JN, Feltkamp MC. 2005. [Human papillomavirus in the aetiology of skin cancer]. Nederlands tijdschrift voor geneeskunde 149:518-522.

80. Boxman IL, Russell A, Mulder LH, Bouwes Bavinck JN, ter Schegget J, Green A. 2000. Case-control study in a subtropical Australian population to assess the relation between non-melanoma skin cancer and epidermodysplasia verruciformis human papillomavirus DNA in plucked eyebrow hairs. Int J Cancer 86:118-121.

81. Speck SH, Ganem D. 2010. Viral latency and its regulation: lessons from the γ-herpesviruses. Cell host & microbe 8:100-115.

82. Redpath S, Angulo A, Gascoigne NR, Ghazal P. 2001. Immune checkpoints in viral latency. Annu Rev Microbiol 55:531-560.

83. Doorbar J. 2013. Latent papillomavirus infections and their regulation. Current opinion in virology 3:416-421.

84. Gravitt PE. 2012. Suppl 2: Evidence and Impact of Human Papillomavirus Latency. Open Virol J 6:198.

85. Jamieson DJ, Duerr A, Burk R, Klein RS, Paramsothy P, Schuman P, Cu-Uvin S, Shah K. 2002. Characterization of genital human papillomavirus infection in women who have or who are at risk of having HIV infection. Am J Obstet Gynecol 186:21-27.

86. Theiler RN, Farr SL, Karon JM, Paramsothy P, Viscidi R, Duerr A, Cu-Uvin S, Sobel J, Shah K, Klein RS. 2010. High-Risk Human Papillomavirus Reactivation in Human Immunodeficiency Virus–Infected Women: Risk Factors for Cervical Viral Shedding. Obstet Gynecol 115:1150-1158.

87. Strickler HD, Burk RD, Fazzari M, Anastos K, Minkoff H, Massad LS, Hall C, Bacon M, Levine AM, Watts DH, Silverberg MJ, Xue X, Schlecht NF, Melnick S, Palefsky JM. 2005. Natural history and possible reactivation of human papillomavirus in human immunodeficiency virus-positive women. J Natl Cancer Inst 97:577-586.

88. Neale RE, Weissenborn S, Abeni D, Bavinck JN, Euvrard S, Feltkamp MC, Green AC, Harwood C, de Koning M, Naldi L, Nindl I, Pawlita M, Proby C, Quint WG, Waterboer T, Wieland U, Pfister H. 2013. Human papillomavirus load in eyebrow hair follicles and risk of cutaneous squamous cell carcinoma. Cancer Epidemiol Biomarkers Prev 22:719-727.

89. Schneider I, Lehmann MD, Kogosov V, Stockfleth E, Nindl I. 2013. Eyebrow hairs from actinic keratosis patients harbor the highest number of cutaneous human papillomaviruses. BMC Infect Dis 13:186.

90. Antonsson A, Erfurt C, Hazard K, Holmgren V, Simon M, Kataoka A, Hossain S, Håkangård C, Hansson BG. 2003. Prevalence and type spectrum of human papillomaviruses in healthy skin samples collected in three continents. J Gen Virol 84:1881-1886.

91. Antonsson A, Forslund O, Ekberg H, Sterner G, Hansson BG. 2000. The ubiquity and impressive genomic diversity of human skin papillomaviruses suggest a commensalic nature of these viruses. J Virol 74:11636-11641.

92. Proby C, Harwood C, Neale R, Green A, Euvrard S, Naldi L, Tessari G, Feltkamp M, De Koning M, Quint W. 2011. A case–control study of betapapillomavirus infection and cutaneous squamous cell carcinoma in organ transplant recipients. American journal of transplantation : official journal of the

American Society of Transplantation and the American Society of Transplant Surgeons 11:1498-1508.

93. McLaughlin-Drubin ME. 2015. Human Papillomaviruses and Non-melanoma Skin Cancer. Semin Oncol 42:284-290.

94. Larson DA, Derkay CS. 2010. Epidemiology of recurrent respiratory papillomatosis. APMIS : acta pathologica, microbiologica, et immunologica Scandinavica 118:450-454.

95. Steinberg BM, Topp WC, Schneider PS, Abramson AL. 1983. Laryngeal papillomavirus infection during clinical remission. The New England journal of medicine 308:1261-1264.

96. Abramson AL, Steinberg BM, Winkler B. 1987. Laryngeal papillomatosis: clinical, histopathologic and molecular studies. The Laryngoscope 97:678-685.

97. Abramson AL, Nouri M, Mullooly V, Fisch G, Steinberg BM. 2004. Latent human papillomavirus infection is comparable in the larynx and trachea. J Med Virol 72:473-477.

98. Doorbar J, Griffin H. 2007. Intrabody strategies for the treatment of human papillomavirus-associated disease. Expert Opin Biol Ther 7:677-689.

99. Lacey CJ. 2005. Therapy for genital human papillomavirus-related disease. J Clin Virol 32:82-90.

100. Von Krogh G, Dahlman-Ghozlan K, Syrjänen S. 2002. Potential human papillomavirus reactivation following topical corticosteroid therapy of genital lichen sclerosus and erosive lichen planus. Journal of the European Academy of Dermatology and Venereology : JEADV 16:130-133.

101. Kalantari M, Garcia-Carranca A, Morales-Vazquez CD, Zuna R, Montiel DP, Calleja-Macias IE, Johansson B, Andersson S, Bernard HU. 2009. Laser capture microdissection of cervical human papillomavirus infections: copy number of the virus in cancerous and normal tissue and heterogeneous DNA methylation. Virology 390:261-267.

102. Gravitt PE. 2011. The known unknowns of HPV natural history. The Journal of clinical investigation 121:4593-4599.

103. Sakakibara N, Chen D, Jang MK, Kang DW, Luecke HF, Wu S-Y, Chiang C-M, McBride AA. 2013. Brd4 is displaced from HPV replication factories as they expand and amplify viral DNA. PLoS Pathog 9:e1003777.

104. Christensen ND, Cladel NM, Reed CA, Han R. 2000. Rabbit oral papillomavirus complete genome sequence and immunity following genital infection. Virology 269:451-461.

105. Maglennon GA, McIntosh P, Doorbar J. 2011. Persistence of viral DNA in the epithelial basal layer suggests a model for papillomavirus latency following immune regression. Virology 414:153-163.

106. Maglennon GA, McIntosh PB, Doorbar J. 2014. Immunosuppression facilitates the reactivation of latent papillomavirus infections. J Virol 88:710-716.

107. Brandsma JL. 2005. The cottontail rabbit papillomavirus model of high-risk HPV-induced disease. Methods Mol Med 119:217-235.

108. Christensen ND. 2005. Cottontail rabbit papillomavirus (CRPV) model system to test antiviral and immunotherapeutic strategies. Antivir Chem Chemother 16:355-362.

109. Amella CA, Lofgren LA, Ronn AM, Nouri M, Shikowitz MJ, Steinberg BM. 1994. Latent infection induced with cottontail rabbit papillomavirus. A model for human papillomavirus latency. The American journal of pathology 144:1167-1171.

110. Zhang P, Nouri M, Brandsma JL, Iftner T, Steinberg BM. 1999. Induction of E6/E7 expression in cottontail rabbit papillomavirus latency following UV activation. Virology 263:388-394.

111. Selvakumar R, Schmitt A, Iftner T, Ahmed R, Wettstein FO. 1997. Regression of papillomas induced by cottontail rabbit papillomavirus is associated with infiltration of CD8+ cells and persistence of viral DNA after regression. J Virol 71:5540-5548.

112. Campo MS, Moar MH, Laird HM, Jarrett W. 1981. Molecular heterogeneity and lesion site specificity of cutaneous bovine papillomaviruses. Virology 113:323-335.

113. Campo MS, Jarrett WF, Barron R, O'Neil BW, Smith KT. 1992. Association of bovine papillomavirus type 2 and bracken fern with bladder cancer in cattle. Cancer Res 52:6898-6904.

114. Campo M, Jarrett W, O'neil W, Barron R. 1994. Latent papillomavirus infection in cattle. Res Vet Sci 56:151-157.

115. Muller H, Gissmann L. 1978. Mastomys natalensis papilloma virus (MnPV), the causative agent of epithelial proliferations: characterization of the virus particle. J Gen Virol 41:315-323.

116. Tan C-H, Tachezy R, Van Ranst M, Chan S-Y, Bernard H-U, Burk RD. 1994. The Mastomys natalensis papillomavirus: nucleotide sequence, genome organization, and phylogenetic relationship of a rodent papillomavirus involved in tumorigenesis of cutaneous epithelia. Virology 198:534-541.

117. Oettle A. 1957. Spontaneous carcinoma of the glandular stomach in Rattus (mastomys) natalensis, an African rodent. Br J Cancer 11:415.

118. Amtmann E, Volm M, Wayss K. 1984. Tumour induction in the rodent Mastomys natalensis by activation of endogenous papilloma virus genomes. Nature 308:291-292.

119. Ingle A, Ghim S, Joh J, Chepkoech I, Bennett Jenson A, Sundberg JP. 2011. Novel laboratory mouse papillomavirus (MusPV) infection. Veterinary pathology 48:500-505.

120. Cladel NM, Budgeon LR, Balogh KK, Cooper TK, Hu J, Christensen ND. 2015. A Novel Pre-Clinical Murine Model to Study the Life Cycle and Progression of Cervical and Anal Papillomavirus Infections. PLoS One 10:e0120128.

121. Handisurya A, Day PM, Thompson CD, Bonelli M, Lowy DR, Schiller JT. 2014. Strain-Specific Properties and T Cells Regulate the Susceptibility to Papilloma Induction by Mus musculus Papillomavirus 1. PLoS Pathog 10:e1004314.

122. Wang JW, Jiang R, Peng SW, Chang YN, Hung CF, Roden RBS. 2015. Immunologic Control of Mus musculus Papillomavirus Type 1. PLoS pathog 11.

123. Shope RE, Hurst EW. 1933. Infectious papillomatosis of rabbits with a note on the histopathology. The Journal of experimental medicine 58:607-624.

124. Rous P, Beard J. 1935. The progression to carcinoma of virus-induced rabbit papillomas (Shope). The Journal of experimental medicine 62:523-548.

125. Kreider JW. 1963. Studies on the mechanism responsible for the spontaneous regression of the Shope rabbit papilloma. Cancer Res 23:1593-1599.

126. Wettstein FO, Stevens JG. 1983. Shope papilloma virus DNA is extensively methylated in non-virus-producing neoplasms. Virology 126:493-504.

127. Ito Y, Evans CA. 1961. Induction of tumors in domestic rabbits with nucleic acid preparations from partially purified Shope papilloma virus and from extracts of the papillomas of domestic and cottontail rabbits. The Journal of experimental medicine 114:485-500.

128. Cladel NM, Budgeon LR, Hu J, Balogh KK, Christensen ND. 2013. Synonymous codon changes in the oncogenes of the cottontail rabbit papillomavirus lead to increased oncogenicity and immunogenicity of the virus. Virology 438:70-83.

129. Mejia AF, Culp TD, Cladel NM, Balogh KK, Budgeon LR, Buck CB, Christensen ND. 2006. Preclinical model to test human papillomavirus virus (HPV) capsid vaccines in vivo using infectious HPV/cottontail rabbit papillomavirus chimeric papillomavirus particles. J Virol 80:12393-12397.

130. Giri I, Danos O, Yaniv M. 1985. Genomic structure of the cottontail rabbit (Shope) papillomavirus. Proc Natl Acad Sci USA 82:1580-1584.

131. Barbosa MS, Wettstein FO. 1987. Transcription of the cottontail rabbit papillomavirus early region and identification of two E6 polypeptides in COS-7 cells. J Virol 61:2938-2942.

132. Danos O, Georges E, Orth G, Yaniv M. 1985. Fine structure of the cottontail rabbit papillomavirus mRNAs expressed in the transplantable VX2 carcinoma. J Virol 53:735-741.

133. Wettstein FO, Barbosa MS, Nasseri M. 1987. Identification of the major cottontail rabbit papillomavirus late RNA cap site and mapping and quantitation of an E2 and minor E6 coding mRNA in papillomas and carcinomas. Virology 159:321-328.

134. Jeckel S, Loetzsch E, Huber E, Stubenrauch F, Iftner T. 2003. Identification of the E9^E2C cDNA and functional characterization of the gene product reveal a new repressor of transcription and replication in cottontail rabbit papillomavirus. J Virol 77:8736-8744.

135. Barbosa MS, Wettstein FO. 1988. The two proteins encoded by the cottontail rabbit papillomavirus E6 open reading frame differ with respect to localization and phosphorylation. J Virol 62:1088-1092.

136. Harry JB, Wettstein FO. 1996. Transforming properties of the cottontail rabbit papillomavirus oncoproteins Le6 and SE6 and of the E8 protein. Journal of virology 70:3355-3362.

137. Barbosa MS, Wettstein FO. 1988. Identification and characterization of the CRPV E7 protein expressed in COS-7 cells. Virology 165:134-140.

138. Ganzenmueller T, Matthaei M, Muench P, Scheible M, Iftner A, Hiller T, Leiprecht N, Probst S, Stubenrauch F, Iftner T. 2008. The E7 protein of the cottontail rabbit papillomavirus immortalizes normal rabbit keratinocytes and reduces pRb levels, while E6 cooperates in immortalization but neither degrades p53 nor binds E6AP. Virology 372:313-324.

139. Haskell KM, Vuocolo GA, Defeo-Jones D, Jones RE, Ivey-Hoyle M. 1993. Comparison of the binding of the human papillomavirus type 16 and cottontail rabbit papillomavirus E7 proteins to the retinoblastoma gene product. J Gen Virol 74 (Pt 1):115-119.

140. Han R, Cladel NM, Reed CA, Christensen ND. 1998. Characterization of transformation function of cottontail rabbit papillomavirus E5 and E8 genes. Virology 251:253-263.

141. Nonnenmacher M, Salmon J, Jacob Y, Orth G, Breitburd F. 2006. Cottontail rabbit papillomavirus E8 protein is essential for wart formation and provides new insights into viral pathogenesis. J Virol 80:4890-4900.

142. Brandsma J, Yang Z, DiMaio D, Barthold S, Johnson E, Xiao W. 1992. The putative E5 open reading frame of cottontail rabbit papillomavirus is dispensable for papilloma formation in domestic rabbits. J Virol 66:6204-6207.

143. Hu J, Cladel NM, Balogh K, Budgeon L, Christensen ND. 2007. Impact of genetic changes to the CRPV genome and their application to the study of pathogenesis in vivo. Virology 358:384-390.

144. Jeckel S, Huber E, Stubenrauch F, Iftner T. 2002. A transactivator function of cottontail rabbit papillomavirus e2 is essential for tumor induction in rabbits. J Virol 76:11209-11215.

145. Peh WL, Brandsma JL, Christensen ND, Cladel NM, Wu X, Doorbar J. 2004. The viral E4 protein is required for the completion of the cottontail rabbit papillomavirus productive cycle in vivo. J Virol 78:2142-2151.

146. Stevens J, Wettstein F. 1979. Multiple copies of Shope virus DNA are present in cells of benign and malignant non-virus-producing neoplasms. J Virol 30:891-898.

147. Watts SL, Ostrow RS, Phelps WC, Prince JT, Faras AJ. 1983. Free cottontail rabbit papillomavirus DNA persists in warts and carcinomas of infected rabbits and in cells in culture transformed with virus or viral DNA. Virology 125:127-138.

148. Wettstein FO, Stevens JG. 1982. Variable-sized free episomes of Shope papilloma virus DNA are present in all non-virus-producing neoplasms and integrated episomes are detected in some. Proc Natl Acad Sci USA 79:790-794.

149. Schneider-Maunoury S, Georges E, Orth G. 1987. Structure and expression of the cottontail rabbit papillomavirus genome and of myc and ras genes during the progression of domestic rabbit skin tumors. Cancer cells 5:229-236.

150. Georges E, Croissant O, Bonneaud N, Orth G. 1984. Physical state and transcription of the cottontail rabbit papillomavirus genome in warts and transplantable VX2 and VX7 carcinomas of domestic rabbits. J Virol 51:530-538.

151. Sugawara K, Fujinaga K, Yamashita T, Ito Y. 1983. Integration and methylation of shope papilloma virus DNA in the transplantable V× 2 and V× 7 rabbit carcinomas. Virology 131:88-99.

152. Lin Y, Borenstein L, Ahmed R, Wettstein F. 1993. Cottontail rabbit papillomavirus L1 protein-based vaccines: protection is achieved only with a full-length, nondenatured product. Journal of virology 67:4154-4162.

153. Lin YL, Borenstein LA, Selvakumar R, Ahmed R, Wettstein FO. 1992. Effective vaccination against papilloma development by immunization with L1 or L2 structural protein of cottontail rabbit papillomavirus. Virology 187:612-619.

154. Selvakumar R, Ahmed R, Wettstein FO. 1995. Tumor regression is associated with a specific immune response to the E2 protein of cottontail rabbit papillomavirus. Virology 208:298-302.

155. Hopfl RM, Christensen ND, Angell MG, Kreider JW. 1993. Skin test to assess immunity against cottontail rabbit papillomavirus antigens in rabbits with progressing papillomas or after papilloma regression. J Invest Dermatol 101:227-231.

156. Okabayashi M, Angell MG, Christensen ND, Kreider JW. 1991. Morphometric analysis and identification of infiltrating leucocytes in regressing and progressing Shope rabbit papillomas. Int J Cancer 49:919-923.

157. Hu J, Peng X, Cladel NM, Pickel MD, Christensen ND. 2005. Large cutaneous rabbit papillomas that persist during cyclosporin A treatment can regress spontaneously after cessation of immunosuppression. J Gen Virol 86:55-63.

158. de Koning MN, Struijk L, Bavinck JNB, Kleter B, ter Schegget J, Quint WG, Feltkamp MC. 2007. Betapapillomaviruses frequently persist in the skin of healthy individuals. J Gen Virol 88:1489-1495.

159. Quint KD, Genders RE, de Koning MN, Borgogna C, Gariglio M, Bouwes Bavinck JN, Doorbar J, Feltkamp MC. 2015. Human Beta-Papillomavirus Infection and Keratinocyte Carcinomas. J Pathol 235:342-354.

160. Kreider JW, Bartlett GL. 1981. The Shope papilloma-carcinoma complex of rabbits: a model system of neoplastic progression and spontaneous regression. Adv. Cancer Res 35:81-110.

161. Culp TD, Christensen ND. 2004. Kinetics of in vitro adsorption and entry of papillomavirus virions. Virology 319:152-161.

162. Seol D, Choe H, Zheng H, Jang K, Ramakrishnan PS, Lim T-H, Martin JA. 2011. Selection of reference genes for normalization of quantitative real-time

PCR in organ culture of the rat and rabbit intervertebral disc. BMC research notes 4:162.

163. Godornes C, Leader BT, Molini BJ, Centurion-Lara A, Lukehart SA. 2007. Quantitation of rabbit cytokine mRNA by real-time RT-PCR. Cytokine 38:1-7.

164. Dewals BG, Vanderplasschen A. 2011. Malignant catarrhal fever induced by Alcelaphine herpesvirus 1 is characterized by an expansion of activated $CD3^{+}CD8^{+}CD4^{-}$ T cells expressing a cytotoxic phenotype in both lymphoid and non-lymphoid tissues. Veterinary research 42:95.

165. Schnupf P, Sansonetti PJ. 2012. Quantitative RT-PCR profiling of the rabbit immune response: assessment of acute Shigella flexneri infection. PLoS One 7:e36446.

166. Clark SJ, Statham A, Stirzaker C, Molloy PL, Frommer M. 2006. DNA methylation: bisulphite modification and analysis. Nature protocols 1:2353-2364.

167. Huber E, Vlasny D, Jeckel S, Stubenrauch F, Iftner T. 2004. Gene profiling of cottontail rabbit papillomavirus-induced carcinomas identifies upregulated genes directly Involved in stroma invasion as shown by small interfering RNA-mediated gene silencing. J Virol 78:7478-7489.

168. Caldelari R, Suter MM, Baumann D, de Bruin A, Müller E. 2000. Long-term culture of murine epidermal keratinocytes. J Invest Dermatol 114:1064-1065.

169. Maglennon G. 2011. Study of papillomavirus latent infection in an animal model. UCL (University College London).

170. Dethlefsen LA, Prewitt J, Mendelsohn M. 1968. Analysis of tumor growth curves. J Natl Cancer Inst 40:389-405.

171. Mehrara E, Forssell-Aronsson E, Ahlman H, Bernhardt P. 2007. Specific growth rate versus doubling time for quantitative characterization of tumor growth rate. Cancer research 67:3970-3975.

172. Bose A, Teh M-T, Mackenzie IC, Waseem A. 2013. Keratin k15 as a biomarker of epidermal stem cells. Int J Mol Sci 14:19385-19398.

173. Casali N. 2003. Escherichia coli host strains, p. 27-48, E. coli Plasmid Vectors. Springer.

174. Rector A, Tachezy R, Van Ranst M. 2004. A sequence-independent strategy for detection and cloning of circular DNA virus genomes by using multiply primed rolling-circle amplification. J Virol 78:4993-4998.

175. Sawtell NM, Thompson RL, Haas RL. 2006. Herpes simplex virus DNA synthesis is not a decisive regulatory event in the initiation of lytic viral protein expression in neurons in vivo during primary infection or reactivation from latency. J Virol 80:38-50.

176. Cladel NM, Hu J, Balogh K, Mejia A, Christensen ND. 2008. Wounding prior to challenge substantially improves infectivity of cottontail rabbit papillomavirus and allows for standardization of infection. Journal of virological methods 148:34-39.

177. Marcuzzi GP, Hufbauer M, Kasper HU, Weißenborn SJ, Smola S, Pfister H. 2009. Spontaneous tumour development in human papillomavirus type 8 E6 transgenic mice and rapid induction by UV-light exposure and wounding. J Gen Virol 90:2855-2864.

178. Zhou AY, Ryeom S. 2014. Cyclosporin A promotes tumor angiogenesis in a calcineurin-independent manner by increasing mitochondrial reactive oxygen species. Molecular cancer research : MCR 12:1663-1676.

179. Datta D, Contreras AG, Basu A, Dormond O, Flynn E, Briscoe DM, Pal S. 2009. Calcineurin inhibitors activate the proto-oncogene Ras and promote protumorigenic signals in renal cancer cells. Cancer Research 69:8902-8909.

180. Gupta A, Dai Y, Vethanayagam RR, Hebert MF, Thummel KE, Unadkat JD, Ross DD, Mao Q. 2006. Cyclosporin A, tacrolimus and sirolimus are potent inhibitors of the human breast cancer resistance protein (ABCG2) and reverse resistance to mitoxantrone and topotecan. Cancer chemotherapy and pharmacology 58:374-383.

181. K Gandhi A, Kang J, Capone L, Parton A, Wu L, H Zhang L, Mendy D, Lopez-Girona A, Tran T, Sapinoso L. 2010. Dexamethasone synergizes with lenalidomide to inhibit multiple myeloma tumor growth, but reduces lenalidomide-induced immunomodulation of T and NK cell function. Current cancer drug targets 10:155-167.

182. Haedicke J, Iftner T. 2013. Human papillomaviruses and cancer. Radiother Oncol.

183. Neale RE, Weissenborn S, Abeni D, Bavinck JNB, Euvrard S, Feltkamp MC, Green AC, Harwood C, de Koning M, Naldi L. 2013. Human Papillomavirus Load in Eyebrow Hair Follicles and Risk of Cutaneous Squamous Cell Carcinoma. Cancer Epidemiol Biomarkers Prev 22:719-727.

184. Blanpain C, Fuchs E. 2006. Epidermal stem cells of the skin. Annu Rev Cell Dev Biol 22:339-373.

185. Moore N, Lyle S. 2010. Quiescent, slow-cycling stem cell populations in cancer: a review of the evidence and discussion of significance. Journal of oncology 2011.

186. Blazkova J, Trejbalova K, Gondois-Rey F, Halfon P, Philibert P, Guiguen A, Verdin E, Olive D, Van Lint C, Hejnar J, Hirsch I. 2009. CpG methylation controls reactivation of HIV from latency. PLoS Pathog 5:e1000554.

187. Bergbauer M, Kalla M, Schmeinck A, Göbel C, Rothbauer U, Eck S, Benet-Pagès A, Strom TM, Hammerschmidt W. 2010. CpG-methylation regulates a class of Epstein-Barr virus promoters. PLoS pathog 6:e1001114.

188. Struijk L, van der Meijden E, Kazem S, ter Schegget J, de Gruijl FR, Steenbergen RD, Feltkamp MC. 2008. Specific betapapillomaviruses associated with squamous cell carcinoma of the skin inhibit UVB-induced apoptosis of primary human keratinocytes. J Gen Virol 89:2303-2314.

189. Pfefferle R, Marcuzzi GP, Akgül B, Kasper HU, Schulze F, Haase I, Wickenhauser C, Pfister H. 2008. The human papillomavirus type 8 E2 protein induces skin tumors in transgenic mice. J Invest Dermatol 128:2310-2315.

190. Schaper ID, Marcuzzi GP, Weissenborn SJ, Kasper HU, Dries V, Smyth N, Fuchs P, Pfister H. 2005. Development of skin tumors in mice transgenic for early genes of human papillomavirus type 8. Cancer Res 65:1394-1400.

191. Viarisio D, Mueller-Decker K, Kloz U, Aengeneyndt B, Kopp-Schneider A, Grone HJ, Gheit T, Flechtenmacher C, Gissmann L, Tommasino M. 2011. E6 and E7 from beta HPV38 cooperate with ultraviolet light in the development of actinic keratosis-like lesions and squamous cell carcinoma in mice. PLoS Pathog 7:e1002125.

192. Siegsmund M, Wayss K, Amtmann E. 1991. Activation of latent papillomavirus genomes by chronic mechanical irritation. J Gen Virol 72:2787.

193. Bavinck JNB, Hardie DR, Green A, Cutmore S, MacNaught A, O'sullivan B, Siskind V, van der Woude FJ, Hardie IR. 1996. THE RISK OF SKIN CANCER IN RENAL TRANSPLANT RECIPIENTS IN QUEENSLAND, AUSTRALIA: A Follow-up Study1. Transplantation 61:715-721.

194. Ramsay H, Fryer A, Hawley C, Smith A, Nicol D, Harden P. 2002. Non-melanoma skin cancer risk in the Queensland renal transplant population. Br J Dermatol 147:950-956.

195. Jensen P, Hansen S, Møller B, Leivestad T, Pfeffer P, Geiran O, Fauchald P, Simonsen S. 1999. Skin cancer in kidney and heart transplant recipients and different long-term immunosuppressive therapy regimens. Journal of the American Academy of Dermatology 40:177-186.

196. Samaniego M, Becker BN, Djamali A. 2006. Drug insight: maintenance immunosuppression in kidney transplant recipients. Nature clinical practice. Nephrology 2:688-699.

197. Amor KT, Ryan C, Menter A. 2010. The use of cyclosporine in dermatology: part I. Journal of the American Academy of Dermatology 63:925-946.

198. Ryan C, Amor KT, Menter A. 2010. The use of cyclosporine in dermatology: part II. Journal of the American Academy of Dermatology 63:949-972.

199. Gratwohl A, Riederer I, Graf E, Speck B. 1986. Cyclosporine toxicity in rabbits. Laboratory animals 20:213-220.

200. Waugh DJ, Wilson C. 2008. The interleukin-8 pathway in cancer. Clinical cancer research : an official journal of the American Association for Cancer Research 14:6735-6741.

201. Apte RN, Dotan S, Elkabets M, White MR, Reich E, Carmi Y, Song X, Dvozkin T, Krelin Y, Voronov E. 2006. The involvement of IL-1 in tumorigenesis, tumor invasiveness, metastasis and tumor-host interactions. Cancer Metastasis Rev 25:387-408.

202. Iwata T, Fujii T, Morii K, Saito M, Sugiyama J, Nishio H, Morisada T, Tanaka K, Yaguchi T, Kawakami Y. 2015. Cytokine profile in cervical mucosa of Japanese patients with cervical intraepithelial neoplasia. International journal of clinical oncology 20:126-133.

203. Grulich AE, van Leeuwen MT, Falster MO, Vajdic CM. 2007. Incidence of cancers in people with HIV/AIDS compared with immunosuppressed transplant recipients: a meta-analysis. Lancet 370:59-67.

204. Kauffman HM, Cherikh WS, McBride MA, Cheng Y, Hanto DW. 2006. Post-transplant de novo malignancies in renal transplant recipients: the past and present. Transplant international : official journal of the European Society for Organ Transplantation 19:607-620.

205. Hojo M, Morimoto T, Maluccio M, Asano T, Morimoto K, Lagman M, Shimbo T, Suthanthiran M. 1999. Cyclosporine induces cancer progression by a cell-autonomous mechanism. Nature 397:530-534.

206. Guba M, von Breitenbuch P, Steinbauer M, Koehl G, Flegel S, Hornung M, Bruns CJ, Zuelke C, Farkas S, Anthuber M. 2002. Rapamycin inhibits primary and metastatic tumor growth by antiangiogenesis: involvement of vascular endothelial growth factor. Nature medicine 8:128-135.

207. Dziunycz PJ, Lefort K, Wu X, Freiberger SN, Neu J, Djerbi N, Iotzowa-Weiss G, French LE, Dotto G-P, Hofbauer GF. 2014. The Oncogene ATF3 Is Potentiated by Cyclosporine A and Ultraviolet Light A. J Invest Dermatol.

208. Wu X, Nguyen B-C, Dziunycz P, Chang S, Brooks Y, Lefort K, Hofbauer GF, Dotto GP. 2010. Opposing roles for calcineurin and ATF3 in squamous skin cancer. Nature 465:368-372.

209. Xu J, Walsh SB, Verney ZM, Kopelovich L, Elmets CA, Athar M. 2011. Procarcinogenic effects of cyclosporine A are mediated through the activation of TAK1/TAB1 signaling pathway. Biochem Biophys Res Commun 408:363-368.

210. Han W, Ming M, He T-C, He Y-Y. 2010. Immunosuppressive Cyclosporin A Activates AKT in Keratinocytes through PTEN Suppression IMPLICATIONS IN SKIN CARCINOGENESIS. J Biol Chem 285:11369-11377.

211. Tiu J, Li H, Rassekh C, van der Sloot P, Kovach R, Zhang P. 2006. Molecular basis of posttransplant squamous cell carcinoma: the potential role of cyclosporine a in carcinogenesis. The Laryngoscope 116:762-769.

212. Vinzon SE, Braspenning-Wesch I, Muller M, Geissler EK, Nindl I, Grone HJ, Schafer K, Rosl F. 2014. Protective Vaccination against Papillomavirus-Induced Skin Tumors under Immunocompetent and Immunosuppressive Conditions: A Preclinical Study Using a Natural Outbred Animal Model. PLoS pathog 10.

213. Molano RD, Pileggi A, Berney T, Poggioli R, Zahr E, Oliver R, Malek TR, Ricordi C, Inverardi L. 2003. Long-term islet allograft survival in nonobese diabetic mice treated with tacrolimus, rapamycin, and anti-interleukin-2 antibody1. Transplantation 75:1812-1819.

214. Euvrard S, Morelon E, Rostaing L, Goffin E, Brocard A, Tromme I, Broeders N, Del Marmol V, Chatelet V, Dompmartin A. 2012. Sirolimus and secondary skin-cancer prevention in kidney transplantation. The New England journal of medicine 367:329-339.

215. Wulff BC, Kusewitt DF, VanBuskirk AM, Thomas-Ahner JM, Duncan FJ, Oberyszyn TM. 2008. Sirolimus reduces the incidence and progression of UVB-induced skin cancer in SKH mice even with co-administration of cyclosporine A. J Invest Dermatol 128:2467-2473.

7 SUPPLEMENTARY

Table S1. Summary of the infection and outcomes of rabbits in this study.

Rabbit ID in this thesis	Infected doses (ng) *	Number of infected sites	Papilloma induction (positive/ total sites)	Efficiency of papilloma induction	Infection date	Euthaniza-tion date	Duration Months (M), Days (D)
Rabbit 1	5700	4	3/4	75%	22.02.2013	19.02.2014	11M,28D
	330	8	7/8	87.5%			
	170	8	7/8	87.5			
	40	8	2/8	25%			
Rabbit 2	5700	4	4/4	100%	22.02.2013	02.10.2013	7M,10D
	330	8	8/8	100%			
	170	8	8/8	100%			
	40	8	3/8	37.5%			
Rabbit 3	5700	4	4/4	100%	23.02.2013	26.03.2014	13M,3D
	330	8	8/8	100%			
	170	8	7/8	87.5%			
	40	8	2/8	25%			
Rabbit LAT1	34	24	10/24	41.67%	28.10.2013	25.07.2014	8M, 28D
Rabbit LAT2	34	24	2/24	8.33%	28.10.2013	22.06.2014	7M, 26D
Rabbit LAT3	34	24	8/24	33.33%	29.10.2013	16.04.2015	17M, 19D
Rabbit LAT4	34	24	5/24	20.08%	29.10.2013	08.06.2015	19M, 11D
Rabbit 5	12	32	1/32	3.13%	04.09.2014	07.09.2016	24M, 4D
Rabbit 6	12	32	3/32	9.38%	04.09.2014	07.09.2016	24M, 4D
Rabbit 7	12	32	3/32	9.38%	19.09.2014	07.09.2016	23M, 20D
Rabbit 8	12	32	1/32	3.13%	19.09.2014	07.09.2016	23M, 20D
Rabbit 9	3800	16	13/16	81.25%	20.04.2015	02.06.2016	13M, 14D
Rabbit 10	3800	16	16/16	100%	20.04.2015	02.05.2016	12M, 13D
Rabbit 11	3800	16	9/16	56.25%	21.04.2015	02.05.2016	12M, 12D
Rabbit 12	3800	16	13/16	81.25%	21.04.2015	28.07.2015	3M, 8D
Rabbit 13	3800	16	6/16	37.5%	21.04.2015	18.08.2016	15M, 29D
Rabbit 14	42	16	1/16	6.25%	05.05.2015	18.08.2016	15M, 14D
Rabbit 15	42	16	4/16	25%	05.05.2015	18.08.2016	15M, 14D
Rabbit 16	42	16	0/16	0	04.05.2015	13.04.2016	11M, 10D
Rabbit 17	42	16	1/16	6.25%	04.05.2015	29.02.2016	9M, 6D
Rabbit 18	42	16	2/16	12.5%	04.05.2015	18.08.2016	15M, 15D

FIG S1. RCA amplified CRPV DNA in latent skin biopsies. M: 1 kb maker, 1: RCA amplified CRPV-pLAII plasmid control, 2: RCA amplified Vx2 cell DNA extracts. 3 to 20: RCA amplified DNAs from the latently infected site. All RCA amplified products were digested with SmaI for 4 hours and then were ran on 0.4% of agarose gel for 1h.

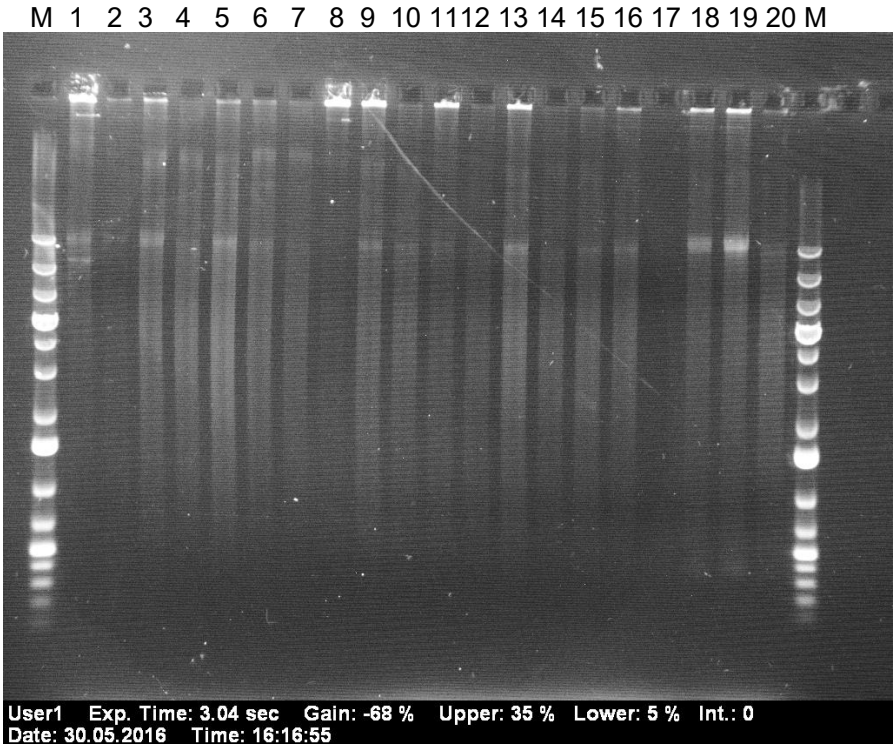

FIG S2. Mechanical irritations of latent infection sites. (A) The irritations of latent infected skin on the tattoo ink marked areas where the viral DNA was inoculated. (B) The effect of mechanical irritations on latent viral copy numbers. Normal skin n = 8, before reactivation n= 10, after reactivation n= 13. The data was log-transformed, and then the unpaired *t*-test was conducted for the statistical significant test.

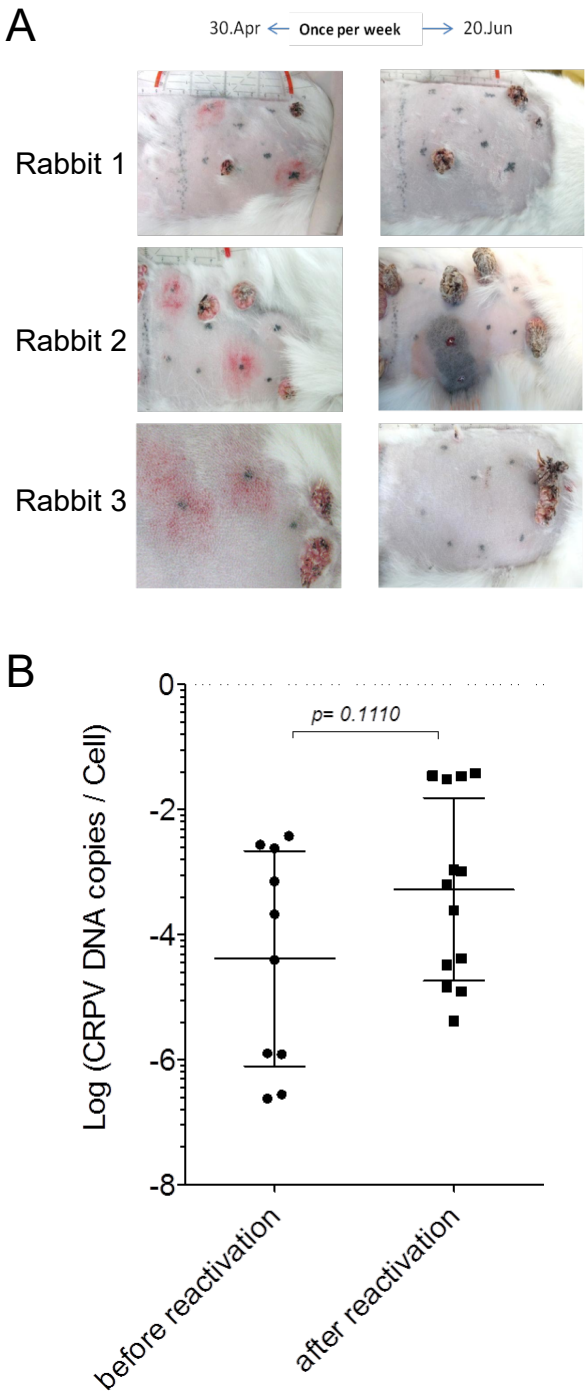

FIG S3. The pre-existing papillomas grew much faster upon drug-induced immunosuppression compared to the untreated control. (A) The growth curve of papillomas. The rabbit LAT1, LAT2 and LAT3 were immunosuppressed, whereas the rabbit LAT4 was non-immunosuppressed control. The rabbit 2 died due to unexpected lung infection 2 weeks post-immunosuppression. The average papilloma GMDs are significantly higher compared to that of the control rabbit. ***: $p < 0.0001$. (B) The representative photo of a papilloma on rabbit LAT1.

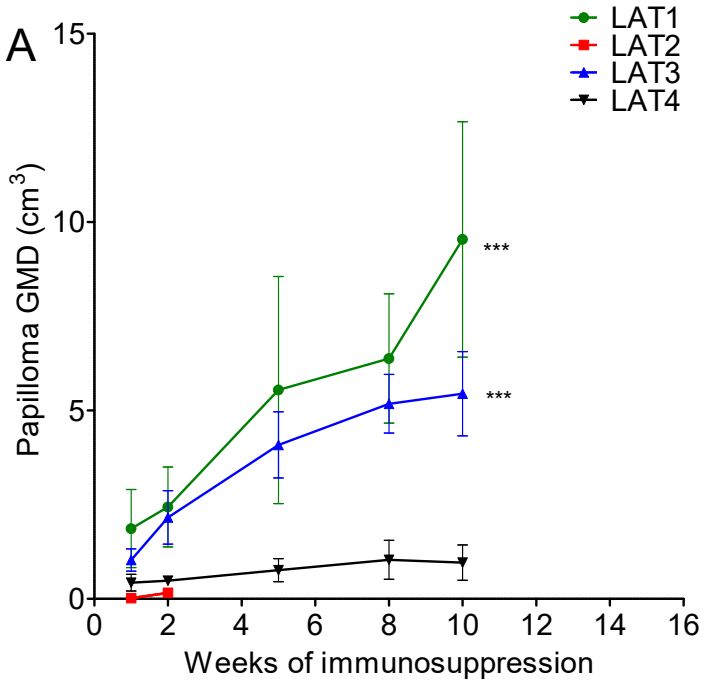

B

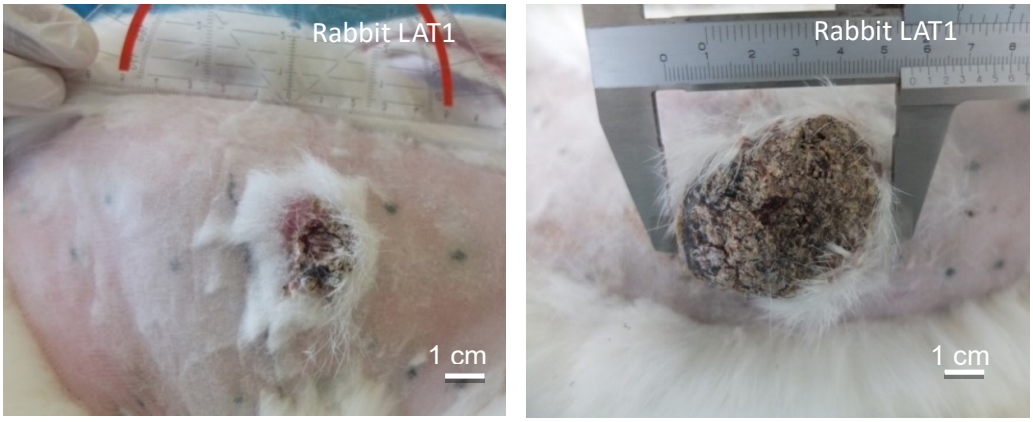

Before immunosuppression

10 weeks after immunosuppression

FIG S4. The effect of BPE, EGF, CsA, Dex, and Sir on rabbit-derived cells (AVS) growth. Photos were taken 5 days after incubation of a therapeutic concentration 250 nM (0.3 ng/μL) CsA, 100nM (0.04 ng/μL) Dex, and 100 nM (0.1 ng/μL) Sir on AVS cells.

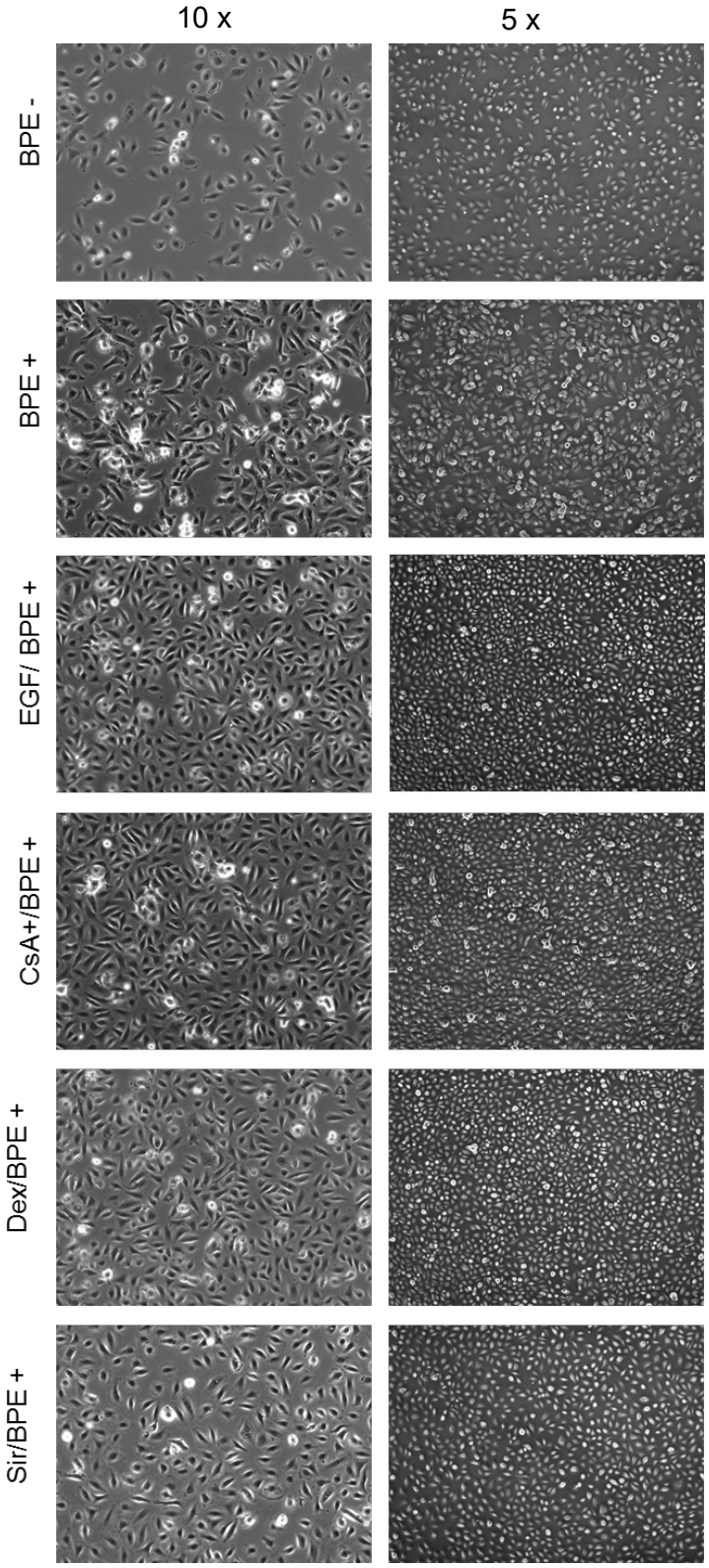

FIG S5. Comparison of latent viral copy number of immunosuppression alone with immunosuppression + UVA/B group. The samples for immunosuppression alone (n= 12) were from rabbit 7 and 8 which under 17 weeks immunosuppression, whereas immunosuppression +UVA/B were from rabbit 16, 17 and 18 (n= 12) with 16 weeks immunosuppression. Each dot represents one sample. The data was log-transformed, and then the unpaired *t*-test was conducted for the statistical significant test.

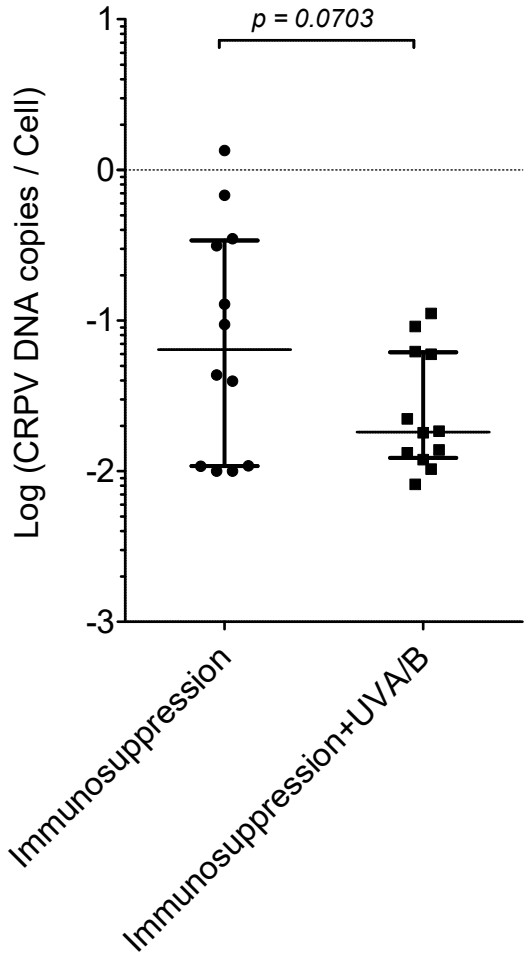

8 ACKNOWLEDGEMENTS

I would like to thank all those who supported me during the preparation of this work.

First of all, my grateful thanks to my supervisor Prof. Dr. Thomas Iftner for offering me the opportunity and interesting project, and his guidance. For me it was a nice experience to work in his lab.

I would like to thank Prof. Dr. Frank Stubenrauch for his helpful suggestions and support on my experiment. Dr. Juliane Haedicke for her efforts on this project, support on my experiment, and translating the abstract of this thesis into German.

My thanks also go to all colleagues in the lab. In particular PhD candidate Markus Schneider for the helping in all animal experiments in this thesis, Dr. Manawapat for providing help on real time PCR, PhD candidate Giada Corradini for the help on immunofluorecent experiments, Dr. Christina Habiger for providing help on FACS analysis, Dr. Olga Rataj for her advice on my WST-1 experiment and help in daily life, MTA Angelika Iftner for helping in primary cell culture experiment, and also Elke Straub, Marcel Dreer for providing help and support on daily basis. My thanks also go to current lab members Dr. Claudia Simon, Saskia, Aylin, Katerin, Julian, Karin.

I also would like to thank secretary Maike for helping me with my VISA and contract, and also Silke for daily support.

Finally I would like to thank my wife Dr. Fengying Liu for her endless support and bring a beautiful daughter Sufei to my life. My thanks to my parents who have been supported me all the time.

You are very important to make this happen.

9 ACADEMIC RESUME

2013 – 2017	**PhD candidate, Biology**
Tübingen, Germany	Division of Experimental Virology, Institute of Medical Virology, University Hospital Tuebingen, Tuebingen University
	Dissertation title: An Out-bred Animal Model of Cottontail Rabbit Papillomavirus Latent Infection
2008 – 2012	**Master of Preventive Veterinary Medicine**
Beijing & Changchun China	Military Veterinary Research Institute, Chinese Academy of Military Medical Sciences
	Dissertation title: Differentiation of the Seven Major Lyssavirus Species by Oligonucleotide Microarray.
2004 – 2008	**Bachelor of Veterinary Medicine**
Chongqing, China	Southwest University
	Thesis title: Infection Rate and Risk Factors Analysis of *Haemotrophic Mycoplasma* (Formerly *Eperythrozoon ovis*) in Chongqing Area

10 PUBLICATION

Jin Xi, Huancheng Guo, Ye Feng, Yunbin Xu, Mingfu Shao, Nan Su, Jiayu Wan, Jiping Li and Changchun Tu. Differentiation of the Seven Major Lyssavirus Species by Oligonucleotide Microarray, 2012, 50(3): 619 - 625. J Clin Microbiol.

Patent: Changchun Tu, **Jin Xi**. Lyssavirus diagnosing and typing chip and manufacturing method thereof. (CN 101921880 B, granted in Oct 17, 2012).

Jin Xi, Markus Schneider, Juliane Haedicke, Angelika Iftner, Frank Stubenrauch and Thomas Iftner. Establishment of an Outbred Latency Model with the Cottontail Rabbit Papillomavirus (CRPV) in New Zealand White Rabbits Allows Measuring the Effects of UV and/or Immunosuppression on Latent Skin Infections. (*in preparation*)

Jin Xi, Markus Schneider, Frank Stubenrauch and Thomas Iftner. Cyclosporine-based Immunosuppression Facilitates Pre-existing Papillomavirus-Induced Tumor Growth in an Out-bred Rabbit Model. (*in preparation*)